UNIVERSITÉ DU QUÉBEC À MONTRÉAL

FUNCTIONAL ANALYSES OF THE YEAST DEAD-BOX RNA HELICASE DBP4 AND ITS HUMAN HOMOLOGUE DDX10 IN RIBOSOME BIOGENESIS

THESIS

PRESENTED

AS PARTIAL REQUIREMENT

OF PhD IN BIOLOGY

BY

SAHAR SOLTANIEH

APRIL 2014

UNIVERSITÉ DU QUÉBEC À MONTRÉAL

ANALYSE FONCTIONELLE DE L'ARN HÉLICASE DBP4 CHEZ LA LEVURE ET SON HOMOLOGUE DDX10 CHEZ L'HUMAIN DANS LA BIOGENÈSE DES RIBOSOMES

THÈSE

PRÉSENTÉE

COMME EXIGENCE PARTIELLE

DU DOCTORAT EN BIOLOGIE

PAR

SAHAR SOLTANIEH

AVRIL 2014

Acknowledgments

I would like to express my deepest gratitude to my supervisor, Dr François Dragon, for his excellent guidance, support, motivation, kindness and patience. Not to mention his priceless advice and unsurpassed knowledge in Molecular Biology and Biochemical Sciences. I would like to thank him for invaluable lessons about the importance of guidance and for the freedom he granted to me during my work in his lab. He has been a tremendous mentor for me, I could not have ever imagined a better supervisor and I am really thankful for allowing me to grow as a research scientist. My research would not have been possible without his continuous support and help.

I would also like to thank my committee members, Dr. Benoit Barbeau, Dr. Jean Danyluk and Dr. Marlene Oeffinger for willing to accept being part of my defense committee.

Many thanks to my laboratory colleagues, and to other colleagues from neighboring laboratories for their help.

Last, but by no means least, I would like to thank my parents for their love, support and encouragements throughout my entire life and I also thank my sister, Samaneh, for her love and being my very best friend.

TABLE OF CONTENT

LIST OF FIGURES

Figure **Page**

LIST OF TABLES

LIST OF ABREVIATIONS

AATF	Apoptosis antagonizing transcription factor
CC	Coiled-coil motif
CRAC	UV crosslinking and analysis of cDNA
CTs	Christmas trees
DC	Dyskeratosis congenita
DFC	Dense fibrillar component
DRIM	Down-Regulated In Metastasis
EM	Electron microscopy
FACS	Fluorescence-activated cell sorting analyses
GC	Granular component
IP	Immunoprecipitation experiment
ITS1	Internal transcribed spacer 1
NAIC	North American Indian childhood cirrhosis
NFBP	NF-κB binding protein
NLS	Nuclear localization signal
NoLS	Nucleolar localization signal
NORs	Nucleolar-organizing regions
PARP	Poly (ADP-ribose) polymerase
PDCD11	Programmed cell death 11
RIP	RNA immunoprecipitation experiment

SBDS	Shwachman-Bodian-Diamond syndrome
scaRNA	Small Cajal body-specific RNA
SF	Superfamilies
snoRNP	Small nucleolar ribonucleoprotein
SSU processome	Small subunit processome
TAP	Tandem affinity purification
WCE	Whole-cell extract

Abstract

The phylogenetically conserved DEAD-box protein Dbp4 is one of the nucleolar RNA helicases involved in ribosome biogenesis. Dbp4 is essential for growth of the yeast *Saccharomyces cerevisiae*, indicating that it plays an important function in the cell. There is a genetic link between Dbp4 and the U14 small nucleolar RNA (snoRNA), which is involved in ribosomal RNA (rRNA) processing; this suggests that Dbp4 plays a role in ribosome biogenesis. A more recent study revealed that Dbp4 is implicated in the early cleavages at sites A0, A1 and A2 of the rRNA precursor (pre-rRNA). We showed that Dbp4 is associated with U3 snoRNA but not with U14 snoRNA, using immunoprecipitation experiments (IPs). IPs also showed association with the U3-specific protein Mpp10, suggesting that Dbp4 interacts with the functionally active SSU processome (80S complex), which can be observed at the 5' end of nascent pre-rRNA. Electron microscopy analyses indicated that depletion of Dbp4 impaired SSU processome formation and co-transcriptional cleavage of the pre-rRNA. This suggests that Dbp4 is required for SSU processome formation.

We found that Dbp4 contains a predicted coiled-coil motif, which is implicated in protein-protein interactions. We showed that Bfr2 and Enp2 associate with Dbp4 in a RNA-dependent manner. We also demonstrated that, like Dbp4, Bfr2 and Enp2 are required for the early processing steps that lead to the production of 18S rRNA. Our results demonstrated that Bfr2, Enp2 and Dbp4 associate with the U3 snoRNA, the U3-specific protein Mpp10, and also with different pre-rRNA species. These results lead us to propose that Bfr2, Dbp4 and Enp2 might be components of the SSU processome. Sucrose gradient sedimentation analyses revealed that Dbp4, Bfr2 and Enp2 sediment in a peak of about 50S, as well as in a peak of ~80S. Our studies showed that Bfr2, Dbp4 and Enp2 associate together in the 50S peak, which does not include U3 snoRNA. IPs demonstrated that U14 snoRNA associates with Dbp4 in the 50S complex, but not with Bfr2 or Enp2. However, these proteins associate with U3 snoRNA in the 80S peak. We proposed that Bfr2, Dbp4 and Enp2 form a 50S complex with other ribosome biogenesis factors, which would be incorporated at late steps into the SSU processome.

DEAD-box RNA helicase DDX10 is the human homologue of yeast Dbp4. We showed that DDX10 and Che-1/AATF (Apoptosis Antagonizing Transcription Factor) co-localize with the nucleolar marker fibrillarin, suggesting that DDX10 and Che-1 (the human homologue of Bfr2) could participate in ribosome biogenesis. We tested different siRNAs against *DDX10* to evaluate the effect of DDX10 depletion on rRNA maturation and proliferation of HeLa cells. Loss of DDX10 and Che-1 resulted in decreased production of 18S rRNA. In line with the 18S rRNA defect, immunoprecipitation experiments demonstrated that DDX10 is associated with the U3 snoRNA, Che-1 and the U3-specific protein DRIM/UTP20. Flow cytometry

analyses revealed that cells treated with siDDX10 slightly accumulated in the G1 phase of the cell cycle. Immunofluoresence microscopy showed that treatment with siDDX10 strongly reduced the expression of the proliferation marker Ki-67. Taken together our data indicate that DDX10 is required for cell growth and proliferation, and that it plays a role in pre-18S rRNA maturation.

Keywords: Ribosome biogenesis, DEAD-box RNA helicase, SSU processome, snoRNA

Résumé

La protéine nucléolaire Dbp4 est une ARN hélicase de la famille « DEAD-box ». Dbp4 est phylogénétiquement conservée et elle est essentielle à la survie de la levure *Saccharomyces cerevisiae*, ce qui souligne son importance fonctionnelle dans la vie cellulaire. Il existe un lien génétique entre Dbp4 et U14, un petit ARN nucléolaire (snoRNA) essentiel à la production d'ARN ribosomique (ARNr) 18S. De plus, il a été démontré que Dbp4 est nécessaire pour les clivages aux sites A0, A1 et A2 qui mènent à la production de l'ARNr 18S. Nous avons trouvé que Dbp4 n'est pas associée à U14 mais plutôt au snoRNA U3, ainsi qu'à la protéine Mpp10 une protéine « spécifique à U3 » et composante essentielle du SSU processome. Ce complexe d'environ 80S représente la forme fonctionnelle de U3. Nos analyses par microscopie électronique ont démontré que la dépletion de Dbp4 empêche la formation du SSU processome et le clivage co-transcriptionel du pré-ARNr.

Suite à des analyses bioinformatiques nous avons identifié un motif « coiled-coil » putatif dans la partie C-terminale de Dbp4, une région qui est essentielle au fonctionnement de l'enzyme. Les « coiled-coil » sont des motifs d'interaction protéine-protéine, ce qui suggère que Dbp4 interagit avec d'autres protéines. Nous avons trouvé que Dbp4 participe à la maturation des pré-ARNr en formant un complexe avec les protéines Bfr2 et Enp2. Dbp4, Bfr2 et Enp2 s'associent avec le snoRNA U3 et Mpp10. Ces protéines sont également impliquées dans les premiers clivages qui mènent à la maturation de l'ARN 18S. Ces résultats suggèrent que Dbp4, Bfr2 et Enp2 seront possiblement des composant de SSU processome. Les analyses de sédimentation dans des gradients de saccharose ont révélé que Dbp4, Bfr2 et Enp2 co-sédimentent dans un complexe de 50S. Les expériences d'immunoprécipitation ont démontré que Dbp4 s'associe au snoRNA U14 dans le complexe de 50S. Bfr2, Enp2 et Dbp4, sont également détectées dans un complexe de 80S avec le snoRNA U3. Il y a donc une réorganisation dynamique de ces complexes pendant la biogenèse des ribosomes.

DDX10 est une ARN hélicase très conservée dans l'évolution. Son homologie avec l'hélicase Dbp4 et sa localisation nucléolaire suggéraient déjà une éventuelle implication de DDX10 dans la biogenèse des ribosomes. Nous avons testé une variété de siRNA ciblant DDX10 afin d'évaluer l'effet de la perte de DDX10 sur la maturation des ARNr ainsi que sur la prolifération et la croissance cellulaire. DDX10 et Che-1/AATF (Apoptosis Antagonizing Transcription Factor) localisent au nucléole. Une perte de DDX10 et de Che-1 entraine une diminution de la synthèse de l'ARNr 18S. Des expériences d'immunoprécipitation ont mis en évidence l'association de DDX10 avec le snoRNA U3, Che-1 et la protéine spécifique à U3 DRIM/UTP20. Les résultats en cytométrie de flux soulignent un arrêt de la croissance cellulaire en phase G1 en absence de DDX10. Les analyses par microscopie à immunoflueresence ont démontré une diminution du niveau d'expression du marqueur de prolifération Ki-67 en présence de siRNA ciblant DDX10. Finalement,

toutes ces données démontrent que DDX10 serait nécessaire à la prolifération et la croissance cellulaire et qu'elle joue un rôle dans la maturation de l'ARNr 18S.

Mots-clés: ARN hélicase, biogenèse des ribosomes, SSU processome, petit ARN nucléolaire.

Chapter I

Introduction

1.1 The nucleolus

In 1839, Valentin chose the name for the nucleolus. He found out that most cells had a secondary nucleus or a "nucleus within a nucleus" (Valentin, 1839). Montgomery described in detail the structure of the nucleolus in 1898 (Montgomery, 1898).

The nucleolus is a membraneless nuclear substructure that organizes around chromosome fragments containing nucleolar-organizing regions (NORs). NORs are tandem repeats of ribosomal genes that consists of a transcribed sequence and an intergenic spacer, which are located on one or numerous chromosomes (Raska *et al.*, 2006). The nucleolus is the center of rDNA transcription and ribosome biogenesis (Busch *et al.*, 1970; Carmo-Fonseca *et al.*, 2000; Olson *et al.*, 2000; Scheer and Hock, 1999), but it also has additional functions, including cell growth and cell cycle regulation, response to cellular stress, telomerase activity, signal recognition particle (SRP) biogenesis, p53 metabolism, small RNA processing, mRNA transport, and viral maturation and infection (Garcia and Pillus, 1999; Hiscox, 2007; Martindill and Riley, 2008; Mayer and Grummt, 2005; Olson *et al.*, 2000; Pederson, 1998a, 1998b; Rubbi and Milner, 2003). It has been proposed that the nucleolus plays different roles in health and disease (Matthews and Olson, 2006; Stark and Taliansky, 2009). Nucleolar perturbations have been observed in different cellular diseases, from auto-immunity to cancer (Montanaro *et al.*, 2008). For example, a decrease in ribosome synthesis induces apoptosis either in a p53-dependent or

independent manner (David-Pfeuty *et al.*, 2001; Pestov *et al.*, 2001), and p53 stabilization is mediated by nucleolar disruption (Rubbi and Milner, 2003).

The nucleolus is composed of three types of components, showing a tripartite organization (Leger-silvestre and Gas, 2004; Raska, 2003; Scheer and Hock, 1999; Shaw and Jordan, 1995) (see Figure 1.1). It is considered that the fibrillar centers (FCs) are the interphase counterparts of mitotic NORs (Goessens, 1984). FCs are normally surrounded by the dense fibrillar component (DFC). The DFC seems as densely packed fibrils. In electron micrographs of mammalian nucleoli, the DFC is heavily stained. The granular component (GC) shows a grainy appearance, containing RNP granules in different stages of maturation (McKeown and Shaw, 2009).

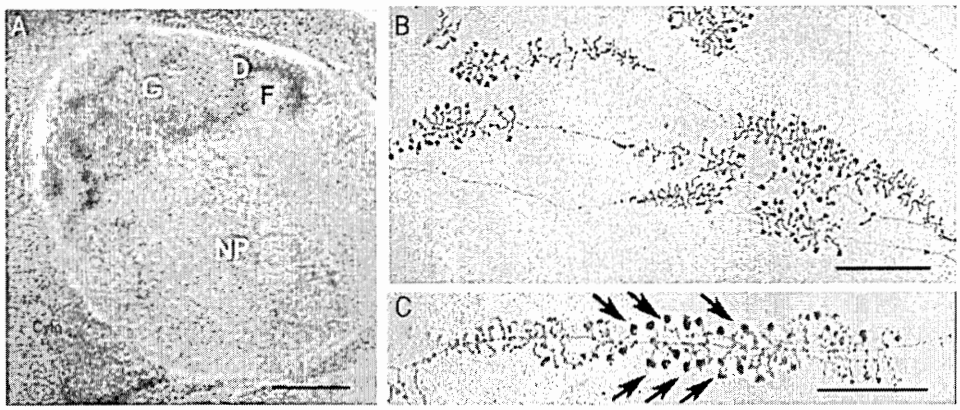

Figure 1.1. Electron micrographs of the nucleolus, and spread preparations of nucleolar chromatin forming Christmas trees (CTs). Thin-sectioned nucleolus (A) and CTs from yeast (B, C). The nucleolus shows a tripartite structure with FC (F), DFC (D) and GC (G). The large terminal knobs are indicated with arrows. Adapted from Raska et al. (2006).

The major part of the nucleolar volume consists of this peripheral nucleolar region (Busch *et al.*, 1970; Leger-silvestre and Gas, 2004; Mosgoller, 2004). The nucleolar

structure is different between kingdoms, species, cell types and individual cells (McKeown and Shaw, 2009), (see Figure 1.2). The DFC is bigger in plants than in animals. In *Saccharomyces cerevisiae*, it is not easy to make the distinction between the DFC and the GC. The regions of the nucleolus function in different steps of rRNA synthesis. The FC contains RNA polymerase I and the transcription factor UBF (Emmott and Hiscox, 2009). The DFC contains the RNA methyltransferase fibrillarin and nucleolin, which have different functions in nucleolar and cellular biology (Mongelard and Bouvet, 2007).

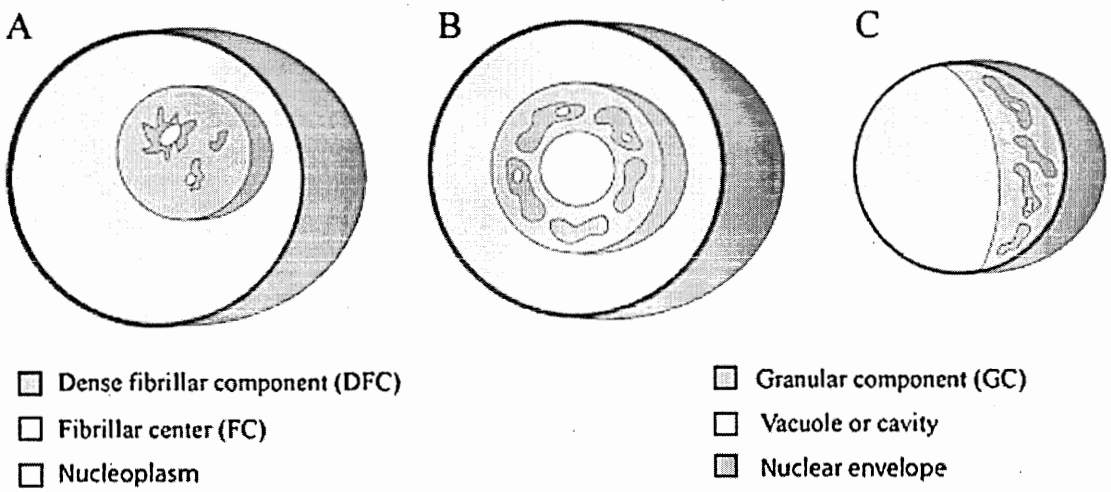

Figure 1.2. Substructure of nucleoli. A) animal nucleolus, B) plant nucleolus and C) yeast nucleolus. Taken from (McKeown and Shaw, 2009).

The visualisation of active rDNA genes in the form of Christmas trees (CTs) by electron microscopy (EM) was a very important progress in understanding the nucleolus (Miller and Beatty, 1969). This technique revealed the gene axis with many

RNA polymerase I molecules and the attached nascent transcripts, which are increasing in length, and the globular RNP particles (knobs) at the 5' end of the transcripts. In mammalian cells as well as onion and pea root cells, CTs are observed in the DFC and the border region between the DFC and FC (Casafont *et al.*, 2006; Cmarko *et al.*, 2000; Gonzalez-Melendi *et al.*, 2001; Melcak *et al.*, 1996; Raska, 2004; Shaw and Brown, 2004). The nucleolus is a distinct structure because particular proteins bind to the rDNA and form a relatively stable center so the rest of nucleolar interactions and dynamic processes are built onto it. There is a constant exchange of components between the nucleolus and the surrounding nucleoplasm. The nucleolar residence time of non-nucleolar proteins that do not associate with interacting partners in the nucleolus is shorter than that of nucleolar proteins, which leads to the steady□state composition of the nucleolus. Therefore, the nucleolus is a steady□state structure in which components are in dynamic equilibrium with the surrounding nucleoplasm (Raska *et al.*, 2006). Contrary to the well known nuclear localization signal (NLS) (Cokol *et al.*, 2000; la Cour *et al.*, 2004), the nucleolar localization signal (NoLS) is not well characterized (Emmott and Hiscox, 2009). Nucleolin, a very abundant nucleolar protein, does not contain any defined NoLS. It is suggested that the RNA-binding domains of nucleolin mediates its nucleolar accumulation (Schmidt-Zachmann and Nigg, 1993). The nucleolus is organized by RNA polymerase I transcription and the presence of rDNA genes as nucleation sites, and they maintain the steady state nucleolar structure (Scheer and Hock, 1999).

1.2 Ribosome biogenesis

1.2.1 Maturation of rRNAs

Ribosomes are large ribonucleoprotein complexes essential for the translation of mRNAs into proteins in a cell. Their mechanism of action seems to be based essentially on rRNA. They therefore are ribozymes (Green and Noller, 1997; Nissen *et al.*, 2000; Noller *et al.*, 1992), based on the crystal structure of the complete *Thermus thermophilus* 70S ribosome, the center of the interface between the 30S small subunit and the 50S large subunit, where the tRNA substrates bind, consists mainly of RNA, and proteins are located mostly at the periphery, which is consistent with rRNA based ribosomal function (Yusupov *et al.*, 2001). The small subunit of the ribosome contains the mRNA decoding site and the large subunit contains the peptidyl transferase center (PTC). Interestingly, the PTC is composed exclusively of RNA (Nissen *et al.*, 2000). Ribosome synthesis is a highly complex and regulated process that starts in the nucleolus but continues in the nucleoplasm and the cytoplasm of eukaryotic cells. Ribosome biogenesis involves rRNA synthesis, maturation, and assembly of rRNA with ribosomal proteins into the small and large ribosomal subunits (40S and 60S in eukaryotes). This process is conserved throughout eukaryotes (Tollervey, 1996b), and is regulated throughout the cell cycle, predominantly at the level of rRNA synthesis (Hannan *et al.*, 1998a). rDNA transcription takes place during the S and G2 phases, stops as cells enter mitosis, and then restarts as cells exit from mitosis (Grummt, 1999). Pre-rRNA processing has been studied very well in *Saccharomyces cerevisiae* (Kressler *et al.*, 1999; Venema

and Tollervey, 1999; Woolford and Baserga, 2013). The operon organisation of rRNAs is similar between different eukaryotic species. Human cells contain about 400 rDNA genes which are located on the short arms of the five acrocentric chromosomes (13, 14, 15, 21 and 22) (Hadjiolov, 1985) and *Saccharomyces cerevisiae* contains about 100–200 tandem repeats (9.1 kbp) in one cluster, which is on the long arm of chromosome XII (Planta, 1997). In most species, including mammals, each rDNA repeat consists of the coding sequence of the mature ribosomal RNAs, two transcribed internal and two external spacers (ITS and ETS) and a non□transcribed intergenic spacer (Fatica and Tollervey, 2002; Hadjiolov, 1985). RNA polymerase I produces a large polycistronic precursor rRNA (35S pre-rRNA in yeast, 47S pre-rRNA in mammals) that contains the 18S, 5.8S, 25-28S rRNAs. In the budding yeast *S. cerevisiae*, each of the rDNA transcription unit also contains a 5S rRNA gene within the ''non□transcribed'' spacer region (Neigeborn and Warner, 1990), which is transcribed by RNA polymerase III in the opposite direction. In human cells, the main 5S rRNA cluster is on chromosome region 1q42.11-q42.1 (Sorensen and Frederiksen, 1991)

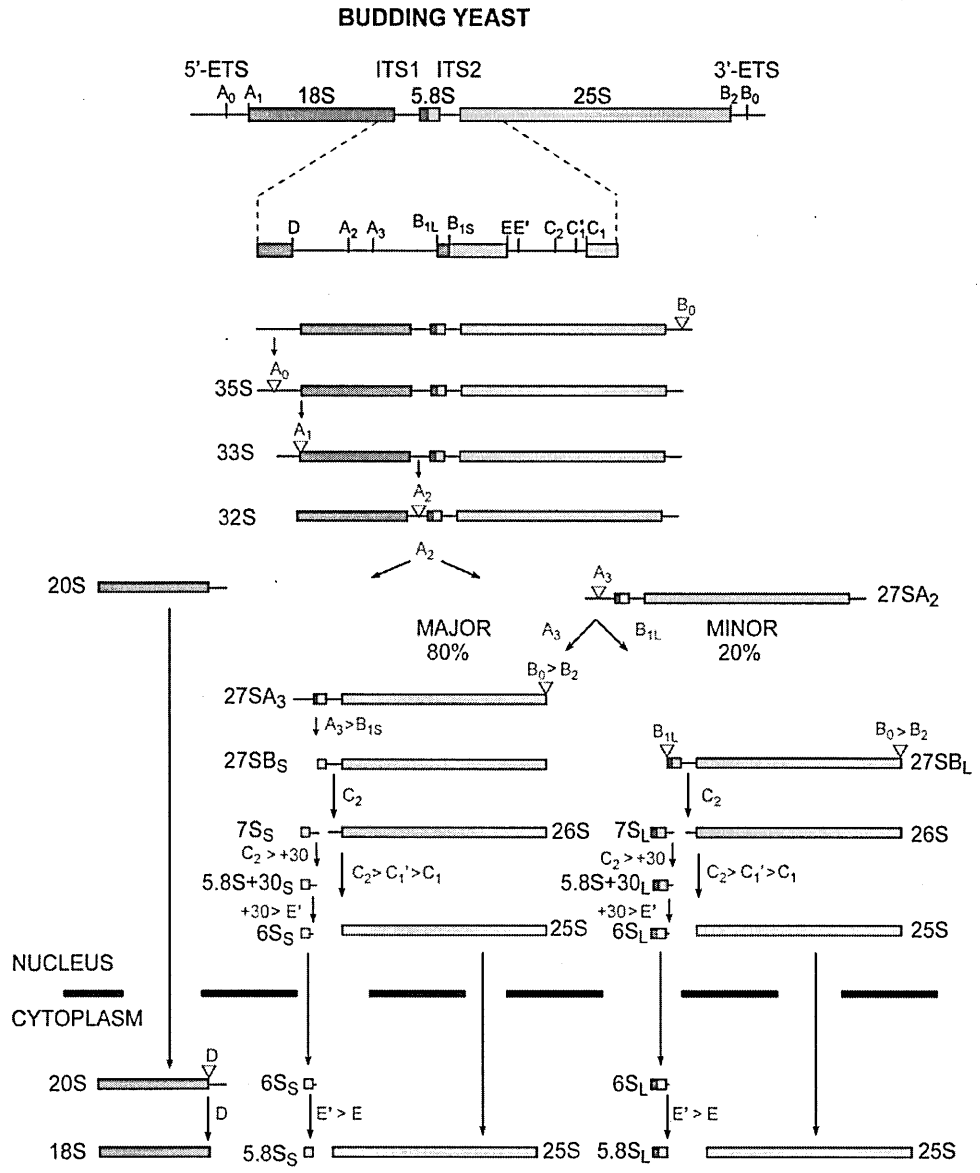

Figure 1.3. Schematic representation pre-rRNA processing pathway in *Saccharomyces cerevisiae*. The maturation of rRNAs is explained in detail in the text. Taken from (Mullineux and Lafontaine, 2012).

The 35S pre-rRNA undergoes a series of modifications including 3'-external transcribed spacer cleavage, 2'-O-ribose methylation and pseudouridylation, followed by 5'-external transcribed spacer and internal transcribed spacer cleavages (Venema and Tollervey, 1999) to produce the mature 18S, 5.8S and 25S rRNAs (Figure 1.3). The 35S pre-rRNA is cleaved in the 5'ETS at site A0 (generating the 33S pre-rRNA), then at site A1, which produces the mature 5'-end of 18S rRNA (generating the 32S pre-rRNA) and at site A2 in ITS1 (generating the 20S and 27SA2 pre-rRNAs). Further processing steps of the 20S rRNA occur in the cytoplasm by cleavage at site D to generate the mature 18S rRNA, but processing of the 27SA2 pre-rRNA continues in the nucleus. The cleavage at site A0 requires U3 and snR30 snoRNAs whereas cleavages at the sites A1 and A2 involve U3, U14, snR10 and snR30 snoRNAs. The 27SA2 precursor is matured by two alternative pathways. The majority of the 27SA2 pre-rRNA is cleaved at site A3 in ITS1 by RNase MRP, and a small amount of 27SA2 is cleaved directly at site B1L by an unknown endonuclease. Then, a series of cleavages by different exonucleases (Rat1, Xrn1, RrP17 and the exosome) produce the mature 5.8S and 25S rRNA (Fromont-Racine *et al.*, 2003; Oeffinger *et al.*, 2009; Venema and Tollervey, 1999). As described in the previous section, the active rRNA transcription unit could be seen with the appearance of Christmas trees (CTs) in electron microscopy images from chromatin spread preparations. The terminal knobs on the nascent pre-rRNA transcripts correspond to rRNA processing complexes. These complexes contain the U3 snoRNP, which base□pairs with sequences near the 5' end of the pre□rRNA (Mougey *et al.*, 1993;

Scheer and Benavente, 1990; Sharma and Tollervey, 1999). The terminal knobs are dynamic entities. Primarly, they are about 15 nm in size. Later during transcription, these knobs transform into a larger knob (40 nm), which corresponds to the so□called small subunit (SSU) processome (Dragon *et al.*, 2002). The large knobs are cleaved co□transcriptionally from the nascent transcript, which releases the pre□40S ribosome (Gallagher *et al.*, 2004; Granneman and Baserga, 2005; Kos and Tollervey, 2010; Osheim *et al.*, 2004).

The rRNAs are assembled with ribosomal proteins into pre-ribosomal particles in the nucleolus. Most of the ribosomal proteins associate with pre-rRNA at early steps preceding cleavage (Kruiswijk *et al.*, 1978), while others associate later in the final assembly steps, which produce the mature 40S and 60S ribosomal subunits. The composition of the pre-ribosomal subunits is highly dynamic, and more than 200 non-ribosomal proteins (trans-acting factors) including 19 putative RNA helicases (Jankowsky *et al.*, 2011), 76 small nucleolar ribonucleoproteins (snoRNP) and different endo- and exonucleases are implicated in the assembly of the ribosome (Dragon *et al.*, 2002; Fatica and Tollervey, 2002; Fromont-Racine *et al.*, 2003; Granneman and Baserga, 2005; Nagahama *et al.*, 2004; Nissan *et al.*, 2004; Tschochner and Hurt, 2003; Venema and Tollervey, 1999; Yager and Davidson, 2006). At last, pre-40S and pre-60S subunits are exported to the cytoplasm for final maturation.

Ribosome biogenesis in mammalian cells is more complex than in yeast. The mature human rRNAs are similar in length except that the 28S rRNA is 1.5 fold

longer than the 25S rRNA. The non-coding spacers are extended 5-fold or even more. In addition the human nucleolus contains about ten times more proteins than the yeast nucleolar proteome (Ahmad *et al.*, 2009; Huh *et al.*, 2003; Mullineux and Lafontaine, 2012). rDNA is transcribed into a 47S pre-rRNA, which is cleaved at sites 01 in 5'-ETS and 02 in 3'-ETS to generate the 45S pre-rRNA (Mullineux and Lafontaine, 2012), (see Figure 1.4). The 45S is matured by two alternative pre-rRNA processing pathways, 1 and 2. In pathway 1, the first cleavage is at A0 followed by cleavage at site 1 (in 5'-ETS). Normally these two cleavages are coupled, producing the 41S pre-rRNA but if they are not concomitant it generates the 43S pre-rRNA. The 41S is cleaved at site 2 into 21S and 32S pre-rRNA. In pathway 2, the first cleavage is at site 2 (in ITS1) producing the 30S and 32S pre-rRNA. The 21S is generated by simultaneous cleavage at sites A0 and 1, or via the 26S intermediate, which is produced by uncoupled cleavage of these sites. The 21S is trimmed to sites C and E generating the 21S-C and 18S-E pre-rRNA. The 18S-E is exported from the nucleus to the cytoplasm, and is matured to the 18S rRNA by cleavage at site 3. In parallel, the 32S is processed at site 3' (in ITS2) generating the 12S pre-rRNA and 28S rRNA. The 12S is further processed by a series of exoribonucleolytic cleavages (Lafontaine, 2015).

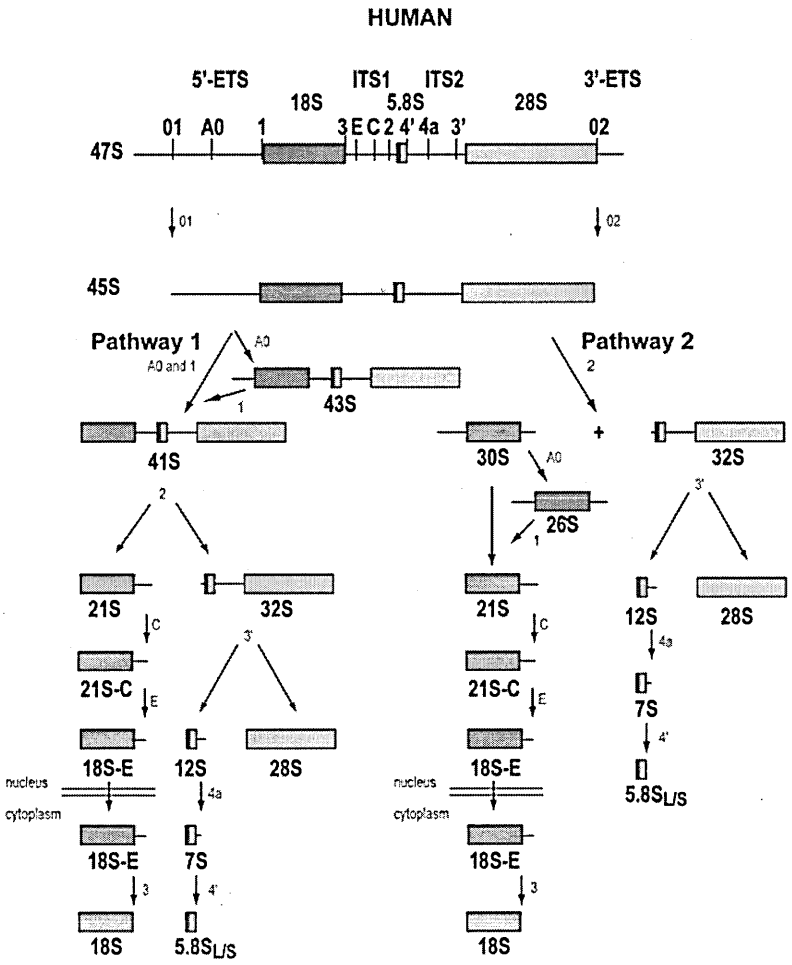

Figure 1.4 Schematic representation of the pre-rRNA processing pathway in humans. The maturation of rRNAs is explained in detail in the text. Taken from (Mullineux and Lafontaine, 2012).

The 12S is cleaved at site 4a into 7S, and afterwards at site 4' to produce the 5.8S rRNA.

1.2.2 The small nucleolar RNAs (snoRNAs)

The two most abundant post-transcriptional modifications of cellular RNAs are 2'-O-ribose methylation and pseudouridylation. Modification sites are found in

functionally important regions of the ribosome (Decatur and Fournier, 2002), and could facilitate the folding and stability of rRNA (King *et al.*, 2003; Ofengand, 2002). In eukaryotes, these modifications are conducted by small nucleolar ribonucleoproteins (snoRNPs) in the nucleolus. Similar RNPs are found in archaebacteria; they are called small RNPs (sRNPs) (Dennis and Omer, 2005; Omer *et al.*, 2003).

SnoRNAs are non-coding RNAs of different length generally ranging from ~60-300 nucleotides. Besides being implicated in modification reactions of rRNAs, a small number of snoRNAs are necessary for pre-rRNA endonucleolytic cleavages.

The snoRNAs are classified into two families, the C/D and H/ACA snoRNAs (Brown *et al.*, 2003; Lestrade and Weber, 2006; Piekna-Przybylska *et al.*, 2007; Samarsky and Fournier, 1999). The C/D and H/ACA snoRNAs associate with specific conserved proteins to form C/D and H/ACA snoRNPs. The third family is RNase MRP, which processes the pre-rRNA endonucleolytically at the A3 site. Its RNA component is structurally similar to that of RNase P. In yeast, RNase MRP contains 9 proteins: Snm1 is specifically associated with RNase MRP, but the other 8 proteins are common with RNase P (Kressler *et al.*, 1999; Venema and Tollervey, 1999; Xiao *et al.*, 2001). Few snoRNAs were identified with no obvious sequence complementarity to common substrates like rRNAs. They are called orphan snoRNAs because they have no known targets (Huttenhofer *et al.*, 2001). Thus, they probably target other RNAs like mRNAs (Bratkovic and Rogelj, 2011). In addition, there is

another class of small RNAs called small Cajal body-specific RNAs (scaRNAs), which accumulate in Cajal bodies, a membraneless sub-compartment of the nucleus. They are involved in modification of snRNAs and snoRNAs, and in their assembly leading to the production of mature small RNAs (Stanek and Neugebauer, 2006). The scaRNAs contain motifs of C/D and H/ACA snoRNAs, and also a specific CAB box (motif UGAG), which is a Cajal body localization signal (Henras *et al.*, 2004; Richard *et al.*, 2003).

1.2.2.1 Guide snoRNPs

The C/D snoRNPs carry out site specific 2'-O-ribose methylation (Kiss-Laszlo *et al.*, 1996; Nicoloso *et al.*, 1996; Tycowski *et al.*, 1996) and the H/ACA snoRNPs catalyze the isomerization of specific uridines to pseudouridines (Ψ) (Ganot *et al.*, 1997a; Ni *et al.*, 1997). The C/D snoRNAs form a stem-bulge-stem structure and contain two consensus sequences (see Figure 1.5A). The box C motif RUGAUGA (R is a purine) is positioned near the mature 5'-end of the snoRNA, while the box D sequence CUGA is located near its 3' end. Many C/D snoRNAs contain a second set of conserved sequences, the C' and D' boxes, located in the central region of the RNA (Reichow *et al.*, 2007). Both the C/D and C'/D' boxes are conserved in *Archaea* and form a kink-turn motif (Klein *et al.*, 2001). In eukaryotes, the C'/D' motif is less conserved and often lacks the kink-turn motif. A sequence of 10–20 nucleotides upstream of the D and/or D' box of the snoRNA base pairs with the

substrate RNA (Henras *et al.*, 2004; Reichow *et al.*, 2007). The methylation reaction is observed 5 nucleotides upstream of the conserved CUGA motif (Kiss-Laszlo *et al.*, 1996; Kiss-Laszlo *et al.*, 1998). The secondary structure of H/ACA snoRNAs consists of two hairpins (Figure 1.5B). The two stem-loops are linked by a hinge region that contains the box H sequence ANANNA (N is any nucleotide) and downstream of the second hairpin is a single-stranded segment with the ACA tri-nucleotide box sequence positioned three nucleotides upstream of the mature 3' end of the snoRNA. The stem-loops contain internal loops with 9-13 nucleotides on each strand that form the pseudouridylation pocket. The pseudouridylation site is situated 14–16 nucleotides upstream of either the H or ACA box motifs (Balakin *et al.*, 1996; Ganot *et al.*, 1997a; Ganot *et al.*, 1997b; Ni *et al.*, 1997). The class-specific sequence elements are conserved from *Archaea* to vertebrates, and are necessary for the assembly of functional RNPs (Balakin *et al.*, 1996; Henras *et al.*, 2004; Maxwell and Fournier, 1995; Tollervey and Kiss, 1997). The C/D snoRNAs associate with common proteins Nop1 (fibrillarin in humans), Nop56, Nop58 and Snu13 (15.5K in humans), which is the kink-turn binding protein, whereas the H/ACA snoRNAs associate with proteins Cbf5 (dyskerin in humans), Gar1, Nhp2 and Nop10. Nop1 is the 2'-O-ribose methylase enzyme and Cbf5 is the pseudouridine synthase. The class specific core snoRNP proteins are necessary for enzymatic activity, stability and nucleolar localisation of the snoRNPs (Bachellerie *et al.*, 2002; Eliceiri, 1999; Meier, 2005; Tollervey and Kiss, 1997).

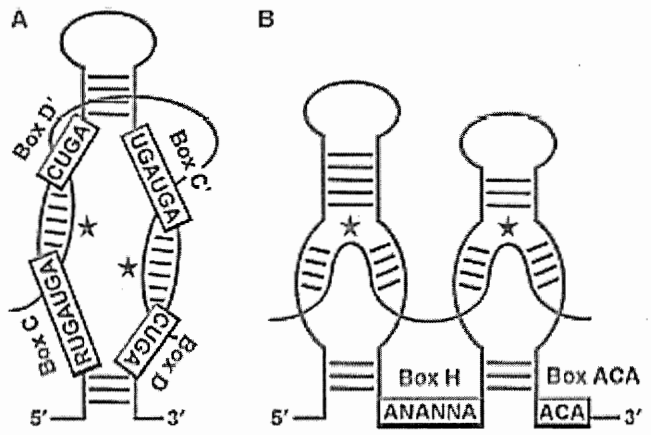

Figure 1.5. The secondary structure of snoRNAs. The class C/D (A) and H/ACA (B) snoRNAs (grey) contain conserved motifs "boxes" (blue). Their target RNA is colored in magneta. The sites for nucleotide modification are marked with a star. Taken from Reichow et al. (2007).

In eukaryotic, genomes the snoRNAs are expressed in different ways (Brown *et al.*, 2003; Filipowicz and Pogacic, 2002; Terns and Terns, 2002). In vertebrates, most of the snoRNAs are present in introns of protein coding genes or non coding pol II transcribed genes (Maxwell and Fournier, 1995). In plants, snoRNAs are found in polycistronic clusters (Leader *et al.*, 1997; Leader *et al.*, 1994). In yeast, snoRNAs are encoded mostly from independent mono- or polycistronic transcripts and only few of them are located in introns (Chanfreau *et al.*, 1997; Chanfreau *et al.*, 1998; Maxwell and Fournier, 1995).

1.2.2.2 Processing snoRNPs

A number of snoRNPs are necessary for the early pre-rRNA cleavages, including U14 and U3 (C/D snoRNAs), snR10 and snR30 (H/ACA snoRNAs), which are

involved in the maturation of 18S rRNA (Dunbar and Baserga, 1998; Hughes and Ares, 1991; Liang and Fournier, 1995; Savino and Gerbi, 1990; Tollervey, 1987; Tollervey and Guthrie, 1985; Venema and Tollervey, 1999). RNase MRP is implicated in the maturation of the 5.8S rRNA by cleaving the pre-rRNA in the internal transcribed spacer 1 (ITS1) at the A3 cleavage site (Chu *et al.*, 1994; Gutmann *et al.*, 2012; Lygerou *et al.*, 1996; Schmitt and Clayton, 1993).

1.2.3 U3 snoRNP

The U3 snoRNP is the most abundant of the snoRNPs, and it is required for processing of pre-rRNA. The role of U3 snoRNA has been studied in mice, *Xenopus laevis* and *Saccharomyces cerevisiae* and these studies demonstrated that the U3 snoRNA is necessary for pre-18S rRNA processing (Borovjagin and Gerbi, 1999; Hughes and Ares, 1991; Kass *et al.*, 1990; Mougey *et al.*, 1993; Savino and Gerbi, 1990). In yeast, the U3 snoRNA consists of two secondary domains (Figure 1.6): a 5' domain (nt 1-39), which is linked via a hinge region to a 3' domain (nt 73 to 3' end) (Mereau *et al.*, 1997; Samarsky and Fournier, 1998). The U3 snoRNA base pairs with the pre-rRNA at three sites. The 5' end of U3 containing sequence elements called GAC box, A' and A box binds to the 18S rRNA, the 5' of the hinge binds to the 5'-ETS of the pre-rRNA and the 3' hinge of U3 binds the 5'-ETS (Beltrame *et al.*, 1994a; Beltrame and Tollervey, 1992, 1995; Dutca *et al.*, 2011; Hughes, 1996; Sharma and Tollervey, 1999; Sharma *et al.*, 1999). According to the group of Baserga (Dutca *et al.*, 2011), this later interaction recruits U3 snoRNA to the pre-rRNA. U3 snoRNA is a component of the SSU processome that is necessary for

endonucleolytic cleavage at sites A0, A1, and A2, which leads to the production of mature 18S rRNA (Beltrame *et al.*, 1994b; Beltrame and Tollervey, 1992, 1995; Dragon *et al.*, 2002; Hughes, 1996; Hughes and Ares, 1991; Sharma and Tollervey, 1999). Defects in cleavage at sites A0, A1, and A2 lead to decreased levels of 18S rRNA. This reduction causes accumulation of the 35S and 23S pre-rRNAs, and a decrease in the levels of the 27SA2 and 20S pre-rRNAs (Venema and Tollervey, 1999). The U3 snoRNA is also involved in the formation of the 5'-end pseudoknot in the 18S rRNA (Henras *et al.*, 2008; Hughes, 1996).

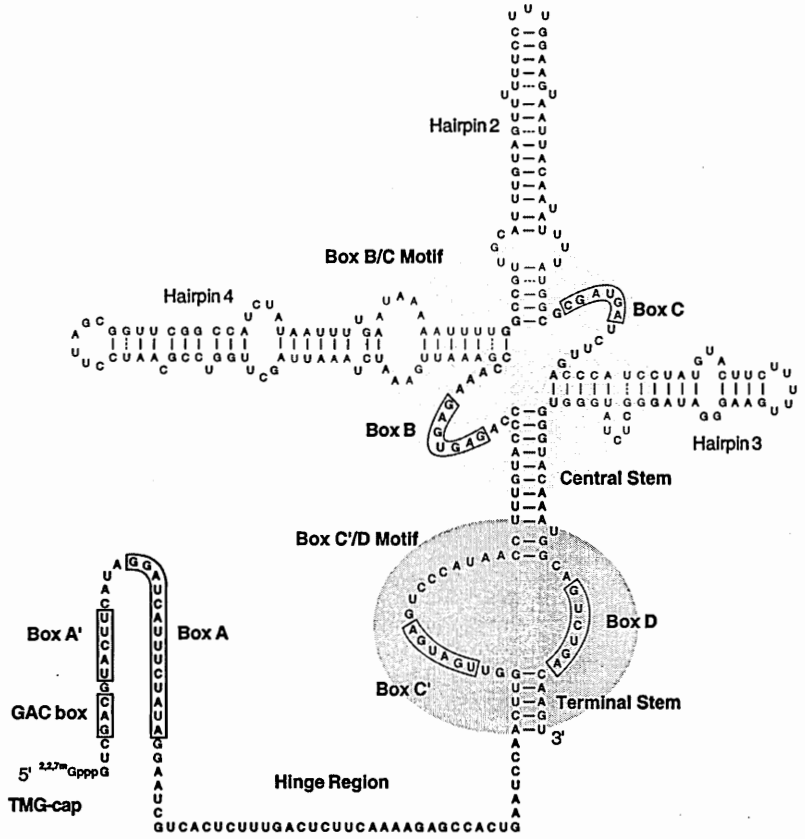

Figure 1.6. Secondary structure of U3 snoRNA from *S. cerevisiae*. The 5' extension consist of conserved boxes A and A' and a non-conserved element, called the GAC box, which is implicated in direct interaction with pre-rRNA and necessary for snoRNA function but not production. The 5' end interacting with pre-rRNA and the 3' extension with RNA binding proteins are linked by a hinge region. The TMG cap protects the 5' and the hinge region from degradation. The box C'/D stem motif is homologous to the box C/D stem motifs in other box C/D snoRNAs. The pairing of the central stem forms the box C'/D stem structure. Boxes B and C probably form a box B/C structure motif serving as a recognition element for a *trans*-acting factor(s). Hairpins 2, 3, and 4 are not essential for U3 accumulation and function. The nucleotides necessary for functional U3 are showed by boldface letters. The putative protein recognition sites are shaded. Taken from Samarsky and Fournier (1998).

1.2.4 U14 snoRNP

U14 is necessary for processing of 18S rRNA in yeast and it is involved in ribose methylation (Kiss-Laszlo *et al.*, 1996; Li and Fournier, 1992). U14 is present in several yeasts, vertebrates and plants (Leader *et al.*, 1994; Maxwell and Fournier, 1995; Zafarullah *et al.*, 1992) and is characterized by four common sequence elements, the C and D boxes, and domains A and B (Jarmolowski *et al.*, 1990) (Figure 1.7). A terminal stem links boxes C and D, and this C/D-helix motif is necessary for processing and accumulation of U14 snoRNA (Balakin *et al.*, 1994; Huang *et al.*, 1992; Watkins *et al.*, 1996). Domains A and B base pair with conserved complementary elements in 18S rRNA (Liang and Fournier, 1995). Domain A is required for processing activity (Jarmolowski et al, 1990). Domain B is dispensable and is involved in the methylation of C414 (Kiss-Laszlo, 1996). Yeast U14 contains a unique structure not found in higher eukaryotes. This structure, called Y domain, is essential for viability (Li and Fournier, 1992). Different studies, like

deletion and substitution variants and hybrid yeast-mouse RNAs, indicated that the Y domain of U14 is essential in *S. cerevisiae* and complete deletion of the Y domain led to lethality (Li and Fournier, 1992; Liang et al, 1997).

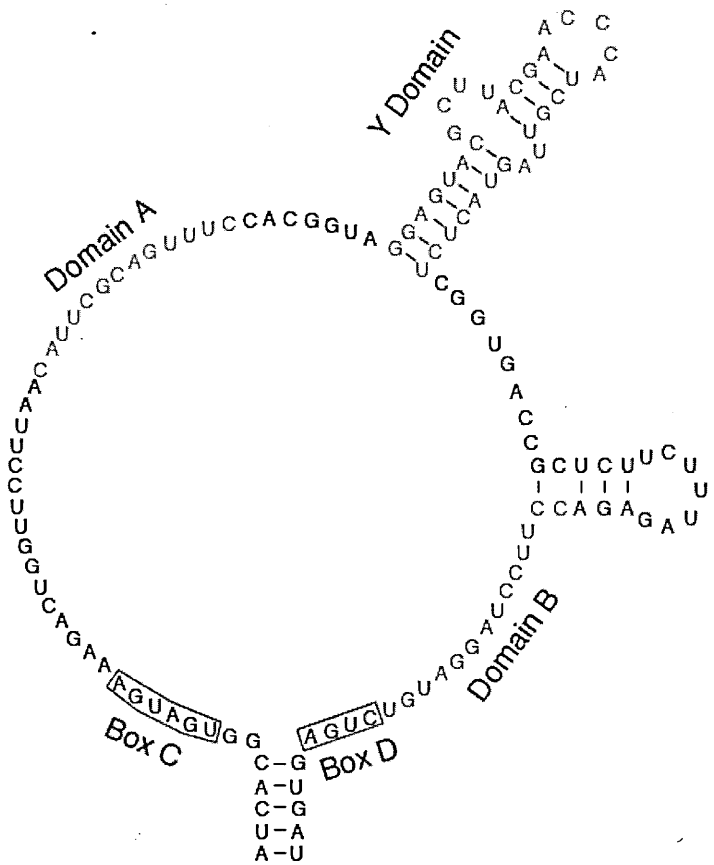

Figure 1.7 Secondary structure of box C/D U14 snoRNA. U14 contains two regions of complementarity to 18S rRNA: domain A (in green) is required for processing activity and cell viability whereas domain B (in blue) targets a methylation site in 18S

rRNA. In yeasts, U14 contains the Y domain (in purple) that is implicated pre-18S rRNA processing. Adapted from Liang et al. (1997).

1.2.5 The small subunit (SSU) processome

The SSU processome is a large ribonucleoprotein complex that sediments at ~80S and is required for pre□18S rRNA processing (Dragon *et al.*, 2002). The SSU processome contains the U3 snoRNA and around 72 different proteins: these proteins include U3-specific proteins, named U three-associated proteins (Utps), ribosome biogenesis factors and ribosomal proteins (Bernstein *et al.*, 2004; Dragon *et al.*, 2002; Lim *et al.*, 2011). This complex also consists of RNA helicases, ATPases and GTPases, endonucleases, kinases and other regulatory factors (Bleichert and Baserga, 2007; Karbstein *et al.*, 2005; Strunk and Karbstein, 2009). The majority of SSU processome components were identified by tandem affinity purification and mass spectrometry, and few of them by biochemical or genetic approaches (Bernstein *et al.*, 2004; Dosil and Bustelo, 2004; Dragon *et al.*, 2002; Krogan *et al.*, 2004; Rudra *et al.*, 2007). Criterias for proteins to be labelled a "SSU processome component" according to the group of Baserga are as follows: a) nucleolar localization, b) 18S rRNA processing defects upon depletion, c) co-immunoprecipitation with U3 snoRNA and/or another SSU processome protein (Lim *et al.*, 2011). The pre-ribosome particle implicated in ribosome biogenesis is called the 90S pre-ribosome. According to Grandi et al. (2002), the characteristics of the 90S components are as

follows: a) nucleolar localization, b) sedimenting at about 90S on a sucrose gradient, c) co-immunoprecipitating with 35S pre-rRNA and U3 snoRNA.

A number of SSU processome components are grouped together and form the following sub-complexes : t-Utp/UtpA, UtpB, UtpC, Mpp10, Bms1/Rcl1 and U3 snoRNP sub-complex (Champion *et al.*, 2008; Dosil and Bustelo, 2004; Freed and Baserga, 2010; Krogan *et al.*, 2004; Lee and Baserga, 1999; Rudra *et al.*, 2007; Wegierski *et al.*, 2001). The U3 snoRNP contains the U3 snoRNA, the four common C/D box snoRNA proteins (see section 2.1.2) and the U3 specific Rrp9/U3-55K protein (Granneman *et al.*, 2002; Venema *et al.*, 2000). Some of these sub-complexes associate with the pre-rRNA in an orderly and stepwise manner (Dutca *et al.*, 2011; Gallagher *et al.*, 2004; Perez-Fernandez *et al.*, 2011; Perez-Fernandez *et al.*, 2007). Thirty one of the 72 SSU processome components were identified as members of the sub-complexes mentioned above. A number of these proteins might associate with the SSU processome individually, and the rest are probably part of unknown sub-complexes yet to be identified, see Figure 1.8.

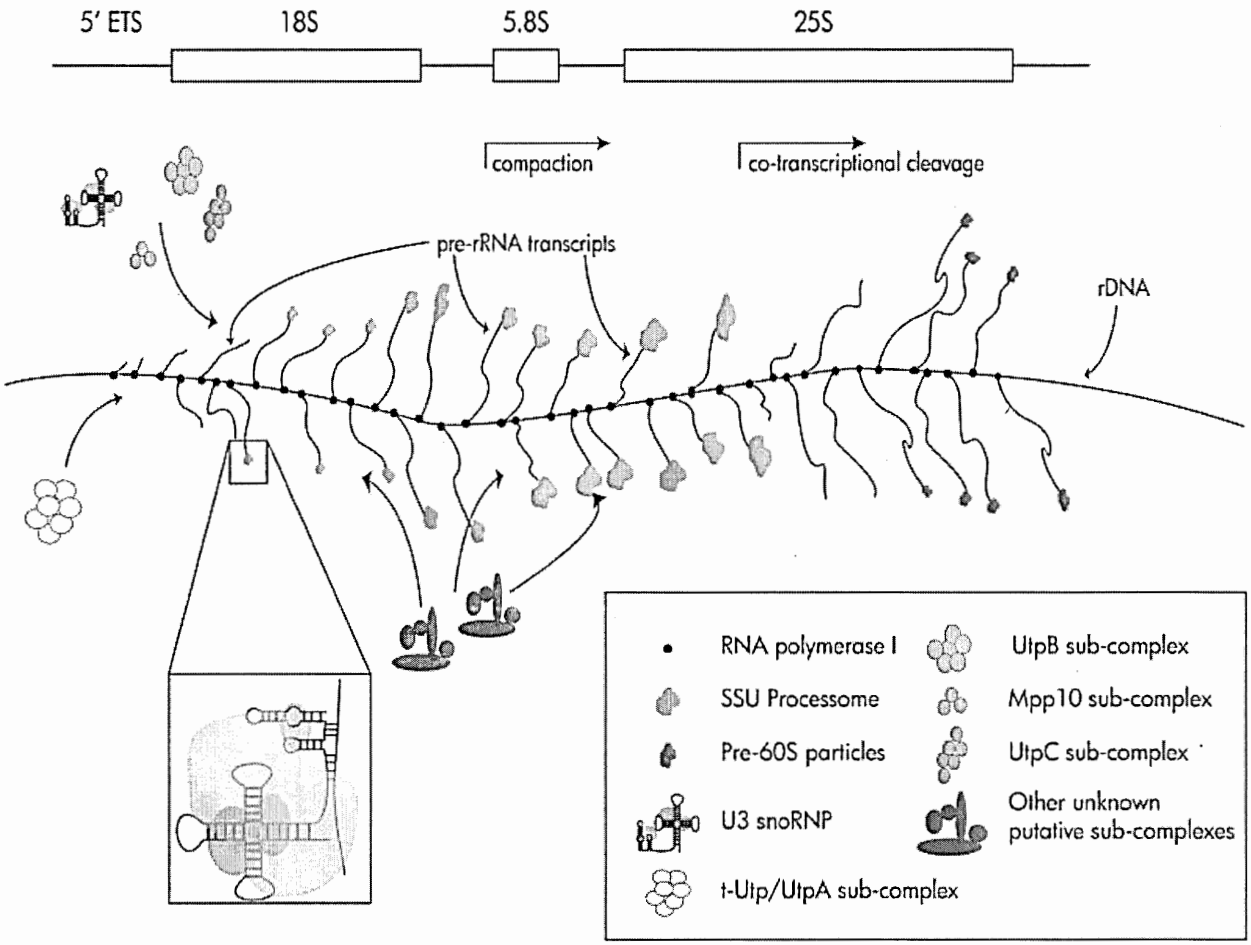

Figure 1.8. Schematic representation of SSU processome assembly. The different sub-complexes assemble onto the nascent transcript in order to form the SSU processome. One rDNA tandem repeat is shown at the top in order to show the relative positions of the 35S pre-rRNA. Taken from (Phipps *et al.*, 2011b)

1.3 Ribosome biogenesis defects, diseases and cancer in humans

Ribosome biogenesis is a very complex and highly regulated process. This process affects cellular metabolism and survival. A series of different genetic diseases related to defects in ribosome biogenesis are called ribosomopathies (Freed *et al.*, 2010; Narla and Ebert, 2010). The following are some examples of these diseases: Mutations in ribosome biogenesis factors of the small and large subunit can cause North American Indian Childhood Cirrhosis, NAIC, (*Cirhin* gene) (Chagnon *et al.*, 2002; Prieto and McStay, 2007) and Shwachman-Bodian-Diamond syndrome (*SBDS* gene) (Boocock *et al.*, 2003; Goobie *et al.*, 2001; Rujkijyanont *et al.*, 2009), respectively. They are both autosomal recessive disorders: NAIC causes neonatal jaundice leading to biliary cirrhosis, and SBDS patients manifest growth problems and skeletal abnormalities. Dyskeratosis congenita (DC) is a X-linked or an autosomal recessive disease caused by mutations in H/ACA snoRNP protein genes (*DKC1, NOP10, NHP2*) (Vulliamy *et al.*, 2008; Walne and Dokal, 2009; Walne *et al.*, 2007; Woolford and Baserga, 2013). The clinical signs of DC are mucocutaneous abnormalities and bone marrow failure. Mutations in the following ribosomal genes *RPS7, RPS17, RPS19, RPS24, RPL5, RPL11, RPL35A, RPS14* cause Diamond-Blackfan anemia, an autosomal dominant disorder. Anemia, bone marrow failure and cardiac defects are among the observed symptoms of this disease.

Changes in nuclear and nucleolar structure are observed in cancer cells (Maggi and Weber, 2005; Montanaro *et al.*, 2008; Ruggero and Pandolfi, 2003). The number of nucleoli, their size and morphology are altered; these phenotypic changes

have been used as diagnostic markers (Jiao *et al.*, 2013; Maggi and Weber, 2005; Ruggero and Pandolfi, 2003). Impaired ribosome biogenesis is also related to changes in cell cycle, cell growth and proliferation, and it could increase the risk of cancer (Montanaro *et al.*, 2008; Ruggero and Pandolfi, 2003). Ribosomal proteins regulate the expression of the p53 tumor suppressor and c-Myc oncogene (Dai and Lu, 2008; Oskarsson and Trumpp, 2005; White, 2005). P53 is a transcription factor that is implicated in cell cycle arrest, DNA damage response, senescence and apoptosis (Lowe *et al.*, 2004; Vogelstein *et al.*, 2000; Vousden and Lane, 2007). MDM2, an E3 ubiquitin ligase, affects p53 activation by either proteasomal degradation or by p53 binding with subsequent inhibition of its transactivation activity (Haupt *et al.*, 1997; Kruse and Gu, 2009; Kubbutat *et al.*, 1997; Momand *et al.*, 1992). Impaired ribosome biogenesis leads to accumulation of non-incorporated ribosomal proteins, which bind MDM2 and inhibit its ubiquitin ligase activity on p53, thus stabilizing p53 (Deisenroth and Zhang, 2010; Fanciulli *et al.*, 2000; Zhang and Lu, 2009). RPL5, RPL11 and RPL23 (ribosomal proteins of the large subunit), and RPS7 (ribosomal protein of the small subunit) bind MDM2 and induce p53 stabilization (Chen *et al.*, 2007; Dai and Lu, 2004; Dai *et al.*, 2004; Zhang *et al.*, 2003; Zhu *et al.*, 2009).

RPL11 also affects c-Myc activity, a transcription factor involved in cell growth, proliferation and apoptosis (Adhikary and Eilers, 2005; Pelengaris *et al.*, 2002a; Pelengaris *et al.*, 2002b). It uses a negative feedback regulation to inhibit c-Myc activity (Dai *et al.*, 2007a; Dai *et al.*, 2007b).

1.4 RNA Helicases

1.4.1 Structure of RNA helicases

Helicases are found in all domains of life: *Bacteria, Archaea* and *Eukaryota*, and many viruses encode them (Anantharaman *et al.*, 2002; Leipe *et al.*, 2002). Impaired function and expression of helicases are related to different diseases, like cancer, neurodegenerative diseases and developmental defects (Abdelhaleem, 2004; Clark *et al.*, 2008; Hanada and Hickson, 2007). The eukaryotic and prokaryotic genomes encode DNA and RNA helicases (Shiratori et al, 1999; Silverman et al, 2003). There are two types of helicases, the ones forming ring-like hexameric structures and the ones not forming rings (Singleton *et al.*, 2007). The classification of these proteins was based on the characteristics of conserved motifs in the primary sequence (Gorbalenya and Koonin, 1993). They are classified into different superfamilies (Savitsky *et al.*), SF1 to SF6 (Gorbalenya and Koonin, 1993; Singleton *et al.*, 2007).

SF1 and SF2 families include DNA and RNA helicases, which function as monomers or dimers (Tuteja and Tuteja, 2004a; Tuteja and Tuteja 2004b). SF3, SF4, SF5 and SF6 consist mainly of hexameric helicases, having bacterial or viral origin (Patel and Picha, 2000). Among the different families of helicases, the DEAD-box family seems to include only RNA helicases (Fairman-Williams *et al.*, 2010).

The crystal structure of SF1 and SF2 helicases show two covalently linked globular domains, each of which usually contains five β-strands surrounded by five α-helices, that resemble the folding of the RecA ATPase (Story and Steitz, 1992). RecA is an allosteric enzyme that uses ATP in order to catalyze strand exchange in homologous sequences in ssDNA and dsDNA. Thus it has both a helicase-like strand separation activity and a strand annealing activity (Story and Steitz, 1992). SF1 and SF2 contain 12 characteristic sequence motifs, (see Figure 1.9) (Fairman-Williams *et al.*, 2010; Gorbalenya and Koonin, 1993; Jankowsky and Fairman, 2007). Helicases possess the conserved Walker A (motif I) and B (motif II) motifs (Walker et al, 1982), which are also found in many NTPases in general.

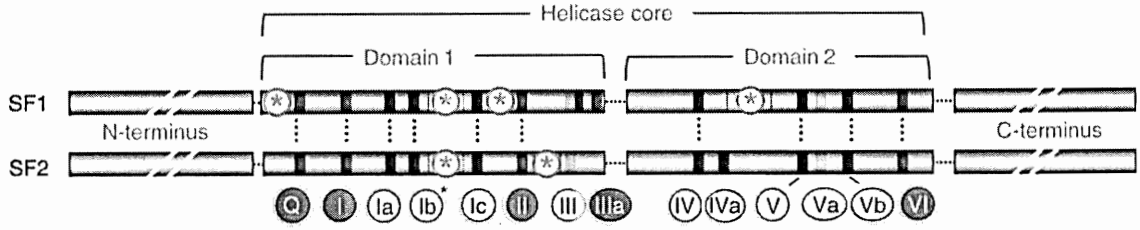

Figure 1.9. The catalytic core of SF1 and SF2 proteins. The motifs are colored based on their biochemical function: red, ATP binding and hydrolysis; yellow, coordination between NTP and nucleic acid binding sites; blue, nucleic acid binding. Motif Ib with asterisk is not present in all SF1 and SF2 families. Green circles with asterisk correspond to insertion of additional domains taken from (Jankowsky, 2011).

The Q motif, which binds the adenine base of ATP is less conserved among SF1 and

SF2 members (Tanner *et al.*, 2003). Motifs III and Va coordinate NTP and nucleic acid binding sites, motifs Ia, Ib, Ic, IV, IVa, V and Vb bind nucleic acids, and motif IIIa in SF1 appears to provide a stacking platform for the base of NTP (Fairman-Williams *et al.*, 2010). In several SF1 and SF2 proteins, the catalytic core is flanked by N- and C-terminal extensions. Many of these extensions have specific functions like nuclease activity, DNA or RNA binding (e.g. Zn-fingers, dsRBDs), and involvement in protein-protein interactions (CARD-domains) (Bernstein and Keck, 2003; Cui *et al.*, 2008; He *et al.*, 2010; Yoneyama and Fujita, 2008; Zhang and Grosse, 2004). Besides providing additional enzymatic activities, these extensions could promote oligomerization, recruit specific complexes, affect interactions with other proteins or influence recognition of specific nucleic acid regions (Karginov *et al.*, 2005; Killoran and Keck, 2008; Klostermeier and Rudolph, 2009; Shereda *et al.*, 2009; Trubetskoy *et al.*, 2009; Yoneyama and Fujita, 2008).

1.4.2 Function of RNA helicases

RNA helicases are enzymes that function in an energy-dependent manner. They dissociate RNA-RNA duplexes (RNA helicase activity or unwindase) or RNA-protein interactions (RNPase activity) by using the free energy of NTP binding and hydrolysis. There are three types of unwinding: translocation on nucleic acids (Lohman *et al.*, 2008; Pyle, 2008; Singleton *et al.*, 2007), translocation without unwinding (Myong *et al.*, 2009; Seidel *et al.*, 2008; Soultanas *et al.*, 2000) and unwinding without translocation (Bizebard *et al.*, 2004; Tijerina *et al.*, 2006; Yang

et al., 2007; Yang and Jankowsky, 2006). RNA binding and unwinding of RNA helicases require NTP-dependent changes in the orientation of the two domains (Jankowsky and Fairman, 2007; Lohman *et al.*, 2008; Pyle, 2008; Singleton *et al.*, 2007). In the absence of ATP, the cleft between two domains opens (Jankowsky and Fairman, 2007); the binding of ATP usually mediates the closure of the two domains (Jankowsky and Fairman, 2007; Lohman *et al.*, 2008; Pyle, 2008; Singleton *et al.*, 2007). In addition to unwinding activity, RNA helicases have other activities. Some RNA helicases are involved in strand annealing or RNA folding (Jankowsky and Fairman, 2007). Many RNA helicases are implicated in specific processes in the cell, (see Figure 1.10).

1.4.3 DEAD-box RNA helicases

According Gorbalenya and Koonin (1993), the DExD/H helicase family is a member of SF2 and is divided to the DEAD-, DEAH-, DExD- and DExH-box families. These families share conserved motifs (Tannner and Linder, 2001; Caruthers and McKay, 2002) and the variations in their conserved motifs make them distinguishable. The DEAD-box family is the largest family and it has twelve conserved motifs that are implicated in ATPase and helicase activity, and in their regulation (Tanner et al, 2003). The conserved motifs of DExD/H helicases are found in a central core region of about 350 to 400 amino acids (Tanner and Linder, 2001; Caruthers and McKay, 2002). The N- and C-terminal extensions that flank the conserved core are extremely variable in size and composition.

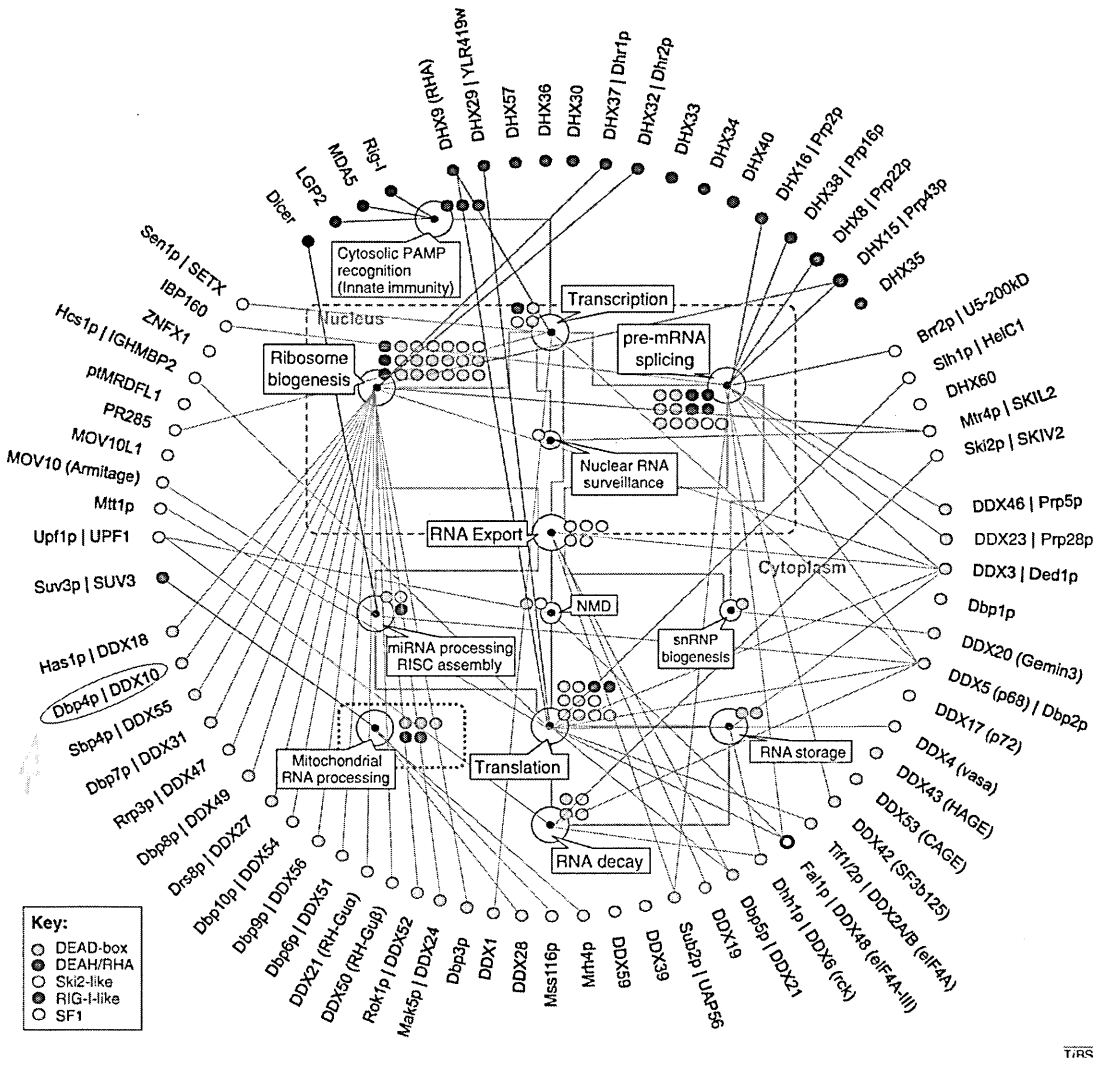

Figure 1.10. Different functions of RNA helicases in eukaryotic cells. The processes of RNA metabolism are indicated by white circles. The connection between processes are shown by grey lines. Yeast RNA helicases and their human orthologs are color-coded based on their families (see legend left corner side). Dbp4 and its human ortholog DDX10 is shown with a pink arrow. Adapted from Jankowsky 2011.

DEAD-box proteins are found in all eukaryotes and most prokaryotes (Aubourg et al, 1999; de la Cruz et al, 1999; Rocak and Linder, 2004). They were identified in the 1980s after alignments were done with eight homologues of yeast translation initiation factor eIF4A, which showed the presence of several conserved motifs (Linder *et al.*, 1989). The name of the family was derived from the amino acid sequence D-E-A-D (Asp-Glu-Ala-Asp) of motif II. Since then, a large number of DEAD-box proteins have been identified, and RNA helicases from DEAD-box and related families were shown to be very important components of living organisms (Silverman et al, 2003).

The N-terminal portion of the core (domain 1) consists of the ATP binding motifs I (Walker A), II (Walker B), the ATP hydrolysis motif III and the RNA binding motifs Ia and Ib. The C-terminal portion of the core (domain 2) includes the RNA binding motifs IV and V and motif VI, which may coordinate the ATPase and unwinding activities. The Q motif, which is an ATP binding motif (Tanner, 2003) and a conserved upstream aromatic residue are specific to DEAD-box proteins. The ATPase activity of DEAD-box proteins is dependent on or stimulated by RNA. The ATPase activity usually doesn't necessitate a specific RNA substrate *in vitro* (Rocak and Linder, 2004). Many studies showed a cooperativity between RNA binding and ATP binding: in the presence of ATP, RNA binding is stronger, but it is severely decreased upon binding of ADP (Cordin *et al.*, 2004; Lorsch and Herschlag, 1998; Peck and Herschlag, 2003). A more recent study revealed that no conformational

change in the helicase core is observed when ADP, ATP or RNA binds alone but the simultaneous binding of ATP and RNA induces a conformational change (Theissen *et al.*, 2008). DEAD-box proteins are involved in bidirectional unwinding (5' to 3' and 3' to 5' unwinding), thus they show no unwinding polarity (Bizebard *et al.*, 2004; Jankowsky, 2011; Jarmoskaite and Russell, 2011; Pyle, 2008; Rogers *et al.*, 1999; Tijerina *et al.*, 2006; Yang and Jankowsky, 2006). The DEAD-box protein loads directly onto the duplex and unwinds it in an ATP-dependent manner, which is called local strand separation (Yang *et al.*, 2007; Yang and Jankowsky, 2006).

Furthermore the DEAD-box protein Ded1 shows an RNPase activity (Fairman *et al.*, 2004): It displaces an RNA-bound protein complex, called the exon junction complex (EJC), in an ATP-dependent manner, and independently from the RNA structure.

DEAD-box proteins are involved in all processes involving RNA including transcription, mRNA splicing, tRNA maturation, ribosome biogenesis, nuclear-cytoplasmic export, translation, mitochondrian gene expression to RNA degradation (de la Cruz *et al.*, 1999). There are at least 37 DEAD-box proteins in humans and 26 in *Saccharomyces cerevisiae* (Fairman-Williams *et al.*, 2010). In yeast, 20 DEAD-box proteins are required for ribosome biogenesis and rRNA maturation (Bleichert and Baserga, 2007; Jankowsky *et al.*, 2011; Rodriguez-Galan *et al.*, 2013).

1.4.3.1 Dbp4 (DEAD-box protein 4)

DEAD-box protein Dbp4, a nucleolar RNA helicase, is phylogenetically conserved

and essential for growth in yeast, indicating that it plays a critical function in the cell (Garcia *et al.*, 2012; Garcia and Uhlenbeck, 2008; Huh *et al.*, 2003; Liang *et al.*, 1997). Dbp4 was identified in a multicopy suppressor screen carried out to isolate factors that interact with the Y domain of U14 snoRNA. Over-expression of Dbp4 suppressed growth defects caused by mutations in the Y domain (Liang *et al.*, 1997). This genetic link suggested a role for Dbp4 in ribosome biogenesis because the U14 snoRNA is involved in processing reactions leading to the production of 18S rRNA. Another study showed that the absence of Dbp4 impaired the early cleavages at sites A0, A1 and A2, and that Dbp4 was necessary for the release of U14 from the pre-rRNA, therefore suggesting that Dbp4 plays a specific role in intramolecular RNA or RNA-protein interactions (Kos and Tollervey, 2005). The ATPase activity of Dbp4 is RNA-dependent but with no specificity for yeast rRNA (Garcia and Uhlenbeck, 2008). The unwinding activity of Dbp4 was shown by the group of Uhlenbeck, and 5' or 3' single-stranded extensions increased its unwinding activity (Garcia *et al.*, 2012).

1.4.3.2 RNA helicase DDX10

DEAD-box RNA helicase DDX10 is the human homologue of yeast Dbp4. It was identified among candidate genes for ataxia-telangiatasia, a genetic disorder, located on chromosome 11q22-q23 (Savitsky *et al.*, 1996). The chromosome translocation, inv(11)(p15q22), which involves *DDX10* (11q22) and *NUP98* (11p15), a member of the nucleoporin family, leads to the production of a chimeric NUP98-DDX10 protein

implicated in therapy-related myeloid malignancies (Arai *et al.*, 1997). There is a considerable increase in proliferation and self-renewal of primary human CD34+ cells when NUP98-DDX10 is present (Yassin *et al.*, 2010). Mutation in motif VI in the DDX10 portion of NUP98-DDX10 decreases the *in vitro* transforming ability of this fusion protein showing that it plays a role in leukemogenesis (Yassin *et al.*, 2010). DDX10 was also identified as a candidate breast cancer gene (Sjoblom *et al.*, 2006). The group of Sjoblom recently showed that knock down of DDX10 inhibited breast cancer cell growth (Jiao *et al.*, 2013). Another study showed that RNA helicase DDX10 is involved in ribosome biogenesis (Tafforeau *et al.*, 2013). DDX10 is associated with a 50S complex including the U3 snoRNA, which is probably recruited to the pre-rRNA via binding nucleolin and RRP5, both of which are RNA-binding proteins (Turner *et al.*, 2009).

1.5 Hypotheses

Ribosome biogenesis engages by far the largest number of RNA helicases, most of which are members of the DEAD-box family. DEAD-box RNA helicase Dbp4 is phylogenetically conserved and essential for growth. DEAD-box RNA helicase DDX10 is the human homologue of Dbp4. Due to the complexity of ribosome biogenesis, little is known about the specific function of these helicases *in vivo* and the discrete pre-rRNA processing steps in which these helicases might function.

Hypothesis 1: Overexpression of Dbp4 suppresses phenotypes of mutant U14 snoRNA showing a genetic link between Dbp4 and U14 snoRNA. Thus, there might be a physical link between these two molecules. In addition, U14 snoRNA is involved in rRNA maturation and it required for cleavages at sites A1 and A2 but not A0. This suggests that Dbp4 might also be implicated in ribosome biogenesis.

Hypothesis 2: Dbp4 has a predicted coiled-coil (CC) motif in its C-terminal extension. This suggests that Dbp4 might function in a complex with one or more proteins to perform its role in ribosome biogenesis.

Hypothesis 3: The proteins and RNAs of the ribosome, and the factors involved in ribosome biogenesis are very well conserved from yeast to humans, and the pre-rRNA processing and assembly pathways appear to be similar. Dbp4 is implicated in

the processing reactions leading to the production of the mature 18S rRNA. This suggests that DDX10, the human homologue of Dbp4, could also be involved in ribosome biogenesis. DDX10 was identified as a candidate breast cancer gene (Sjoblom *et al.*, 2006), suggesting that DDX10 probably plays a role in cellular growth and proliferation.

1.6 Objectives

In order to answer my first hypothesis, the physical interaction between Dbp4 and U14 snoRNA was studied by IPs, and the function of Dbp4 in molecular mechanisms and interactions leading to the production of 18S rRNA was studied by sucrose gradient sedimentation analyses.

To test my second hypothesis, we attempted to identify partners of Dbp4. Potential partners of Dbp4 from a yeast two-hybrid screen and database mining were selected and their *in vivo* association was examined by IPs and GST pull-down.

To verify my third hypothesis, the possible role of DDX10 in pre-rRNA processing was evaluated, and the effect of DDX10 knock down during rRNA maturation and also on cellular growth and proliferation was examined by northern hybridization, FACS and western blot analyses using Ki-67 proliferation marker.

Chapter II

2.1 Preface

The U14 snoRNA is required for the processing reactions at cleavage sites A1 and A2 but it is also involved in ribose methylation (C414 in 18S rRNA). Dbp4 was found in a screen carried out to find interactors of the yeast-specific Y domain of U14. Overexpression Dbp4 suppressed the Y domain mutant phenotypes. Because of this genetic link between Dbp4 and U14, we decided to investigate the physical link between these two molecules. We did immunoprecipitations experiments (IP) followed by 3'-end labeling, which suggested that Dbp4 might be associated with U3 snoRNA and not U14 snoRNA. We confirmed these results by nothern hybridization using specific probes against the snoRNAs of interest. Different conditional strains were generated to perform sucrose gradient analyses in order to study the sedimentation behavior of Dbp4, U3, U14, Mpp10 (U3-specific protein) and some guide snoRNAs in the presence or absence of one of these molecules. In collaboration with the group of Dr. Ann Beyer, chromatin spread preparations were carried out in undepleted and Dbp4-depleted cells showing that Dbp4 is necessary for the SSU processome formation.

I did the major part of all the experiments under the supervision of Dr. François Dragon, the 3'-end labeling was done by Krasimir Spasov, Figure 3 was done by Christian Trahan, and the electron microscopy images, maps and gene tracing of the chromatin spread preparations were performed by Yvone Osheim and Ann Beyer.

DEAD-box RNA helicase Dbp4 is required for SSU processome formation and function

Sahar Soltanieh[1,*], Yvonne N. Osheim[2], Krasimir Spasov[1,*], Christian Trahan[1,*], Ann L. Beyer[2], and François Dragon[1]#

Molecular and Cellular Biology 2015, vol. 35, no. 5, pp. 816-830

doi: 10.1128/MCB.01348-14

[1] Département des sciences biologiques and Centre de recherche BioMed, Université du Québec à Montréal, C.P. 8888 Succursale Centre-ville, Montréal (Québec), Canada H3C 3P8

[2] Department of Microbiology, Immunology and Cancer Biology, University of Virginia Health System, Charlottesville VA 22908-0734, U.S.A.

Footnote:

* Present address: S. Soltanieh and C. Trahan, Institut de recherches cliniques de Montréal, Montréal (Québec), Canada H2W 1R7; K. Spasov, Department of Pharmacology, Yale University School of Medicine, New Haven, CT 06520-8066, U.S.A.

Corresponding author: dragon.francois@uqam.ca

2.2 Abstract

DEAD-box RNA helicase Dbp4 is required for 18S rRNA synthesis: cellular depletion of Dbp4 impairs the early cleavage reactions of the pre-rRNA, and causes the U14 small nucleolar (sno) RNA to remain associated with pre-rRNA. Immunoprecipitation experiments (IPs) carried out with whole cell extracts (WCEs) revealed that HA-tagged Dbp4 is associated with U3 snoRNA but not with U14 snoRNA. IPs with WCEs also showed association with the U3-specific protein Mpp10, which suggests that Dbp4 interacts with the functionally active U3 RNP; this particle, called the SSU processome, can be observed at the 5' end of nascent pre-rRNA. Electron microscopy analyses indicated that depletion of Dbp4 compromised SSU processome formation and co-transcriptional cleavage of the pre-rRNA. Sucrose density gradient analyses revealed that depletion of U3 snoRNA or Mpp10 protein inhibited the release of U14 snoRNA from pre-rRNA, just as seen with Dbp4-depleted cells, indicating that alteration of SSU processome components has significant consequences on U14 snoRNA dynamics. We also found that the C-terminal extension flanking the catalytic core of Dbp4 plays an important role in the release of U14 snoRNA from pre-rRNA.

2.3 Introduction

Ribosome biogenesis in the nucleolus of eukaryotic cells begins with transcription of large rRNA precursors (pre-rRNAs), which are matured and assembled into the small (40S) and large (60S) ribosomal subunits. It is well established that a key step in the making of ribosomes is the production of mature rRNAs, the functional components of ribosomes (Venema and Tollervey, 1999; Moore and Steitz, 2002).

In yeast, RNA polymerase I synthesizes a long precursor of 35S that encodes the 18S, 5.8S and 25S rRNAs, while the 5S rRNA is independently transcribed by RNA polymerase III (Venema and Tollervey, 1999; Kressler *et al.*, 1999). The 35S pre-rRNA is subjected to an orderly maturation process that requires over 200 *trans*-acting factors (Fromont-Racine *et al.*, 2003; Henras *et al.*, 2008; Kressler *et al.*, 2010). In addition, tens of small nucleolar (sno) RNAs base pair with pre-rRNAs and direct site-specific post-transcriptional modification of rRNAs (Henras *et al.*, 2004). The snoRNAs are grouped in two large families, called C/D and H/ACA, and they assemble into RNPs with specific proteins to carry out 2'-*O*-ribose methylation and pseudouridylation, the conversion of uridines into pseudouridines (Ψ), respectively (Kiss, 2001; Decatur and Fournier, 2003; Henras *et al.*, 2004).

In contrast to the plethora of snoRNAs guiding post-transcriptional modifications, very few snoRNAs are required for the endonucleolytic cleavages that remove spacer sequences from pre-rRNAs. U3, U14 and snR30 snoRNAs are essential for the early cleavage reactions that lead to the production of 18S rRNA;

snR10 is also implicated in these cleavages but it is not essential for growth (Maxwell and Fournier, 1995;(Venema and Tollervey, 1999; King *et al.*, 2003; Liang *et al.*, 2010). U3 (C/D class) and snR30 (H/ACA class) are involved in the three early processing reactions, i.e. the cleavages at sites A0, A1 and A2 (for details on the processing pathway see (Woolford and Baserga, 2013). U14 and snR10 are unique in that they have dual functions: they are involved in pre-rRNA processing at sites A1 and A2 but not at A0, and U14 targets 2'-*O*-methylation of C414 in 18S rRNA while snR10 directs formation of Ψ2923 in 25S rRNA (Piekna-Przybylska *et al.*, 2007). Another essential snoRNA is RRP2, the RNA component of RNase MRP; this RNA does not belong to the C/D or H/ACA class but it is required for cleavage at site A3 and production of $5.8S_S$ rRNA (Venema and Tollervey, 1999; Woolford and Baserga, 2013).

The small subunit (SSU) processome is a very large RNP of ~80S that forms the terminal knob observed at the 5'-end of nascent pre-rRNA transcripts (Dragon *et al.*, 2002; Osheim *et al.*, 2004). The SSU processome is constituted of the U3 snoRNA and over 70 proteins, most of which are U3-specific and required for its function (Dragon *et al.*, 2002 ; Bernstein *et al.*, 2004; Phipps *et al.*, 2011a; Lim *et al.*, 2011; Perez-Fernandez *et al.*, 2011; Woolford and Baserga, 2013). At present it is not known whether U14 snoRNP contains specific proteins required for its function. Yeast U14 snoRNA has an extra stem-loop structure called the Y domain, which is essential for growth (Maxwell and Fournier, 1995). In a search for protein(s) that

interact with the Y domain, Liang et al. (Liang *et al.*, 1997) identified Dbp4 in a multi-copy suppressor screen; growth defects caused by deleterious mutations in the Y domain of U14 could be suppressed by over-expression of Dbp4, a phylogenetically conserved DEAD-box RNA helicase (Liang *et al.*, 1997; Garcia *et al.*, 2012).

RNA helicases are viewed as molecular motors that rearrange RNA structures or RNA-protein complexes in an energy-dependent fashion (Jankowsky, 2011). These enzymes are characterized by signature motifs that form a central, catalytic domain of about 400 amino acids. The catalytic core is flanked by N- and C-terminal extensions that vary in length and amino acid composition; these regions are thought to be important for substrate recognition and function of individual helicases, (Silverman *et al.*, 2003; Cordin *et al.*, 2006). Of the 45 putative RNA helicases identified in yeast (de la Cruz *et al.*, 1999), 20 are required for ribosome biogenesis (Bleichert and Baserga, 2007; Rodriguez-Galan *et al.*, 2013): this reflects the complexity of RNA-RNA and RNA-protein rearrangements that are needed for the production of functional ribosomes.

DEAD-box RNA helicase Dbp4 is essential for viability, indicating that its function cannot be complemented by another helicase (Liang *et al.*, 1997). A role for Dbp4 in ribosome biogenesis was demonstrated by Kos and Tollervey (Kos and Tollervey, 2005): they showed that depletion of Dbp4 impaired early cleavage reactions at sites A0, A1 and A2 of the pre-rRNA, a phenotype that is normally seen with cells depleted of the U3 snoRNA or U3-specific proteins (Granneman and

Baserga, 2004). Cellular depletion of Dbp4 also impaired the release of U14 snoRNA from pre-rRNA, suggesting that Dbp4 is the RNA helicase that unwinds the U14 snoRNA:pre-rRNA duplex (Kos and Tollervey, 2005). We recently showed that Dbp4 is associated with U14 snoRNA in a complex that sediments at about 50S in sucrose density gradients (Soltanieh *et al.*, 2014). The human homologue of Dpb4 is also present in a complex of 50S but it is associated with the U3 snoRNA and not with U14 (Turner *et al.*, 2009), indicating that the Dbp4 complex of 50S is different in yeast and humans (Soltanieh *et al.*, 2014).

Here we report that Dbp4 is associated with the U3 snoRNA and the U3-specific protein Mpp10, which are components of the SSU processome. Electron microscopy analyses of chromatin spreads indicated that cellular depletion of Dbp4 inhibited SSU processome formation. We also show that trapping of U14 snoRNA on pre-rRNA is observed not only in Dbp4-depleted cells but also upon depletion of the U3 snoRNA or Mpp10 protein. Moreover, we found that the C-terminal extension of Dbp4 plays an important role in the release of U14 snoRNA from high molecular weight complexes, and that it is necessary for its association with U14 in the 50S complex.

2.4 Materials and Methods

2.4.1Yeast strains and media

Yeast strains used in this study are listed in Table 1. Strains were usually grown in rich YP medium (1% yeast extract, 2% peptone) supplemented with either 2%

dextrose (YPD) or 2% galactose (YPGal). For selection of auxotrophic markers, cells were grown in synthetic medium (0.17% yeast nitrogen base) supplemented with the appropriate dropout mix (Clontech) and 2% galactose or glucose, as required. Media in culture plates included 2% bacto-agar. Yeast strains expressing HA-tagged proteins were generated as described by (Knop *et al.*, 1999) using appropriate oligonucleotides (sequences of oligonucleotides are available on request): cells were plated on non-selective YPD or YPGal agar plates, as required, and then replica plated onto selective agar plates containing 200 μg/ml geneticin (Gibco). Strain DBP4-HA was further engineered into a depletion strain by replacing its promoter with the inducible *GAL1* promoter as described by Longtine et al. (Longtine *et al.*, 1998). Depletion strain GAL::DBP4-HA was used for complementation assays with constructs that were constitutively expressed from the single copy plasmid pCM188 (Gari *et al.*, 1997). Plasmid-borne Dbp4 contained a myc tag at its C-terminus.

2.4.2 Immunoprecipitations

Immunoprecipitation experiments (IPs) with WCEs were done essentially as described previously (Dragon *et al.*, 2002). For each IP, four mg of protein A-Sepharose CL-4B (GE Healthcare) were first saturated with mouse monoclonal anti-HA antibody (12CA5): binding was carried out overnight on a nutator at 4°C in TMN100 buffer (25 mM Tris-HCl, pH 7.6, 10 mM $MgCl_2$, 100 mM NaCl, 0.1% Nonidet P-40, 1mM DTT). The "HA beads" were then washed three times with 1 ml TMN100 and subsequently incubated with 500 μl of WCE on a nutator at 4°C for 1

hour. WCEs were prepared from exponentially growing cells (A_{600} = 0.5-0.7), and the equivalent of 5 A_{600} units of cells were used for each IP. Cells were disrupted with glass beads (Sigma) in TMN100 buffer containing Complete™ Protease Inhibitor Cocktail (Roche). After vigorous vortexing (seven times for 45 sec with intervals of 45 sec on ice), lysates were cleared by centrifugation at 4°C in a microcentrifuge (5 min at 18,000×g). After incubation, the beads were washed 5 times with 1 ml TMN100, TMN200 or TMN400 respectively (the numbers indicate the concentration of NaCl in mM). IPs with complexes isolated from sucrose gradient fractions were carried out as described in (Soltanieh *et al.*, 2014). Co-immunoprecipitated RNAs were recovered by phenol/chloroform extraction, followed by ethanol precipitation in the presence of 40 µg glycogen (Roche). For protein analyses, the beads were mixed with 2× SDS loading buffer and the proteins were eluted by incubation at 90°C for 5 min.

2.4.3 3'-end labeling of RNAs

Labeling of RNAs at their 3'-end was done essentially as described previously (Dragon *et al.*, 2000). RNAs were mixed with T4 RNA ligase reaction buffer (50 mM HEPES, pH 8.3, 10 mM $MgCl_2$, 50 µM ATP, 3.3 mM DTT, 10% (v/v) DMSO, 40 units RNasin (Promega) 10 µCi [5'-^{32}P]pCp and 20 units T4 RNA ligase (New England Biolabs). The reaction mixture (30 µl) was incubated at 4°C for 16 hours, and an equal volume of Stop Solution (USB) was added to the reaction. Samples

were heat-denatured for 3 min at 90°C and immediately put on ice. Aliquots of 6 µl were separated on 8% polyacrylamide sequencing gels.

2.4.4 Northern blotting

Small RNAs recovered from IPs or sucrose gradient fractions were extracted with phenol-chloroform, precipitated with ethanol, separated on a denaturing polyacrylamide (8%) gel, transferred onto a nylon membrane, cross-linked under UV light, and hybridized with specific 5'-end labeled antisense oligonucleotides (sequences are available on request; (Soltanieh *et al.*, 2014)). Hybridization was done for 16 hours at 37°C. Following two washes in 5× SSPE containing 0.1% SDS and one wash in 0.5× SSPE containing 0.1% SDS, the membranes were exposed to a phosphor screen and analyzed with a Molecular Imager F/X (Bio-Rad).

2.4.5 Western blotting

Proteins recovered after immunoprecipitations or from the sucrose gradient fractions were separated by SDS-PAGE and transferred onto a PVDV membrane (Immobilon-P, Millipore). The blots were incubated for 1 hour with one of the following primary antibodies: mouse monoclonal 12CA5 anti-HA antibody, mouse monoclonal 9E10 anti-myc antibody, rabbit polyclonal anti-Mpp10 antibodies (Dunbar *et al.*, 1997), rabbit polyclonal anti-Tsr1 antibodies (Strunk *et al.*, 2012), rabbit polyclonal anti-Rpl3 and anti-Rpl30 antibodies. Note that anti-Rpl30 (formerly L32) also recognize

Rps2 (formerly S4; (Vilardell and Warner, 1997)). After three washes, the blots were incubated with the appropriate HRP-conjugated secondary antibodies (GE Healthcare) following the manufacturer's recommendations. The blots were washed and revealed using the ECL-Plus Western Blotting Detection System (GE Healthcare).

2.4.6 Sucrose density gradient analyses

Prior to harvesting cells, cultures were incubated with cycloheximide (100 µg/ml; Sigma), and cycloheximide was maintained in all following steps. Cells (30 A_{600} units) were harvested by centrifugation, washed with cold water, and resuspended in 0.5 ml of TMK100 buffer (same as TMN100 but KCl was substituted for NaCl) containing Complete™ Protease Inhibitor Cocktail (Roche) and cycloheximide. Cellular extracts were prepared with glass beads (Sigma) by vigorous vortexing (seven times for 45 sec with intervals of 45 sec on ice), and lysates were cleared by centrifugation at 4°C in a microcentrifuge (5 min at 2,500×g). Fifteen A_{260} units of extract were loaded onto 7-47% (w/v) linear sucrose gradients prepared in TMK100. The gradients were spun in a SW41 rotor at 39000 rpm for 165 min. Fractions were collected using an ISCO density gradient fractionator equipped with a UA-6 detector with constant monitoring of the absorbance at 254 nm to follow the presence of 40S and 60S ribosomal subunits, 80S ribosomes and polysomes. Each fraction was separated in two aliquots: an aliquot of 200 µl was used for RNA analyses by

northern hybridization (see above), and 300 µl were subjected to TCA precipitation before analyzing proteins by western blotting.

2.4.7 Cellular depletion of individual components

Conditional strains were first grown to exponential phase ($A_{600} \approx 0.5$) at 30°C in liquid YPGal medium and then transferred into pre-warmed YPD medium. When required, cultures were diluted with pre-warmed YPD to maintain exponential growth. Cellular growth was monitored at different time points by measuring the A_{600}.

2.4.8 Electron microscopy

Miller spreads were performed as described in (Osheim *et al.*, 2004). Briefly, 1 ml of the appropriate yeast culture was added to 5 mg zymolyase for 4 min, centrifuged briefly and the pellet was resuspended in 1 ml 0.025% Triton, pH 9.2. After thorough mixing, the solution was added to 6 ml 11 mM KCl, pH 7, and allowed to disperse for about 40 minutes with swirling. One-tenth volume of 0.1 M sucrose, 10% formalin, pH 8.65, was added and grids were made 15 min later.

2.5 Results

2.5.1 Dbp4 specifically associates with the U3 snoRNA

Deleterious mutations in the Y domain of U14 snoRNA can be suppressed by over-expression of DEAD-box protein Dbp4 (Liang *et al.*, 1997). To examine the possible association of Dbp4 with U14 snoRNA, we carried out immunoprecipitation experiments (IPs) with cellular extracts prepared from yeast strain DBP4-HA, a derivative of YPH499 (Sikorski and Hieter, 1989). DBP4-HA expresses Dbp4 with a triple HA epitope at its C-terminus (hereafter named Dbp4-HA); it is important to mention that in this strain, Dbp4-HA is not over-expressed because transcription is under the control of its endogenous promoter (Knop *et al.*, 1999). No growth defects were observed with strain DBP4-HA, indicating that the triple HA tag at the C-terminus of Dbp4 did not affect its essential function (data not shown).

We conducted IPs with cellular extracts prepared from the DBP4-HA strain and other control strains, and we analyzed the co-immunoprecipitated RNAs. The immunoprecipitates were washed with increasing salt concentrations to assess the stability of complexes. In a first series of experiments, RNAs that co-immunoprecipitated with Dbp4-HA were directly labeled at their 3'-end with [5'-^{32}P]pCp and separated on a sequencing gel. These experiments revealed a faint band of about 330 nucleotides (nt) that progressively disappeared with increasing salt concentrations (Figure 1A, lanes 3-5). This band co-migrated with the U3 snoRNA, which gave a very strong signal in control IPs with HA-tagged Nop1, a protein

common to all C/D snoRNPs (Henras *et al.*, 2004); Figure 1A, lanes 7-9). In marked contrast with the Nop1-HA IPs, no band corresponding to U14 snoRNA (126 nt) was detected in the Dbp4-HA immunoprecipitates (compare lanes 3-5 with 7-9 in Figure 1A). Note that tRNAs, 5S rRNA and 5.8S rRNA were also detected in these experiments but those RNAs are known as sticky, non-specific contaminants (see (Dunbar *et al.*, 1997; Dragon *et al.*, 2002; Lemay *et al.*, 2011)). To identify the RNAs that co-immunoprecipitated with Dbp4 we carried out northern hybridization analyses with ^{32}P-labeled oligonucleotides. These experiments showed that HA-tagged Dbp4 is specifically associated with the U3 snoRNA (Figure 2.1B). The signal for U3 decreased with increasing salt concentrations, showing that the association of Dbp4 with U3 was salt-sensitive, in contrast with the U3-Nop1 association (compare lanes 8-10 and 13-15 in Figure 2.1B). Control experiments with the untagged parental strain did not reveal the presence of U3 in immunoprecipitates (Figure 2.1B, lanes 3-5), ruling out the possibility that the faint U3 band observed in Dbp4-HA IPs resulted from a non-specific interaction.

2.5.2 Dbp4 interacts with the SSU processome, the active U3 particle

U3 is a dynamic RNP that can be detected in alternative states of ~12-15S and ~80S; the larger form is the functionally active U3 RNP and is coined the SSU processome (Fabrizio *et al.*, 1994; Billy *et al.*, 2000; Dragon *et al.*, 2002). Being an RNA helicase, Dbp4 could be required for assembly of the U3 RNP at an early (~12-15S) or late stage (~80S). To assess this latter possibility we asked whether Dbp4 co-

immunoprecipitated with the U3-specific protein Mpp10, which is an integral constituent of the SSU processome (Dunbar *et al.*, 1997; Dragon *et al.*, 2002; Osheim *et al.*, 2004). Western blotting analyses indicated that Dbp4 was associated with Mpp10, and that this association was salt-sensitive (Figure 2.2A, lanes 10-12). The co-IP of Mpp10 with Dbp4-HA was much less efficient than with the core component Nop1-HA (compare lanes 6-8 and 10-12 in Figure 2.2A), but the signal was well above background levels (compare lanes 2-4 and 10-12 in Figure 2.2A), indicating that co-IP of Mpp10 with Dbp4 was specific and not due to fortuitous interactions. Sucrose gradient sedimentation analyses indicated that Dbp4-HA was enriched in the lower density fractions of the gradient, forming a peak at 40-50S, as observed by (Soltanieh *et al.*, 2014), and that a very small portion of Dbp4-HA co-sedimented with Mpp10 and the U3 snoRNA in the 80S region of the gradient (Figure 2.2B). These results are consistent with IPs showing that only a fraction of the U3 snoRNA and Mpp10 co-immunoprecipitated with Dbp4-HA (Figures 2.1B and 2A). We recently proposed that Dbp4 is a SSU processome component (Soltanieh *et al.*, 2014); here we showed that association of Dbp4 with the SSU processome is not stable, which could reflect the transient nature of the interaction between RNA helicase Dbp4 and the SSU processome.

2.5.3 Loss of Dbp4 alters the sedimentation of snoRNPs

We generated the conditional strain GAL::DBP4-HA that expresses Dbp4-HA under the control of the *GAL1* promoter (Longtine *et al.*, 1998). This promoter is active in

galactose-containing medium (YPGal) but is turned off when cells are grown in the presence of glucose (dextrose; YPD). We found that the growth rate of strain GAL::DBP4-HA was identical to that of the parental strain DBP4-HA and wild-type strain YPH499 when cells were grown in YPGal (data not shown). When exponentially growing cells were shifted from YPGal to YPD, growth of strain GAL::DBP4-HA began to slow down within 3-4 hours after the shift to YPD, whereas strains DBP4-HA and YPH499 maintained exponential growth rates (Figure 2.3A).

To avoid possible secondary effects caused by the depletion of Dbp4, we chose to analyze cellular extracts prepared at early time points after the shift to YPD. Cells were harvested at 4 and 6 h following the shift to YPD (indicated by arrows in Figure 2.3A), and cellular extracts were analyzed by ultracentrifugation through sucrose density gradients. Continuous monitoring of the absorbance at 254 nm during gradient fractionation generated a sedimentation profile of ribosomal particles (40S and 60S ribosomal subunits, 80S ribosomes, and polysomes). For comparison, extracts were prepared from non-depleted, exponentially growing cells (0 h in YPD) and were analyzed in parallel. Note that the 60S peak was less pronounced than the 40S peak in non-depleted cells (this was also seen with extracts from other non-depleted strains or the parental DBP4-HA strain), and switching cells from galactose- to dextrose-containing medium restored the normal smaller size of the 40S peak (data not shown). Depletion of Dbp4 caused a strong decrease in the amount of free 40S ribosomal subunits and a gradual increase of free 60S ribosomal subunits over time

(Figure 2.3B). These results are consistent with the implication of Dbp4 in 18S rRNA production (Liang *et al.*, 1997; Kos and Tollervey, 2005). Indeed, impairment of 18S rRNA synthesis leads to a deficit in 40S subunits, which is accompanied by a concomitant excess of free 60S subunits because 80S ribosomes can no longer be formed. Curiously however, the intensity of the 80S peak did not diminish, even 6 hours after the shift to YPD. This phenomenon is unique to Dbp4-depletion, and it was not observed for depletion of U14, U3 or Mpp10 (see below).

The distribution of snoRNAs in sucrose density gradients was analyzed by northern hybridization (Figure 2.3C). In comparison with non-depleted cells (0 h in YPD), the distribution pattern of U3 and U14 snoRNAs changed: U14 moved from the 50S to higher molecular weight fractions of the gradient, indicating that U14 was trapped in higher-order complexes. U3 normally sediments as free RNPs (~12-15S) and active particles (~80S) but during depletion of Dbp4, free RNPs were barely detected and the bulk of U3 accumulated in high-density regions of the gradient (≥80S). Individual fractions were also analyzed for the presence of the U3-specific protein Mpp10 by western blotting (Figure 2.3D). In depleted cells, the sedimentation profile of Mpp10 was similar to that of the U3 snoRNA, with the exception that a larger portion of Mpp10 was found in free form at the top of the gradient; it is known that the Mpp10 complex, which is small and contains Imp3 and Imp4, independently joins the nascent SSU processome (Wehner *et al.*, 2002; Perez-Fernandez *et al.*, 2007; Dutca *et al.*, 2011; Lim *et al.*, 2011; Perez-Fernandez *et al.*, 2011).

We also examined the sedimentation profile of modification guide RNAs because depletion of Dbp4 can alter their sedimentation (Kos and Tollervey, 2005). In Dbp4-depleted cells, the box C/D guide snoRNAs snR41 and snR77 showed an increased distribution in fractions corresponding to very large complexes (polysome size fractions), and snR47 moved from the 40S-60S to the 60S-80S region of the gradient. In contrast, we did not observe major changes in the distribution of H/ACA guide snoRNAs snR10 and snR46 or the processing H/ACA snoRNA snR30. Overall, these sedimentation profiles suggest that depletion of Dbp4 can alter the dynamics of snoRNPs, with a more pronounced effect on C/D snoRNPs.

2.5.4 Effects of depleting the U14 snoRNA

Considering the link between Dbp4 and U14 snoRNA (Liang *et al.*, 1997), (Kos and Tollervey, 2005), we analyzed the effects of depleting U14. Strain YS626, which expresses U14 under the control of the *GAL1* promoter (Liang *et al.*, 1997), was further engineered to encode HA-tagged Dbp4 under the control of its endogenous promoter (Knop *et al.*, 1999). This new strain was named YSS1 and used for our analyses. Exponentially growing cells were transferred from YPGal to YPD, and the growth rate decreased gradually after the shift (Figure 2.4A). Depletion times of 4 and 8 hours were chosen for further experiments with strain YSS1. We examined the sedimentation profile of ribosomal particles before and after the shift to YPD (Figure 2.4B). Consistent with the essential role of U14 in 18S rRNA production, the peak of free 40S ribosomal subunits was almost undetectable upon depletion of U14. As

expected, this deficit was accompanied by an increase of free 60S ribosomal subunits, and the overall content of 80S ribosomes and polysomes was decreased due to the impaired balance between the amount of 40S and 60S ribosomal subunits (Figure 2.4B). Gradient fractions were subjected to northern and western blotting analyses (Figure 2.4C and 2.4D). Interestingly, depletion of U14 caused a change in the sedimentation profile of the U3 snoRNA: as seen with Dbp4-depleted cells (Figure 2.3), free U3 RNPs were no longer detected in the lower density region of the gradient, and U3 accumulated in large complexes. Before its depletion, U14 sedimented in low molecular weight fractions but after a few hours in YPD it was no longer detected in those low molecular weight fractions.

Depletion of U14 also caused a redistribution of box C/D guide snoRNAs, which was similar to that seen upon depletion of Dbp4. Note, however, that these snoRNAs could be detected in large complexes even before depletion, which is different from what was observed with the GAL::DBP4-HA strain (compare the time 0 h for snR41, snR47 and snR77 in Figures 2.3C and 2.4C). As reported previously, the sedimentation profiles of snoRNAs can differ between strains with different genetic backgrounds (Kos and Tollervey, 2005). Nevertheless, U14-depletion changed the sedimentation profile of these C/D guide snoRNAs in a manner similar to that seen upon depletion of Dbp4. Moreover, depletion of U14 affected sedimentation of the H/ACA processing snoRNA snR30, which largely disappeared from low molecular weight fractions and accumulated in the 80S region of the gradient (Figure 2.4C). H/ACA guide snoRNAs snR10 and snR35 also slightly

accumulated in the 80S region of the gradient upon U14 depletion (Figure 2.4C). Western blot analyses showed that depletion of U14 had little effect on the distribution of Mpp10, while Dbp4 was no longer detected in high-density fractions (Figure 2.4D). Taken together these results indicate that depletion of U14 affects the sedimentation profile of many nucleolar factors.

2.5.6 Depletion of the U3 snoRNA alters the sedimentation of snoRNAs

The U3 snoRNA is the central constituent of the SSU processome. Because U3 and Dbp4 are associated (see Figure 2.1), we analyzed the consequences of depleting the U3 snoRNA. Strain JH84 that conditionally expresses the U3 snoRNA from the *GAL1* promoter (Samarsky and Fournier, 1998) was modified to encode HA-tagged Dbp4 from its endogenous promoter (strain YSS2). As observed previously with depletion of other components, blocking the production of U3 snoRNA caused severe growth defects (Figure 2.5A). We chose to carry out further experiments with cells depleted of the U3 snoRNA for 3 and 6 hours. The sedimentation profile of ribosomal particles was similar to that seen with U14-depleted cells, except that the decrease of the 80S peak was less pronounced (compare Figure 2.5B and Figure 2.4B). The sedimentation profile of the U3 snoRNA itself was like that seen with cells depleted of Dbp4 or U14 snoRNA (compare Figure 2.5C with Figures 2.3C and 2.4C). Surprisingly, depletion of the U3 snoRNA also affected the sedimentation profile of U14, which showed an increased distribution and abundance in the fractions corresponding to large complexes (Figure 2.5C). In fact, the sedimentation profile of

U14 snoRNA was very similar to that observed during depletion of Dbp4 (see Figure 2.3C), indicating that depletion of the U3 snoRNA also resulted in trapping U14 in high molecular weight complexes.

As seen with the U14 depletion strain YSS1 grown in YPGal (Figure 2.4), we noted that snR41 accumulated in two regions of the gradient in non-depleted cells, one at ~50S and the other one corresponding to high-density fractions (Figure 2.5C). Upon U3-depletion this distribution changed, and snR41 moved from the ~50S region to the 60S-80S region of the gradient, while a good proportion of snR41 was maintained in high-density fractions. There were no major changes in the distribution of guide snoRNAs snR10, snR46, and snR77; however, snR47 largely accumulated in the ~80S region of the gradient, as seen previously during depletion of Dbp4 (Figure 2.3C) and U14 snoRNA (Figure 2.4C). Only minor changes were observed in the sedimentation profiles of the H/ACA processing snoRNA snR30 (Figure 2.5C) and with proteins Mpp10 and Dbp4 (Figure 2.5D).

2.5.7 Effects of Mpp10 depletion

The U3-specific protein Mpp10 is required for pre-18S rRNA processing and is a genuine SSU processome component (Dunbar *et al.*, 1997; Dragon *et al.*, 2002). We have shown that Mpp10 and Dbp4 are associated *in vivo* (see Figure 2A). Hence we analyzed the effect of depleting Mpp10 using the depletion strain YSS3 that expresses Mpp10 under the control of a *GAL1-10* promoter (Dunbar *et al.*, 1997) and HA-tagged Dbp4 from its endognous promoter. When exponentially growing cells

were shifted from YPGal to YPD, there was a gradual reduction of growth rate (Figure 2.6A), and further experiments were done 6 and 10 hours after the shift to YPD. The sedimentation profiles of ribosomal particles from Mpp10-depleted cells were very similar to those seen with U14-depleted cells (compare Figures 2.4B and 2.6B). Loss of Mpp10 induced a strong deficit of 80S ribosomes and concomitant accumulation of free 60S subunits. We also examined the sedimentation profile of snoRNAs involved in processing reactions and that of Dbp4 by northern and western blotting (Figures 2.6C and 2.6D). After 6 hours of depletion U3 and U14 snoRNAs were no longer detected in low molecular weight fractions (free RNPs), and accumulated in higher density fractions (~80-90S). After 10 hours of depletion, there was a quite uniform distribution of U3 and U14 snoRNAs throughout the gradient. In contrast, there was almost no change in the distribution of snoRNAs snR10, snR30 as well as Dbp4 protein upon depletion of Mpp10. The effects on snoRNAs are reminiscent of what was seen with Dbp4-depleted cells and suggest that depletion of Mpp10 primarily affected the distribution of U3 and U14 snoRNAs.

2.5.8 Dbp4 is required for SSU processome formation

The SSU processome forms at the 5' end of nascent pre-rRNA and decorates active transcription units, which take the shape of "Christmas trees"; electron microscopy (EM) analyses revealed that depletion of various SSU processome components abolished its formation, although the extent of alterations seen by EM varied between various SSU processome components (Dragon *et al.*, 2002; Osheim *et al.*, 2004;

Gallagher *et al.*, 2004). Because depletion of Dbp4 leads to pre-18S rRNA processing defects related to SSU processome dysfunction, we carried out EM analyses on chromatin spreads of the GAL::DBP4-HA strain to determine if the absence of Dbp4 could affect the formation of "Christmas trees". As shown in Figure 2.7, there was a marked difference between non-depleted cells (0 h in YPD) and cells depleted of Dbp4 for various times. In non-depleted cells, rRNA genes showed the characteristic pattern in which nascent transcripts are first packaged into SSU processomes and then co-transcriptionally cleaved at site A2 (Osheim *et al.*, 2004). After a few hours of depletion, there were fewer transcripts per gene on average and fewer terminal knobs. The few SSU processomes that formed did so on more mature transcripts near the 3' end of the gene (small arrows, Figure 2.7A). This phenotype was exacerbated over time and resulted in nearly complete loss of terminal knobs within 12 h of depletion (see Figures 2.7 and 2.8). The most striking effect of Dbp4-depletion was seen on normal co-transcriptional cleavage of pre-rRNA, which was nearly abolished within 5 h of depletion (Figure 2.8). Taken together these results demonstrate that Dbp4 is required for co-transcriptional SSU processome formation and function.

2.5.9 The C-terminal extension of Dbp4 is required for association with U14

Point mutations in the catalytic core of Dbp4 induced trapping of U14 snoRNA in high molecular weight complexes, suggesting that the ATPase/helicase activity of Dbp4 is required to release U14 from pre-rRNA (Kos and Tollervey, 2005). The extensions flanking the catalytic core of DEAD-box proteins are thought to be

important for substrate recognition (Cordin *et al.*, 2006; Silverman *et al.*, 2003). We therefore tested whether deleting the C-terminal extension of Dbp4 would affect the release of U14 from pre-rRNA. Depletion strain GAL::DBP4-HA was transformed with single copy plasmids that constitutively express full-length Dbp4 (control) or a truncated version lacking the C-terminal extension (Dbp4ΔCt); these constructs bear a myc tag at their C-terminus to distinguish them from chromosome-encoded HA-tagged Dbp4. Expression of myc-tagged Dbp4 restored growth in YPD but Dbp4ΔCt did not (data not shown). Cultures were harvested before depletion or 6 hours after the shift to YPD, and cellular extracts were fractionated on sucrose gradients to analyze the sedimentation pattern of U3 and U14 snoRNAs. The distribution of U3 was the same in cells expressing plasmid-borne Dbp4 or Dbp4ΔCt either in non-depleted (0 h) or depleted cells (6 h) (see top panels of Figure 2.9A). The distribution of U14 was also similar in non-depleted cells expressing plasmid-borne Dbp4 or Dbp4ΔCt (0 h panels for U14 in Figure 2.9A) but in depleted cells, there was a marked difference between cells expressing Dbp4ΔCt and those expressing full-length Dbp4 (see bottom panels in Figure 2.9A). In fact, the distribution of U14 with cells expressing Dbp4ΔCt was identical to that seen in cells depleted of Dbp4 (Figure 3C). These results suggest that, in addition to the helicase activity of Dbp4 (Kos and Tollervey, 2005), the C-terminal extension of Dbp4 is required to release U14 from pre-rRNA.

We examined the sedimentation profile of plasmid-borne Dbp4 and Dbp4ΔCt by western blotting. The distribution of full-length Dbp4 was similar in non-depleted and depleted cells, and the same was observed with Dbp4ΔCt, however, very little Dbp4ΔCt was detected in high molecular weight fractions compared to full-length Dbp4 (Figure 2.9). We also verified that expression of the myc-tagged Dbp4 constructs did not alter the distribution of chromosome-encoded Dbp4 in non-depleted cells (data not shown).

IPs carried out with WCEs indicated that Dbp4 is not associated with U14 snoRNA (Figure 2.1). However, when cellular extracts are fractionated on sucrose gradients and IPs are done with 50S fractions, U14 co-immunoprecipitated with Dbp4 (Soltanieh *et al.*, 2014). We examined if the C-terminal extension of Dbp4 is required for its association with U14 snoRNA in the 50S complex (Figure 2.9). IPs were carried out with sucrose gradient fractions of 50S and 80S (SSU processome) as described previously (Soltanieh *et al.*, 2014), except that extracts were prepared from cells expressing myc-tagged Dbp4 or Dbp4ΔCt. U14 snoRNA did not co-immunoprecipitate with Dbp4ΔCt in the 50S complex (compare lanes 2 and 6 in Figure 2.9C). We conclude that the C-terminal extension of Dbp4 is required for its association with U14 snoRNA.

2.5.10 Dbp4-depleted cells accumulate mature LSU RNAs in the 80S peak

The sucrose gradient sedimentation profile seen with Dbp4-depleted cells was very peculiar: even though in those cells production of 40S subunits was impaired and accompanied by an excess of free 60S subunits (LSU), there was no diminution of the 80S peak that normally contains free ribosomes (see Figure 2.3B). Because Dbp4 is required for pre-rRNA processing (Kos and Tollervey, 2005), the unaltered 80S peak seen in Dbp4-depleted cells could result from accumulation of immature, pre-ribosomal RNPs. We thoroughly examined extracts prepared from cells depleted of Dbp4 for 6 hours and found that the 80S peak was enriched in low molecular weight proteins when compared to the 80S peak of non-depleted cells (compare time 0 h and 6 h in Figure 2.10A). Western blotting analyses with antibodies directed against ribosomal proteins L3 and S2 (also known as uL3 and uS5, respectively; (Ban *et al.*, 2014)) showed that ratios of Rpl3 over Rps2 in the 80S peak were increased upon depletion of Dbp4 (Figure 2.10B). This suggests that the 80S peak of Dbp4-depleted cells is deprived of 40S subunits and does not represent free ribosomes. Northern hybridization revealed that the 80S peak of Dbp4-depleted cells was enriched in mature 25S and 5.8S rRNAs (Figures 2.10C and 2.10D), whereas the abundance of various pre-rRNA species in the 80S peak was the same in depleted and non-depleted cells (compare lanes 3 and 4 in Figure 2.10C). Furthermore, 7S and 6S pre-rRNAs, which are precursors of 5.8S rRNA (Woolford and Baserga, 2013), did not accumulate in the 80S peak of Dbp4-depleted cells (data not shown).

Alteration of SSU biogenesis can lead to relocation of pre-40S RNPs into 80S-like particles (Strunk *et al.*, 2012; Ferreira-Cerca *et al.*, 2014). To determine if

the 80S peak observed upon Dbp4 depletion contained pre-40S particles, sucrose gradient fractions corresponding to 40S and 80S peaks were isolated from non-depleted and Dbp4-depleted cells, and subjected to western blot analyses for the pre-40S assembly factor Tsr1 (Strunk *et al.*, 2012). There was no accumulation of Tsr1 in the 80S peak from Dbp4-depleted cells (compare lane 6 with lane 4 in Figure 2.10E). We conclude that depletion of Dbp4 did not lead to relocation of pre-40S particles in the 80S peak.

2.6 Discussion

A role for Dbp4 in ribosome biogenesis was originally proposed on the basis of its genetic interaction with U14 snoRNA, which is essential for 18S rRNA production (Maxwell and Fournier, 1995; Venema and Tollervey, 1999): over-expression of Dbp4 could suppress growth defects caused by mutations in the Y domain of U14, and it was proposed that Dbp4 would also be required for 18S rRNA synthesis (Liang *et al.*, 1997). It was later shown that cellular depletion of Dbp4 impaired production of 18S rRNA due to cleavage defects at sites A0, A1 and A2, which leads to accumulation of the aberrant 23S pre-rRNA species (Kos and Tollervey, 2005), a phenotype that is identical to that seen in cells depleted of the U3 snoRNA or U3-specific proteins (Venema and Tollervey, 1999; Dragon *et al.*, 2002; Dunbar *et al.*, 1997). Depletion of Dbp4 also caused the U14 snoRNA to remain associated with the 35S pre-rRNA, and it was envisioned that the RNA helicase activity of Dbp4 could release U14 from the pre-rRNA (Kos and Tollervey, 2005).

To examine the physical interaction of Dbp4 with U14 snoRNA we first carried out IPs using whole cell extracts (WCEs) prepared from a yeast strain that expresses HA-tagged Dbp4; it is important to note that in this strain expression of Dbp4-HA is under the control of its endogenous promoter to prevent its over-expression (Knop *et al.*, 1999). IPs with anti-HA mAb indicated that Dbp4 is associated with the U3 snoRNA and the U3-specific proteins Mpp10 (Figures 2.1 and 2.2A). Since U3 and Mpp10 are required for pre-rRNA processing reactions at sites A0, A1 and A2, our results are consistent with the observation that cellular depletion of Dbp4 leads to processing defects at sites A0-A2 (Kos and Tollervey, 2005). The U14 snoRNA did not co-immunoprecipitate with Dbp4 when using WCEs (Figure 2.1B). Although this was also observed in previous experiments (Soltanieh *et al.*, 2014), our results are different from the earlier study of Kos and Tollervey (Kos and Tollervey, 2005) who showed that both U3 and U14 snoRNAs co-immunoprecipitated with Dbp4. This could be due to variations in experimental procedures, such as the difference in the concentration of WCEs, which was about 20-fold higher in the experiments done by Kos and Tollervey (Kos and Tollervey, 2005).

The U3 snoRNA and Mpp10 are components of the SSU processome, a large RNP that sediments at ~80S in sucrose gradients (Dragon *et al.*, 2002). As seen in Figures 1 and 2A, association of Dbp4 with U3 and Mpp10 was not salt-stable. This is in marked contrast with what is generally observed in IPs conducted with genuine SSU processome components (Dragon *et al.*, 2002; Bernstein *et al.*, 2004). The

sensitivity to salt concentrations suggests that interaction of Dbp4 with the SSU processome could depend on electrostatic interactions (Katsamba *et al.*, 2001), (Doetsch *et al.*, 2011), which is plausible because Dbp4 contains patches of positively and negatively charged residues (Liang *et al.*, 1997; Garcia *et al.*, 2012). Sucrose gradient sedimentation analyses indicated that a large fraction of Dbp4 did not co-sediment with U3 and Mpp10 in the ~80S region of the gradient (Figure 2.2B). This observation is in agreement with proteomic studies that did not identify Dbp4 in SSU processome/90S pre-ribosome preparations (Dragon *et al.*, 2002; Grandi *et al.*, 2002; Bernstein *et al.*, 2004), and support the idea that Dbp4 is not a stable component of the SSU processome. Nevertheless, Dbp4 is required for SSU processome formation and function: EM studies on chromatin spreads revealed that depletion of Dbp4 rapidly caused defects in appearance of terminal knobs (Figure 2.7), however, the most striking defect seen in Dbp4-depleted cells was the strong reduction in pre-rRNA co-transcriptional cleavage, which crashed within a few hours of depletion (Figure 2.8). Taken together, our results suggest that Dbp4 is a SSU processome component but its association with the SSU processome is likely to be transient.

Cellular depletion of Dbp4 leads to retention of U14 snoRNA on the pre-rRNA (Kos and Tollervey, 2005); see Figure 2.3C), and it is reasonable to assume that Dbp4 is the RNA helicase that unwinds the U14:pre-rRNA duplex. Here we showed that depletion of two SSU processome components, the U3 snoRNA and Mpp10, also led to trapping of U14 in very large complexes (Figures 2.5C and 2.6C). With extracts from U3- and Mpp10-depleted cells we were expecting that the sucrose

gradient sedimentation profile of Dbp4 and U14 would be the same, which was not the case. In fact, in marked contrast with what happened to U14 snoRNA, depletion of U3 or Mpp10 did not considerably alter the sedimentation profile of Dbp4 (Figures 2.5D and 2.6D), implying that Dbp4 did not follow U14 in very large complexes.

Depletion of U3, Mpp10, U14 or Dbp4 prevents SSU processome formation (Dragon *et al.*, 2002; Osheim *et al.*, 2004); Figure 2.7, and leads to trapping of U14 in large complexes (Figures 3-6). Depletion of Bfr2, another SSU processome component, caused a similar phenotype for U14 snoRNA (Soltanieh *et al.*, 2014). Therefore, assembly of the SSU processome could be a prerequisite for Dbp4 to "find" U14, and release it from pre-rRNA. If trapping of U14 is a consequence of impaired SSU processome formation, one could view U14 as a sentinel or sensor of correct SSU processome assembly and function, and the release of U14 by Dbp4 would be a checkpoint in this process. It is not clear what mediates the interaction of Dbp4 with the SSU processome. Although we showed an association of Dbp4 with the U3 snoRNA (Figure 2.1), a direct interaction of Dbp4 with U3 appears unlikely because many proteins are probably already present in the particle before Dbp4 interacts with it (see also the model proposed by (Soltanieh *et al.*, 2014). Since Dbp4 contains a highly conserved coiled-coil motif in its C-terminal extension (Soltanieh *et al.*, 2014), it is probable that Dbp4 would contact the SSU processome through interactions with SSU processome proteins, many of which contain coiled-coil motifs (Dragon *et al.*, 2002). Such interactions could allow the correct positioning of Dbp4 prior to its action on the U14:pre-rRNA duplex.

Complementation assays with a truncated Dbp4 that lacks its C-terminal extension (Dbp4ΔCt) revealed that this region is essential for growth (data not shown). Dbp4ΔCt changed the sucrose gradient sedimentation pattern of U14 snoRNA, which was trapped in high molecular weight complexes (Figure 2.9A). This phenotype was identical to that seen upon cellular depletion of Dbp4 (Figure 2.3) or when introducing point mutations in the catalytic core of Dbp4 (Kos and Tollervey, 2005). Therefore, in addition to the ATPase/helicase activity of Dbp4, the C-terminal extension plays a critical role in releasing U14 from pre-rRNA. We know that Dbp4 associates with U14 snoRNA in a complex of about 50S (Soltanieh *et al.*, 2014). Here we demonstrated that the C-terminal extension is required to maintain the association of Dbp4 with U14 snoRNA in the 50S complex (Figure 2.9C).

Given that depletion of Dbp4 impairs 18S rRNA synthesis (Kos and Tollervey, 2005), it was stunning to observe that the 80S peak did not diminish upon depletion of Dbp4 (Figure 2.3B). We first suspected that the 80S peak contained 23S pre-rRNA associated with ribosomal proteins and other nucleolar factors, but a detailed analysis indicated that this 80S peak was not enriched in 23S but rather contained large amounts of mature rRNAs of the LSU (25S and 5.8S) and very little mature 18S RNA (Figure 2.10). To determine whether the 80S-like particles could be pre-40S subunits we examined the presence of Tsr1, which is a late pre-40S assembly factor (Strunk *et al.*, 2012; Ferreira-Cerca *et al.*, 2014). Tsr1 did not accumulate in the 80S peak, suggesting it did not contain pre-40S particles (Figure 2.10E). Taken together, the data suggest that Dbp4-depleted cells accumulate LSU particles

containing mature rRNAs; these LSUs likely interact with additional cellular components to form RNPs of ~80S. To our knowledge this is the first time such an observation is reported. Further studies will be required to determine what makes "normal" 60S subunits sediment at 80S.

2.7 Acknowlegments

We are grateful to Susan Baserga, Maurille Fournier, Katrin Karbstein, Jonathan Warner and Karen Wehner for the generous gift of yeast strains and reagents. This work was supported by a grant from the Natural Sciences and Engineering Research Council of Canada to FD (RGPIN 249792), and grants to ALB from the National Science Foundation (MCB-0818818) (YNO) and NIH (R01GM063952) (Garcia *et al.*).

Table 2.1: Yeast strains used in this study

Strain	Genotype	Reference or source
YPH499	*Mat***a**, *ura3-52*, *lys2-801*, *ade2-101*, *trp1-Δ63*, *his3-Δ200*, *leu2-Δ1*	((Sikorski and Hieter, 1989))
DBP4-HA	Same as YPH499 except *DBP4::DBP4-3HA-kanMX6*	This study
GAL::DBP4-HA	Same as DBP4-HA except *TRP1::* P_{GAL1}*-DBP4-3HA*	This study
NOP1-HA	Same as YPH499 except *NOP1::NOP1-3HA-kanMX6*	((Dragon *et al.*, 2002))
YS626	*Mat***a**, *leu2 ura3 trp1 his3 HIS3::GAL1::U14*	((Liang *et al.*, 1997))
YSS1	Same as YS626 except *DBP4::DBP4-3HA-kanMX6*	This study
JH84	*Mat***α**, *leu2-3,12 ura3-52 his3-Δ ade2-1 can1100 u3aΔ* UAS_{GAL} *:U3A::URA3 U3B::LEU2*	((Samarsky and Fournier, 1998))
YSS2	Same as GAL::U3 except *DBP4::DBP4-3HA-kanMX6*	This study
YPH258		((Sikorski

	*Mat***a**, *ura3-52*, *lys2-801*, *ade2-101*, *his3-Δ200*, *leu2-Δ1*	and Hieter, 1989))
GAL::MPP10	Same as YPH258 except *mpp10::HIS3 ADE2 URA3::* $P_{GAL1\text{-}10}$*-MPP10*	((Dunbar *et al.*, 1997))
YSS3	Same as GAL::MPP10 except *DBP4::DBP4-3HA-kanMX6*	This study

2.9 Figure legends

Figure 2.1: Dbp4 is associated with the U3 snoRNA.

(A) 3'-end labeling of RNAs. Whole cell extracts (WCEs) were prepared from yeast strains expressing HA-tagged Dbp4 (lanes 2-5) or HA-tagged Nop1 (lanes 6-9). Beads coated with HA mAb were incubated with WCEs, recovered by centrifugation, and washed with increasing salt concentrations. RNAs were extracted with phenol/chloroform, precipitated with ethanol, labeled at their 3' end with [5'-^{32}P] pCp, and separated on a sequencing gel. T lanes are total RNA from WCEs. DNA molecular weight markers (M) are shown in lane 1 (in nt). The predicted position of some RNAs is indicated on the right.

(B) Northern blotting of recovered RNAs. IPs and RNA isolation were conducted as in (A) with WCEs prepared from an untagged yeast strain (lanes 1-5), or yeast strains expressing HA-tagged Nop1 (lanes 6-10) or HA-tagged Dbp4 (lanes 11-15). Immunoprecipitated RNAs were separated in a denaturing gel, transferred onto a nylon membrane, and probed with radiolabeled oligonucleotides complementary to various snoRNAs (indicated on the right). Lanes T correspond to RNAs isolated from WCEs, and lanes S are RNAs from supernatants.

Figure 2.2: Dbp4 associates with Mpp10 but is not enriched in SSU processome fractions.

(A) Western analysis of IPs conducted as in Figure 1B. WCEs were prepared from an untagged yeast strain (lanes 1-4) or yeast strains expressing HA-tagged Nop1 (lanes 5-8) or HA-tagged Dbp4 (lanes 9-12). Proteins were fractionated by SDS-PAGE, transferred onto a PVDF membrane, and subjected to immunoblotting with anti-Mpp10 antibodies.

(B) Sucrose gradient sedimentation analyses. Top panels are northern blots for U3 and U14 snoRNAs. Bottom panels are western blots for Dbp4 and Mpp10 proteins. The position of 40S and 60S ribosomal subunits, 80S ribosomes, and polysomes is indicated.

Figure 2.3: Depletion of Dbp4 affects sedimentation of U14 and other snoRNAs

(A) Growth curves of the strains YPH499, DBP4-HA and GAL::DBP4-HA after shift into glucose-containing medium. The cultures were diluted as necessary to maintain exponential growth. Absorbance at 600 nm was measured over time. Arrows show depletion time points that were chosen for subsequent analyses.

(B) Sucrose gradient sedimentation profiles of extracts prepared from the GAL::DBP4-HA strain before (0h) and after shift to YPD (4h and 6h, left to right). The position of free 40S and 60S subunits, 80S ribosomes and polysomes is indicated.

(C) Northern analysis of snoRNAs in sucrose gradient fractions. RNAs were extracted from gradient fractions of the GAL::DBP4-HA strain grown in YPGal (0 h) or in YPD to deplete Dbp4 for 4 h or 6 h (time of depletion is indicated on the left).

We used oligonucleotides complementary to different snoRNAs that belong to the C/D or H/ACA class (indicated on the right). Gradients were fractionated in 22 samples (numbered 1 to 22 under the panels). T lanes are total RNAs of the extracts. Sedimentation is from left to right. The position of 40S and 60S subunits, 80S ribosomes and polysomes are indicated on the top. In the snR10 panel, asterisks indicate that snR10 corresponds to the lower band in fractions 3 and 4 (time 0 h). Note that fraction 12 of the 6 h depletion time was lost.

(D) Western blotting analysis of sucrose gradient fractions. The time of growth of the GAL::DBP4-HA strain in YPD medium is indicated on the left of each panel. Samples (numbered 1 to 22 under the panels) were analyzed with an antibody against Mpp10.

Figure 2.4: Effects of depleting the U14 snoRNA

(A) Effect of U14 gene repression on cellular growth. Strain YSS1 was grown to exponential phase in YPGal and shifted to YPD as described in Fig. 3A.

(B) Polysome profile of strain YSS1 at time 0 h (before depletion), 4 h and 8 h after the shift to YPD. The peaks of free 40S and 60S subunits, 80S ribosomes and polysomes are indicated.

(C) Northern hybridization analysis of snoRNAs in sucrose gradient fractions (see Fig. 3C for details).

(D) Sedimentation analysis of Dbp4 and Mpp10 proteins by western blotting. Sucrose gradient fractions were analyzed before and after depletion of U14 snoRNA (time in YPD is indicated on the left).

Figure 2.5: Depletion of U3 snoRNA affects sedimentation of U14

(A) Cellular growth analysis during U3 snoRNA depletion. The experiment with strain YSS2 was done as previously described (Fig. 3A).

(B) Polysome profile of strain YSS2 at time 0 h (before depletion), 3 h and 6 h after depletion. The peaks of free 40S and 60S subunits, 80S ribosomes and polysomes are indicated.

(C) Analysis of the sedimentation profile of different snoRNAs by northern hybridization as shown in Fig. 3C.

(D) Distribution pattern of Dbp4 and Mpp10 in the presence or absence of U3 snoRNA using anti-HA and anti Mpp10 antibodies (time in YPD is indicated on the left).

Figure 2.6: Depletion of Mpp10 affects sedimentation of U14

(A) Cellular growth analysis during Mpp10 depletion. Strain YSS3 was grown in YPD (see details in Fig. 3A).

(B) Polysome profile of strain YSS3 at time 0 h (before depletion), 6 h and 10 h after the shift to YPD. The peaks of free 40S and 60S subunits, 80S ribosomes and polysomes are indicated.

(C) Northern hybridization analysis of processing snoRNAs with strain YSS3 (see Fig. 3C for details).

(D) Western blotting analysis of Dbp4 with strain YSS3 (time in YPD is indicated on the left).

Figure 2.7: Dbp4 is required for SSU processome formation.

Electron micrographs of rRNA genes from strain GAL::DBP4-HA. Examples of genes from the 0 hr (non-depleted) and 5 hr, 6 hr and 12 hr depletions are displayed in (A). Small arrows indicate examples of SSU processomes and large arrows indicate examples of transcripts that have been co-transcriptionally cleaved. Panel (B) shows interpretive line tracings of the genes. Panel (C) contains maps of the genes with the following features highlighted: 5' ETS particles are small and light gray, SSU processomes are larger and black, and LSU particles beginning to form are small and light gray with a black center (see (Osheim *et al.*, 2004)).

Figure 2.8: EM analyses of co-transcriptional pre-rRNA processing.

Semi-quantitative analysis of the state of rRNA genes in strain GAL::DBP4-HA at various times of depletion (cells were grown in YPGal and then switched to YPD for the depletions). Fields of rRNA genes from EM analysis of Miller chromatin spreads were examined and the following features were given a visual score of 0 to 3: transcription level (i.e., density of transcripts/gene), presence of 5' ETS particles, presence of SSU processomes, and normal co-transcriptional cleavage. The scores

were then normalized (0 to 1) and plotted as a bar graph. The number of fields examined ranged from 56 to 133 (average 83) and each field contained multiple genes. As a general rule, the rRNA genes in a given nucleolus display similar morphologies. The transcription level at 0 hr is slightly lower than that at 3 hr depletion because of the transcriptional advantage of growth in glucose.

Figure 2.9: Deletion of the C-terminal extension of Dbp4.

Depletion strain GAL::DBP4-HA was transformed with a plasmid expressing full-length Dbp4 (Dbp4) or a truncated version lacking its C-terminal extension (DBP4ΔCt). In (A) and (B), cells were grown in galactose-containing medium (0 h) and shifted to YPD for 6 hours (6 h). Northern hybridization (A) and western blot analyses (B) were carried out as in Figure 3 except that 16 fractions were collected instead of 22 and immunoblots were done with anti-myc monoclonal antibody (mAb).

C) IPs with anti-myc mAb were done on sucrose gradient fractions corresponding to the 50S and 80S peaks, and U14 snoRNA was detected by northern hybridization (as described in (Soltanieh *et al.*, 2014)).

Figure 2.10: Depletion of Dbp4 leads to accumulation of mature LSU rRNAs in the 80S peak. Extracts were prepared from non-depleted cells (0 h) or cells depleted of Dbp4 for 6 h.

(A) Proteins isolated from the 80S peak of sucrose gradients were analyzed by SDS-PAGE and stained with silver nitrate. Molecular weight markers are indicated in kDa on the left.

(B) Analysis of ribosomal proteins. Proteins of the 60S and 80S peaks of the gradients were fractionated by SDS-PAGE and transferred to a PVDF membrane. The blot was subjected to immunodetection with anti-Rpl3 (LSU protein) and anti-Rps2 (SSU protein) antibodies.

(C) Northern hybridization of precursor and mature rRNAs. Total RNA (Wiederkehr *et al.*) and RNAs from the 80S peak (80S) were fractionated in a denaturing agarose gel and transferred to a nylon membrane. The blot was probed for various pre-rRNAs species or mature rRNAs indicated on the right.

(D) Northern blot of 5.8S rRNA in fractions of sucrose gradients. The blots shown in Fig. 3C (time 0 h and 6 h) were probed for mature 5.8S rRNA.

(E) Analysis of the pre-40S assembly factor Tsr1. Proteins of the extracts (Wiederkehr *et al.*), 40S and 80S peaks of sucrose gradients were from non-depleted (0 h) or Dbp4-depleted cells (6 h), fractionated by SDS-PAGE and transferred to a PVDF membrane. The blot was subjected to immunodetection with anti-Tsr1 antibodies.

2.10 Figures

Figure 2.1

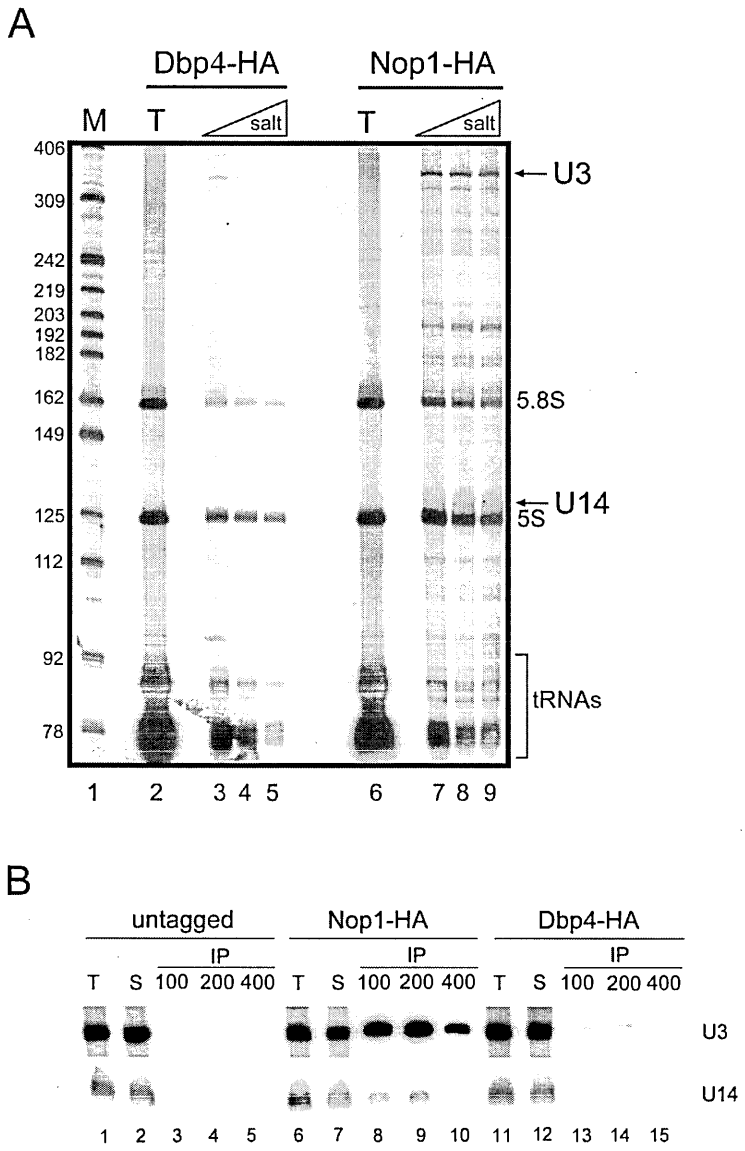

Figure 2.2

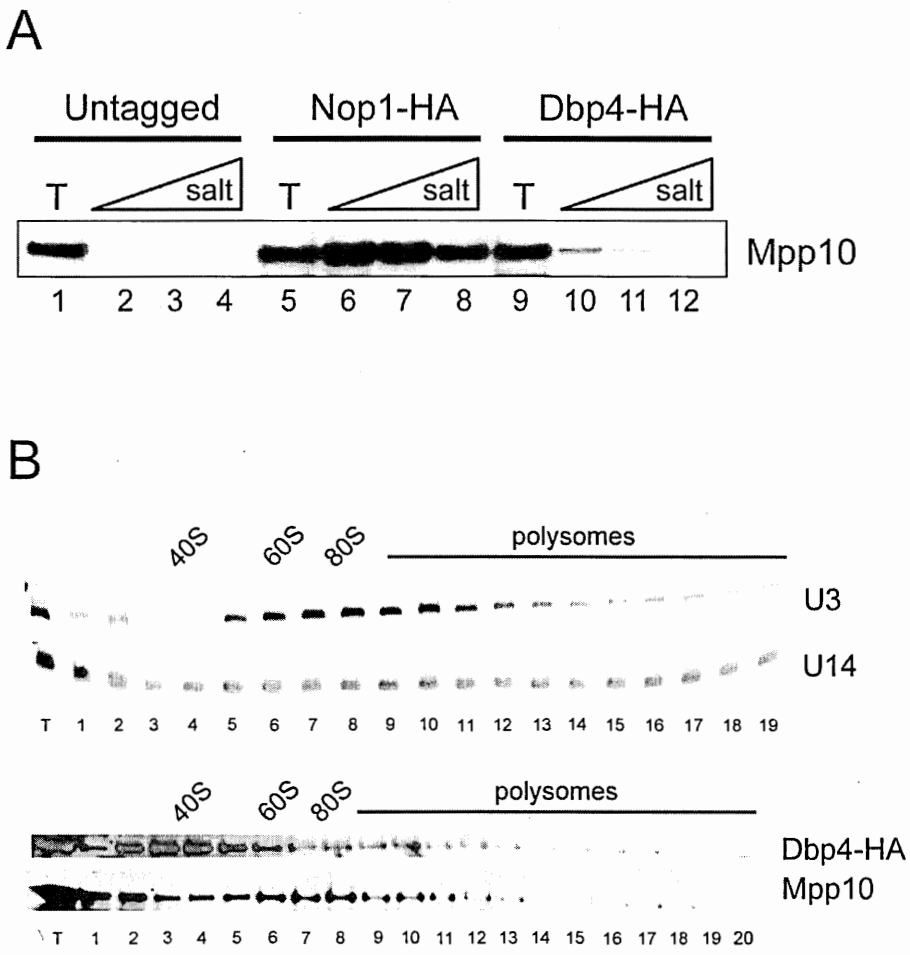
A
Untagged
Nop1-HA
Dbp4-HA
T
salt
T
salt
T
salt
Mpp10
1 2 3 4 5 6 7 8 9 10 11 12
B
40S
60S
80S
polysomes
U3
U14
T 1 2 3 4 5 6 7 8 9 10 11 12 13 14 15 16 17 18 19
40S
60S
80S
polysomes
Dbp4-HA
Mpp10
T 1 2 3 4 5 6 7 8 9 10 11 12 13 14 15 16 17 18 19 20

Figure 2.3

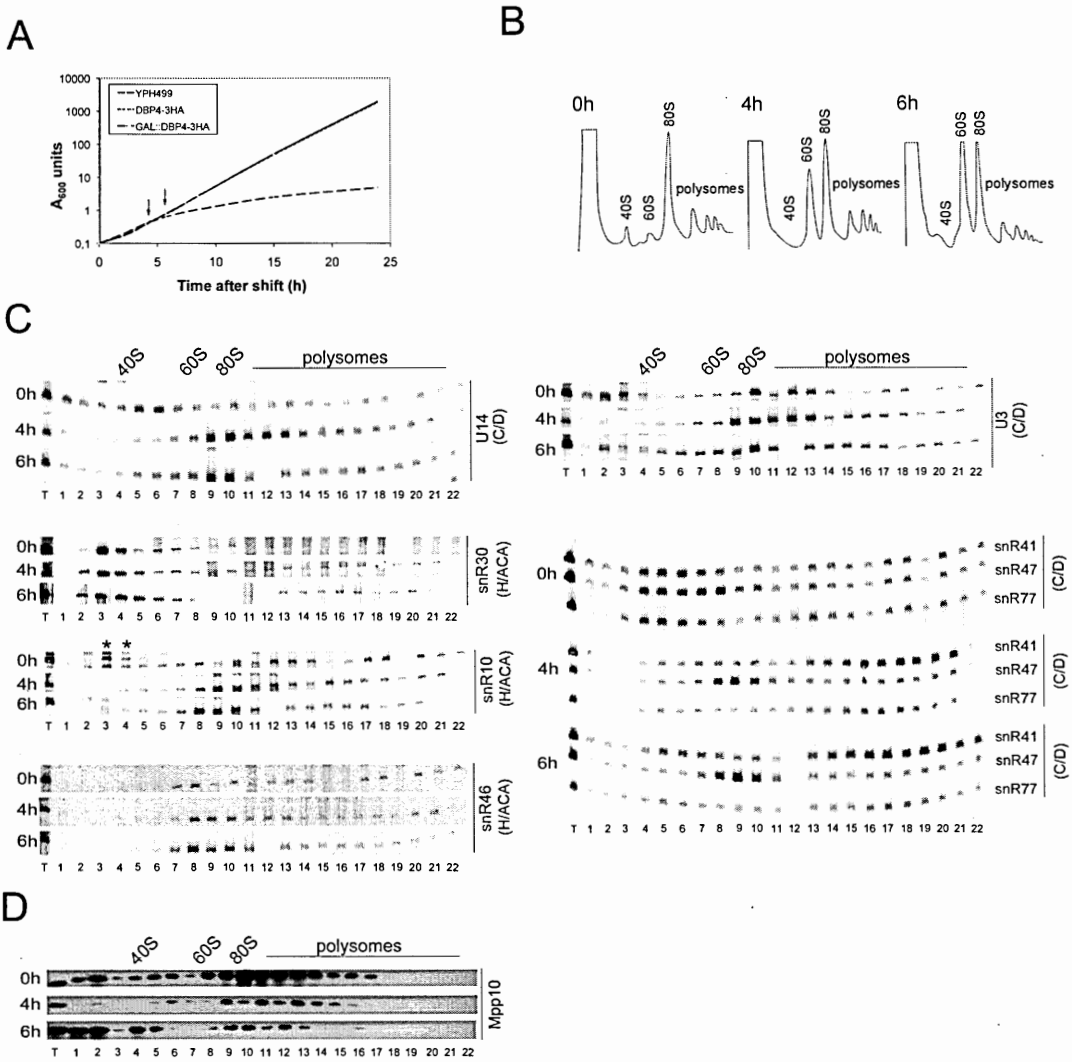
A
YPH499
DBP4-3HA
GAL::DBP4-3HA
A_{600} units
Time after shift (h)
B
0h
4h
6h
40S
60S
80S
polysomes
C
U14 (C/D)
U3 (C/D)
snR30 (H/ACA)
snR10 (H/ACA)
snR46 (H/ACA)
snR41
snR47
snR77
(C/D)
D
Mpp10

Figure 2.4

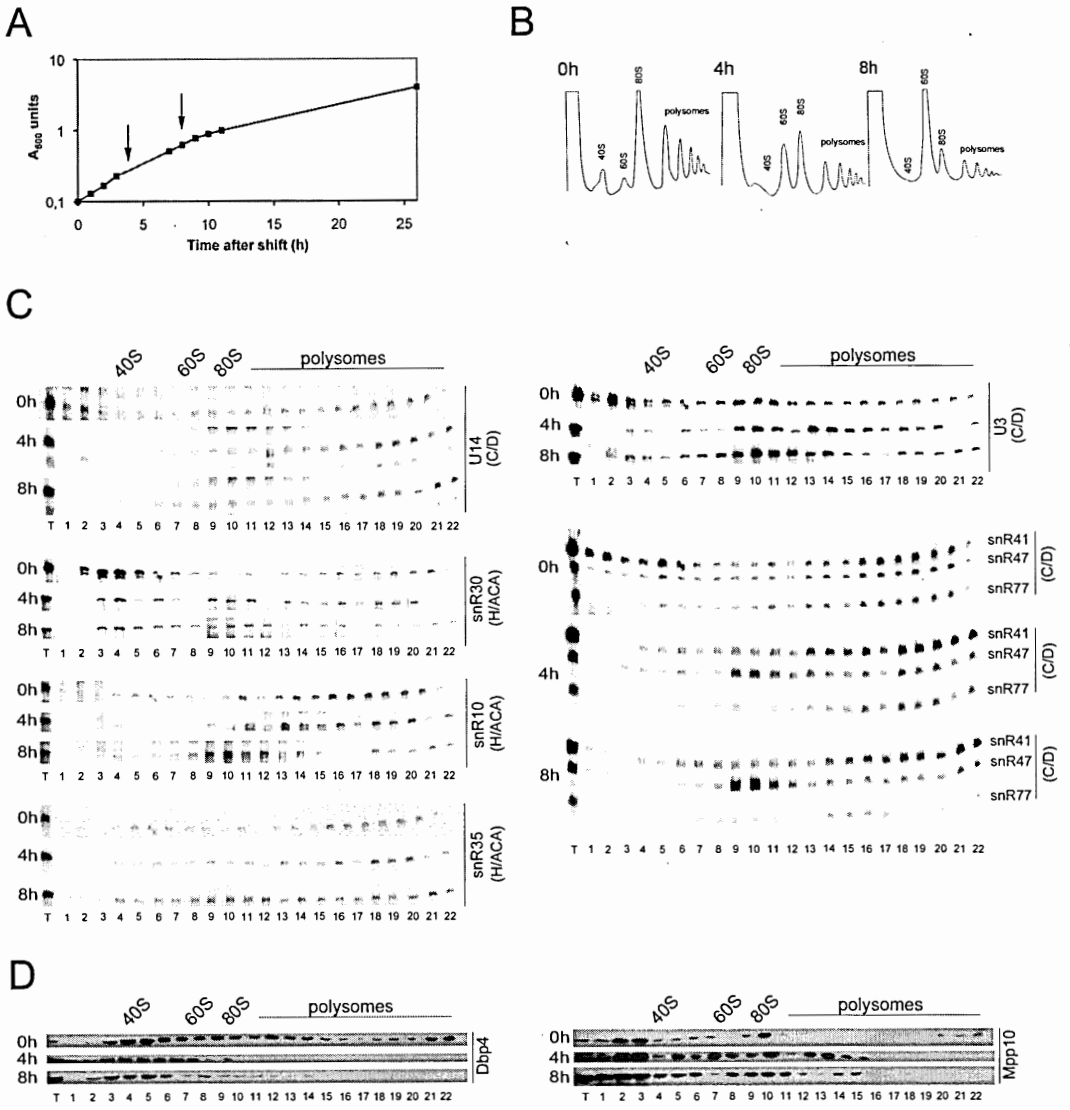
A
B
C
D
Time after shift (h)
0h
4h
8h
40S
60S
80S
polysomes
U14 (C/D)
snR30 (H/ACA)
snR10 (H/ACA)
snR35 (H/ACA)
U3 (C/D)
snR41
snR47
snR77
Dbp4
Mpp10

Figure 2.5

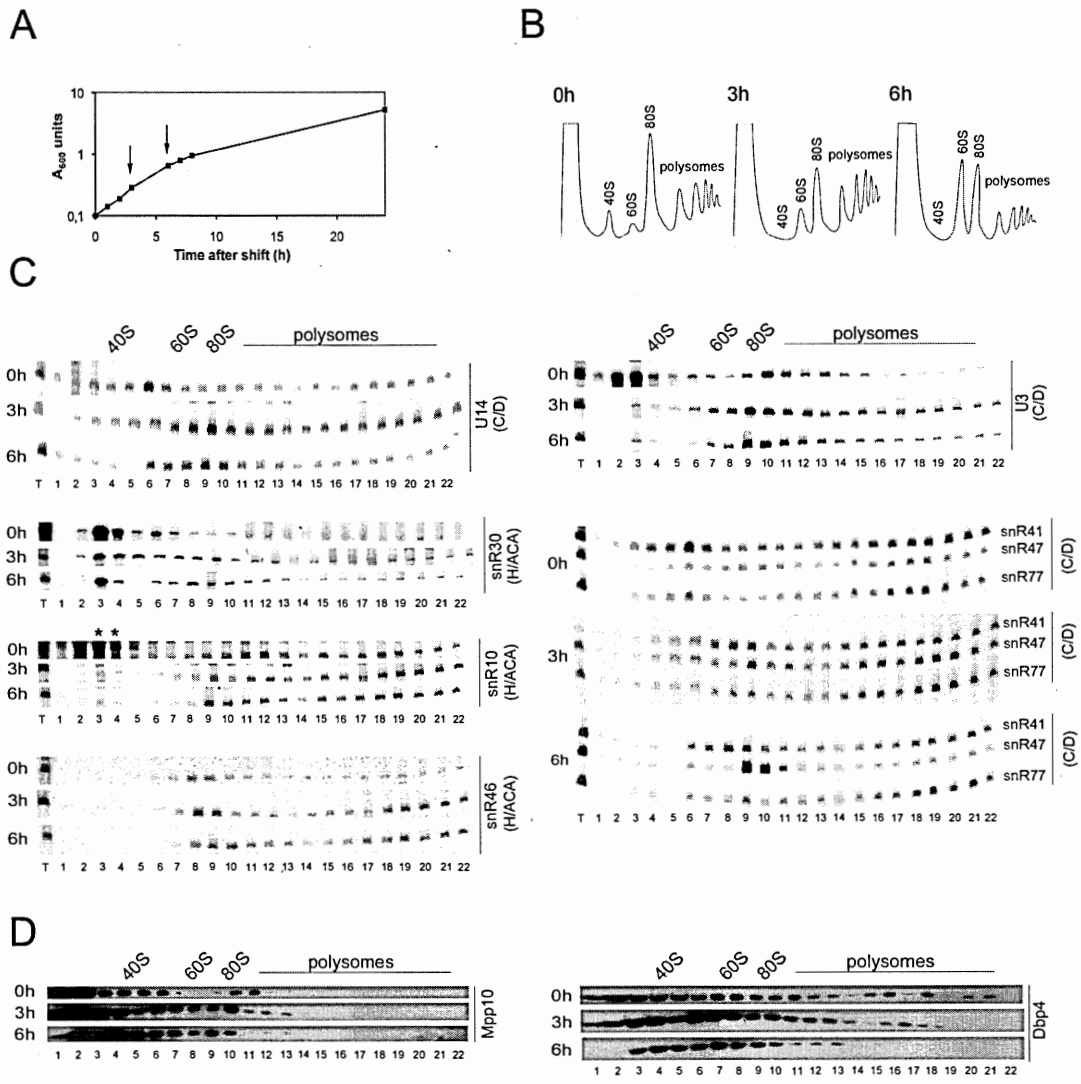
A
B
C
D
Time after shift (h)
0h
3h
6h
40S
60S
80S
polysomes
U14 (C/D)
U3 (C/D)
snR30 (H/ACA)
snR10 (H/ACA)
snR46 (H/ACA)
snR41
snR47
snR77
Mpp10
Dbp4

Figure 2.6

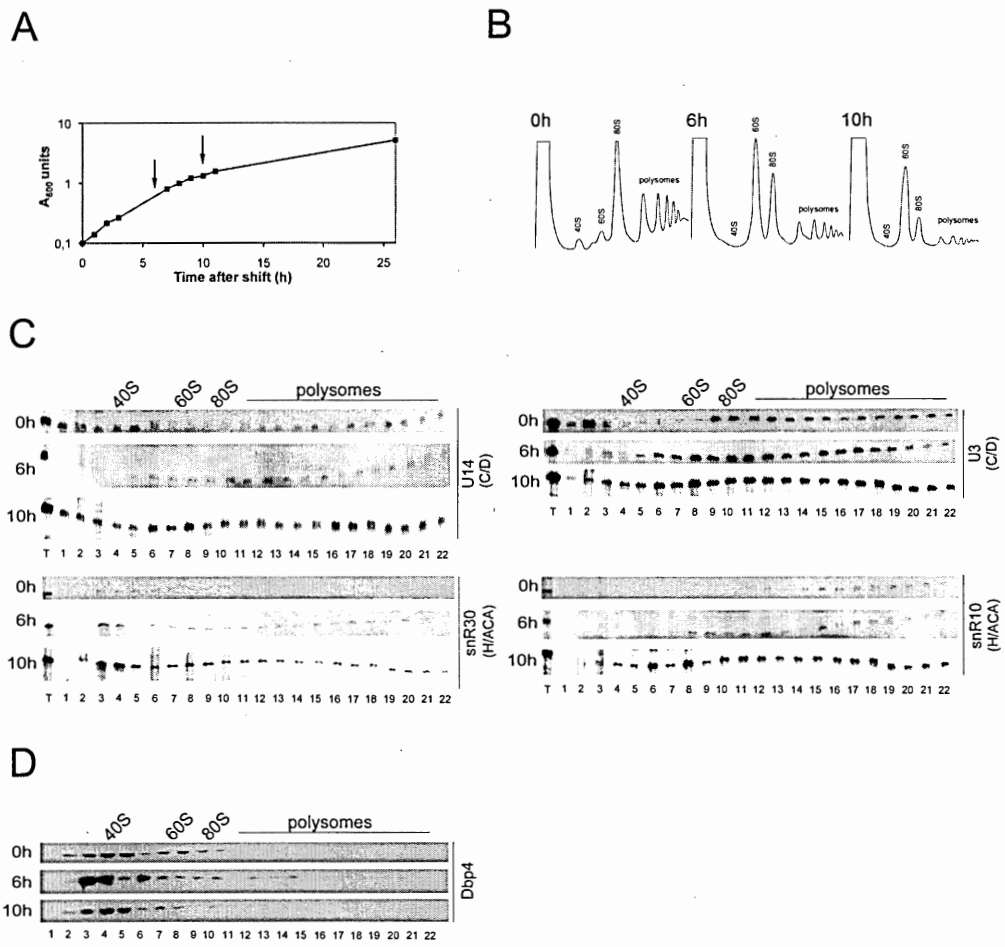
A
B
C
D
10
1
0,1
A_{600} units
0
5
10
15
20
25
Time after shift (h)
0h
6h
10h
40S
60S
80S
polysomes
T 1 2 3 4 5 6 7 8 9 10 11 12 13 14 15 16 17 18 19 20 21 22
U14 (C/D)
U3 (C/D)
snR30 (H/ACA)
snR10 (H/ACA)
Dbp4

Figure 2.7

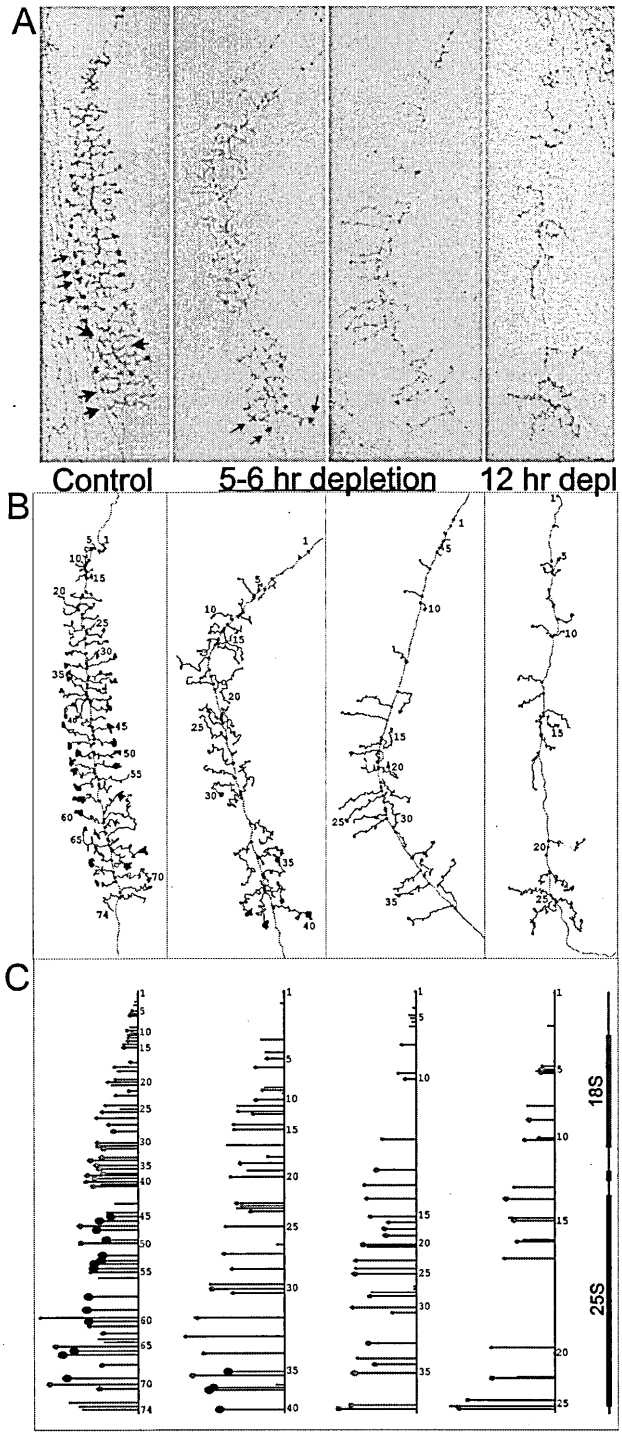

Figure 2.8

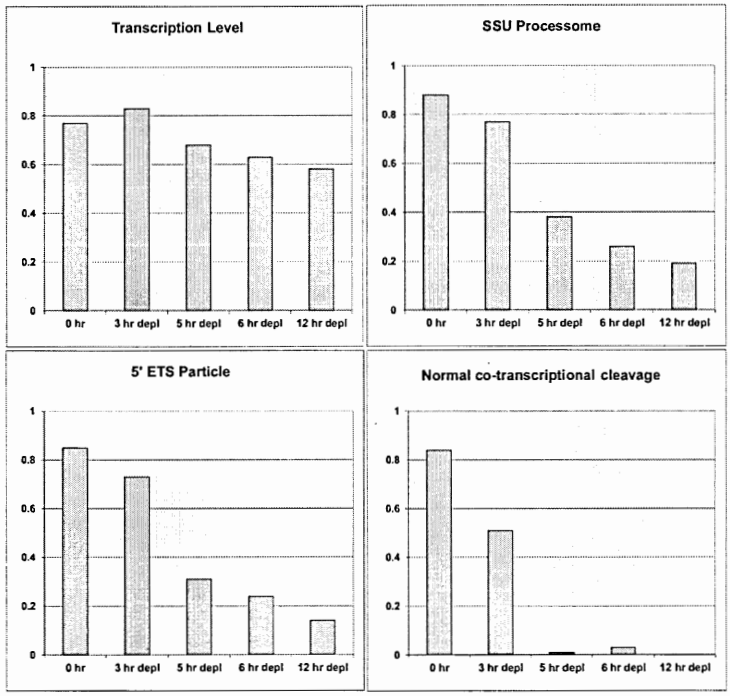
Transcription Level
SSU Processome
5' ETS Particle
Normal co-transcriptional cleavage
1
0.8
0.6
0.4
0.2
0
0 hr
3 hr depl
5 hr depl
6 hr depl
12 hr depl

Figure 2.9

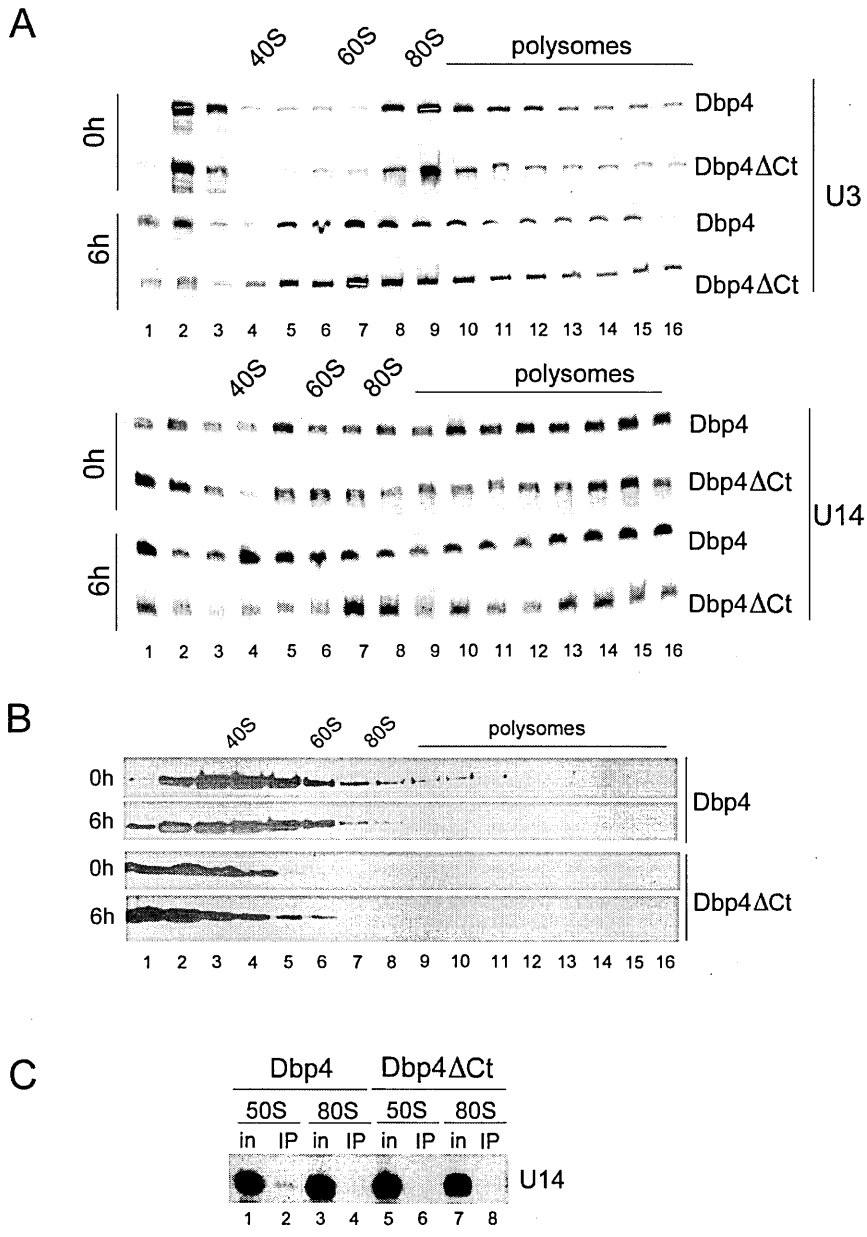
A
40S
60S
80S
polysomes
0h
6h
Dbp4
Dbp4ΔCt
U3
U14
1 2 3 4 5 6 7 8 9 10 11 12 13 14 15 16
B
0h
6h
Dbp4
Dbp4ΔCt
C
50S
80S
in
IP
U14
1 2 3 4 5 6 7 8

Figure 2.10

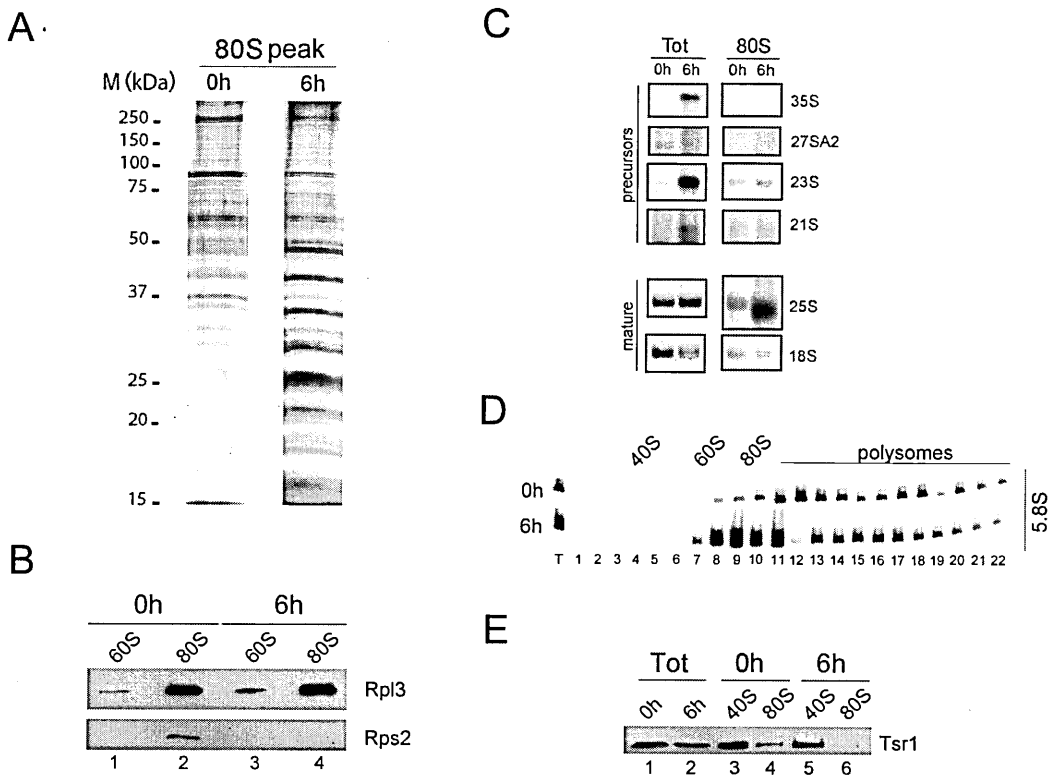
A
80S peak
M (kDa)
0h
6h
250
150
100
75
50
37
25
20
15
B
0h
6h
60S
80S
60S
80S
Rpl3
Rps2
1
2
3
4
C
Tot
80S
0h 6h
0h 6h
precursors
mature
35S
27SA2
23S
21S
25S
18S
D
40S
60S
80S
polysomes
0h
6h
5.8S
T 1 2 3 4 5 6 7 8 9 10 11 12 13 14 15 16 17 18 19 20 21 22
E
Tot
0h
6h
0h
6h
40S
80S
40S
80S
Tsr1
1 2 3 4 5 6

Chapter III

3.1 Preface

The assembly of U3 snoRNP and protein subcomplexes leads to the formation of SSU processome, which takes place in a hierarchical manner. We have found that Dbp4 associates with Bfr2 and Enp2, two conserved nucleolar proteins, and that they are all implicated in the early cleavages leading to 18S rRNA production. We showed that Dbp4, Bfr2 and Enp2 associate with the U3 snoRNA and the U3-specific protein Mpp10, suggesting that they might be components of the SSU processome (80S complex). Sucrose gradient analyses showed that Dbp4, Bfr2 and Enp2 are formed in complexes of 50S and 80S. Our studies revealed that Bfr2, Dbp4 and Enp2 associate together in the 50S peak, which does not include U3 snoRNA. In addition, Dbp4 associates with U14 snoRNA in the 50S peak. However, all these proteins associate with U3 snoRNA in the 80S peak. We proposed that Bfr2, Dbp4 and Enp2 form a 50S complex, which will later be incorporated into the SSU processome.

Martin Lapensée produced the anti-Dbp4 polyclonal antibodies and I did all of the experiments under the supervision of Dr. François Dragon.

Nucleolar proteins Bfr2, Enp2 with DEAD-box RNA helicase Dbp4 in two different complexes

Sahar Soltanieh, Martin Lapensée and François Dragon

Nucleic Acids Research 2014, vol. 42, no. 5, pp. 3194-3206
doi: 10.1093/nar/gkt1293

Département des sciences biologiques and Centre de recherche BioMed,
Université du Québec à Montréal, Montréal, Québec, Canada

Key Words : DEAD-box RNA helicase, ribosome biogenesis,
ribosomal RNA processing

3.2 Abstract

Different pre-ribosomal complexes are formed during ribosome biogenesis, and the composition of these complexes is highly dynamic. Dbp4, a conserved DEAD-box RNA helicase implicated in ribosome biogenesis, interacts with nucleolar proteins Bfr2 and Enp2. We show that, like Dbp4, Bfr2 and Enp2 are required for the early processing steps leading to the production of 18S rRNA. We also found that Bfr2 and Enp2 associate with the U3 snoRNA, the U3-specific protein Mpp10, and various pre-18S rRNA species. Thus, we propose that Bfr2, Dbp4 and Enp2 are components of the SSU processome, a large complex of ~80S. Sucrose gradient sedimentation analyses indicated that Dbp4, Bfr2 and Enp2 sediment in a peak of ~50S and in a peak of ~80S. Bfr2, Dbp4 and Enp2 associate together in the 50S complex, which does not include the U3 snoRNA; however, they associate with U3 snoRNA in the 80S complex (SSU processome). Immunoprecipitation experiments revealed that U14 snoRNA associates with Dbp4 in the 50S complex, but not with Bfr2 or Enp2. The assembly factor Tsr1 is not part of the "50S" complex, indicating this complex is not a pre-40S ribosome. A combination of experiments leads us to propose that Bfr2, Enp2 and Dbp4 are recruited at late steps during assembly of the SSU processome.

3.3. Introduction

The making of eukaryotic ribosomes is an intricate process that is highly conserved. Our knowledge of ribosome biogenesis comes mainly from studies in the budding yeast *Saccharomyces cerevisiae* (Henras *et al.*, 2008; Venema and Tollervey, 1999; Warner, 1989; Woolford, 1991). Ribosome biogenesis initiates within the nucleolus, continues in the nucleoplasm and terminates in the cytoplasm. This process involves rRNA transcription, processing, modification and assembly of rRNAs with ribosomal proteins, which leads to the synthesis of the small and large ribosomal subunits (40S and 60S) (Fromont-Racine *et al.*, 2003; Henras *et al.*, 2008; Lafontaine and Tollervey, 2001; Venema and Tollervey, 1999).

A key process in ribosome biogenesis is the production of mature ribosomal RNAs (rRNAs), the functional components of ribosomes (Moore and Steitz, 2002). Yeast RNA polymerase I synthesizes a long precursor of 35S that encodes the 18S, 5.8S and 25S rRNAs, while the 5S rRNA is independently transcribed by RNA polymerase III (Kressler *et al.*, 1999; Venema and Tollervey, 1999). The 35S pre-rRNA is subjected to an orderly maturation process that requires about 200 *trans*-acting factors (Fromont-Racine *et al.*, 2003; Henras *et al.*, 2008; Kressler *et al.*, 2010; Kressler *et al.*, 1999). In addition, tens of small nucleolar RNAs (snoRNAs) basepair transiently with pre-rRNAs and direct site-specific post-transcriptional modification of rRNAs. Very few snoRNAs are required for the endonucleolytic cleavages that remove spacer sequences from pre-rRNAs. In yeast, only U3, U14 and

snR30 snoRNAs are essential for the cleavage reactions that lead to the production of 18S rRNA (Henras *et al.*, 2004; Maxwell and Fournier, 1995; Venema and Tollervey, 1999). The functionally active U3 RNP is a very large complex of ~80S called the small subunit (SSU) processome, which is formed at the 5' end of nascent pre-rRNA and can be seen under the electron microscope (Dragon *et al.*, 2002; Osheim *et al.*, 2004). In yeast, the SSU processome is implicated in early pre-rRNA cleavages at processing sites A0, A1 and A2 (Dragon *et al.*, 2002; Osheim *et al.*, 2004). The SSU processome is an early pre-ribosomal particle that is necessary for maturation of the 18S rRNA: it contains the U3 snoRNA and about 72 proteins, including ribosome biogenesis factors and ribosomal proteins (Lim *et al.*, 2011). These proteins assemble and interact together to form the SSU processome. A number of studies identified the presence of sub-complexes of the SSU processome. These sub-complexes are called UtpA/tUTP, UtpB, UtpC, Mpp10, Rcl1/Bms1 and U3 snoRNP (Champion *et al.*, 2008; Dosil and Bustelo, 2004; Freed and Baserga, 2010; Gallagher *et al.*, 2004; Granneman *et al.*, 2009; Krogan *et al.*, 2004; Lee and Baserga, 1999; Rudra *et al.*, 2007; Venema *et al.*, 2000; Wegierski *et al.*, 2001; Wehner *et al.*, 2002). However, proteins identified from these sub-complexes account for 43% of the proteins of the SSU processome, indicating that many proteins of the SSU processome have not yet been identified as components of a sub-complex (Lim *et al.*, 2011; Phipps *et al.*, 2011b). There are also studies showing that some of the sub-complexes of the SSU processome associate with the rRNA precursors in a

hierarchical and stepwise manner (Gallagher *et al.*, 2004; Perez-Fernandez *et al.*, 2011; Perez-Fernandez *et al.*, 2007).

Many of the non-ribosomal factors involved in rRNA maturation are RNA helicases. These enzymes are viewed as molecular motors that rearrange RNA structures in an energy-dependent fashion (Bleichert and Baserga, 2007; Cordin *et al.*, 2006; Jankowsky *et al.*, 2011; Jankowsky, 2011; Rajkowitsch *et al.*, 2007; Staley and Guthrie, 1998; Tanner and Linder, 2001). However, some can rearrange RNA-protein complexes, and many could in fact be RNPases (Jankowsky and Bowers, 2006; Tanner and Linder, 2001). DEAD-box protein Dbp4 is a putative RNA helicase that is phylogenetically conserved and essential for yeast viability; Dbp4 was first identified as a multi-copy suppressor of lethal mutations in the Y domain of U14 snoRNA (Liang *et al.*, 1997). More recently it was shown that Dbp4 is required for the production of 18S rRNA and more specifically for the early cleavages at sites A0, A1 and A2 of the pre-rRNA (Kos and Tollervey, 2005). The C-terminal extension that flanks the catalytic core of Dbp4 contains a predicted coiled-coil motif, which is conserved in all Dbp4 orthologs (our unpublished observation). Because this motif is implicated in protein-protein interactions, Dbp4 might function in a complex with other proteins. We found that Dbp4 associates with the essential nucleolar proteins Bfr2 and Enp2 (Bernstein *et al.*, 2004; Chabane and Kepes, 1998; Li *et al.*, 2009). We also show that Bfr2 and Enp2 are implicated in the early cleavages leading to 18S rRNA production, and that Bfr2 and Enp2 associate with the U3 snoRNA and the U3-specific protein Mpp10. Sucrose gradient analyses and

immunoprecipitation assays revealed that Dbp4, Bfr2 and Enp2 associate together in complexes of 50S and 80S. These proteins do not associate with the U3 snoRNA in the 50S peak, however they interact with the U3 snoRNA in the 80S peak.

3.4 Materials and Methods

3.4.1 Yeast strains and media

All conditional yeast strains and strains expressing tagged proteins were derived from YPH499 (*MAT*a, *ura3-52, lys2-80, ade2-101, trp1-Δ63, his3-Δ200, leu2-Δ1*) (Sikorski and Hieter, 1989). We generated strain GAL::HA-BFR2 (alias YSS5) that expresses 3×HA-tagged Bfr2 under the control of the *GAL1* promoter, which was substituted for the natural promoter by chromosomal integration at the *BFR2* locus (Longtine *et al.*, 1998). Strain YSS5 was further engineered to produce 9×myc tagged Enp2 expressed form its natural promoter (Knop *et al.*, 1999): this new strain (YSS7) is hereafter referred to as the double-tagged strain. Strain GAL::ENP2-myc (alias YSS9) expresses C-terminally 9×myc-tagged Enp2 under the control of the *GAL1* promoter (Longtine *et al.*, 1998). Strain GAL::DBP4-HA expresses 3×HA-tagged Dbp4 under the control of the *GAL1* promoter (Longtine *et al.*, 1998). Strain AH109 was obtained form Clontech (*MAT*a, *trp1-901, leu2-3, 112, ura3-52, his3-200, gal4Δ, gal80Δ, LYS2:: $GAL1_{UAS}$-$GAL1_{TATA}$-HIS3, $GAL2_{UAS}$-$GAL2_{TATA}$-ADE2 URA3:: $MEL1_{UAS}$-$MEL1_{TATA}$-LacZ MEL1*). The strains were grown in rich medium YPD (1% yeast extract, 2% peptone, 2% dextrose), YPGal (1% yeast extract, 2% peptone, 2%

galactose) or synthetic minimal media (0.67% yeast nitrogen base) complemented with the proper dropout mix and appropriate carbon source.

3.4.2 Two-hybrid analyses

The ORF encoding Dbp4 was amplified by PCR from genomic DNA isolated from yeast strain YPH499 following the procedure of Asubel et al. (1999). Primers DBP4-Nco 5'-CAT GCC ATG GCC AAA AAA AAT AGA TTG AAC-3' and DBP4-Xma 5'-CCC CCC GGG TTA ACC CTG GAT TAA TTT AGC TGT C-3' were used, and the DNA fragment was cloned between the NcoI and XmaI sites of pGBKT7 (Clontech) to produce pGBK-DBP4. This plasmid was transformed into yeast strain AH109 and used as bait in a two-hybrid screen carried out with yeast genomic libraries (James *et al.*, 1996). Plasmids pGAD-DBP4, pGAD-BFR2 and pGAD-ENP2 were prepared as described above except that primer pairs DBP4-forXma 5'-CCC CCC GGG TAT GGC CAA AAA AAA TAG ATT GAA-3' and DBP4-revXho 5'-CCG CTC GAG TTA ACC ATG GAT TAA TTT AGC TGT C-3', BFR2-forXma 5'-CCC CCC GGG TAT GGA AAA ATC ACT AGC GGA TCA AAT TTC C-3' and BFR2-revXho 5'-CGC CTC GAG TCA ACC AAA GAT TTG GAT ATC ATC GTT TTT AAC-3', ENP2-forXma 5'-CCC CCC GGG TAT GGT TTT GAA ATC TAC TTC CGC AAA TG-3' and ENP2-revXho 5'-CGC CTC GAG CTA CAT ACC ACG GAA CGC ATT TTT G-3', were used to amplify the ORFs of *DBP4*, *BFR2* and *ENP2*, respectively, and the DNA fragments were individually cloned between de XmaI and XhoI sites of pGADT7 (Clontech). The integrity of two-hybrid constructs

was verified by automated sequencing at the McGill University and Génome Québec Innovation Centre.

The interaction between Dbp4 and various proteins was assessed by the yeast two-hybrid assay in strain AH109. To this end, pGBK-DBP4 was used as bait, and prey plasmids included pGAD-DBP4, pGAD-BFR2, pGAD-ENP2 and pGAD-NOP6. Bait and prey plasmids were simultaneously transformed into yeast strain AH109, and double transformants were selected onto SD-Trp-Leu agar plates (Ausubel 1999). For each combination of bait and prey plasmids, transformants were first streaked onto a SD-Trp-Leu plate and after 3 days of incubation at 30°C, the cells were restreaked onto a SD-Trp-Leu-His plate. To increase the stringency of the two-hybrid assay, 3-Amino-1,2,4-triazole (3-AT) was added to SD-Trp-Leu-His plates at concentrations of 2 mM or 20 mM. Empty bait or prey plasmids were used as controls.

3.4.3 Antibodies

The antibodies used in this study are as follows: anti-HA mouse monoclonal antibody (12CA5 hybridoma supernatant), anti-myc mouse monoclonal antibody (9E10 hybridoma supernatant), anti-Mpp10 rabbit polyclonal (Dunbar *et al.*, 1997), anti-Dbp4 rabbit polyclonal antibodies, anti-Tsr1 rabbit polyclonal (Strunk *et al.*, 2011), anti-MBP rabbit polyclonal antibodies (NEB), anti-Penta·His mouse monoclonal antibody (QIAGEN), and anti-GST goat polyclonal antibodies (GE Healthcare).

The anti-Dbp4 antibodies were raised against recombinant Dbp4Δcat, which lacks most of the catalytic domain of Dbp4 to avoid cross-reaction with other DEAD-box RNA helicases. His-tagged Dbp4Δcat was produced in *Escherichia coli* BL21(DE3) pLysA from the pET23a(+) vector, a kind gift of T.H. King and M.J. Fournier (University of Massachusetts, Amherst, U.S.A.); this construct encodes a mutant derivative of Dbp4 lacking most of the catalytic domain due to elimination of the in-frame EcoRI fragment. His-tagged Dbp4Δcat was first isolated on a HisTrap column using the ÄKTApurifier as recommended by the manufacturer (GE Healthcare). During elution, fractions of 500 µL were collected and peak fractions were pooled; recombinant Dbp4Δcat was further purified by electrophoresis in preparative SDS-gels. These gels were subjected to reverse staining (Ortiz *et al.*, 1992), and the 46-kDa band corresponding to Dbp4Δcat was excised, electro-eluted and concentrated (Microcon filters, Millipore). The purified protein was quantified with the Bio-Rad Protein Assay and stored at -80°C. Immunization of rabbits was carried out in-house at the Animal Care Facility.

3.4.4 Immunoprecipitations

Immunoprecipitation experiments (IPs) were conducted with whole cell extracts (WCEs) prepared from exponentially growing cells. Cells were harvested by centrifugation, washed with sterile water and broken with glass beads in TMN100 buffer (25 mM Tris-HCl, pH 7,5, 100 mM NaCl, 10 mM $MgCl_2$, 0.1 % NP-40). For

RNase treatment, the WCEs were pre-incubated with 30 µg RNase A (Sigma) for 10 min at 37°C, and Mock experiments were incubated similarly except that no RNase A was added. Thirty A_{600} units of cells were collected and after preparation of cellular extract, the equivalent of five A_{600} units were used for each IP experiment; when IPs were done to verify association of large RNA precursors, 30 A_{600} units were used. IPs were also carried out on fractions from sucrose density gradients: fractions 3, 4 and 5 (the "50S" peak) were pooled together, while pooled fractions 7 and 8 formed the "80S" peak. Cell lysates were incubated with protein-A agarose beads (Roche) saturated with anti-Dbp4, anti-Mpp10, anti-HA or anti-myc antibodies. IPs were done at 4°C for 1 hour on a Nutator, and immunoprecipitates were washed five times with 1 ml of TMN100 buffer. For protein analyses, the immunoprecipitates were either mixed with 2×SDS-loading buffer or eluted with elution buffer (25 mM Tris-HCl, pH 7.5, 10 mM EDTA, 0.5% SDS) for 10 min at 65°C, and 2xSDS-loading buffer was added afterwards. For RNA analysis, the immunoprecipitates were eluted with the elution buffer, extracted with phenol/chloroform and precipitated with ethanol. The precipitated RNA was either resuspended in 95% formamide or in 51% formamide and 17% formaldehyde in order to analyze the U3 snoRNA or large RNAs, respectively.

3.4.5 Western blotting

Protein samples were separated by SDS-PAGE, transferred onto a PVDF membrane, and subjected to immunodetection with anti-HA (1/100), anti-myc (1/100), anti-Mpp10 (1/10000), anti-Dbp4 (1/3000), anti-MBP (1/10000), anti-His (1/1000) and anti-GST (1/1500), and the appropriate HRP-conjugated secondary antibodies were used (GE Healthcare). Immunoblots were revealed by chemiluminescence with the Immmobilon Western kit (Millipore).

3.4.6 Northern blotting

To analyze precursor and mature ribosomal RNAs, total RNA was extracted with hot acidic phenol (Ausubel 1999). To detect the U3 snoRNA in either sucrose gradient fractions or IP assays, RNA was isolated using phenol/chloroform extraction as described by (Ausubel 1999). Large RNAs were separated on 1,2% formaldehyde-agarose gels and small RNAs were separated on 8% denaturing polyacrylamide gels. Northern hybridization was carried out with a radiolabeled oligonucleotide probes complementary to the U3 snoRNA or to different rRNA precursors. The oligonucleotide used are as follows: anti-U3, 5'- CCA AGT TGG ATT CAG TGG CTC-3 ; 5'-A0, 5'- CGC TGC TCA CCA ATG G- 3' ; D-A2, 5'-GCT CTC ATG CTC TTG CC-3' ; A2-A3, 5'- TTG TTA CCT CTG GGC CC -3' ; anti-18S, 5'-CAT GGC TTA ATC TTT GAG AC-3' ; anti-25S, 5'-CTC CGC TTA TTG ATA TGC-3' ; anti-5.8S, 5'-GCG TTG TTC ATC GAT GC-3' ; anti-U14 CGA TGG GTT CGT AAG CGT ACT CCT ACC GTG G. The mature 18S and 25S rRNAs were

visualized by staining with GelRed™ (Biotium). Membranes were exposed to a phosphor screen and revealed with a Molecular Imager FX (Bio-Rad).

3.4.7 Sucrose density gradients

WCEs were fractionated on 7–47% linear sucrose gradients as described by (Lemay *et al.*, 2011) except that the lysis buffer was TMK100 (25 mM Tris-HCl, pH 7,5, 100 mM KCl, 10 mM $MgCl_2$, 0.1 % NP-40). Sixteen fractions were collected with an ISCO density gradient fractionation system coupled to a UA-6 detector to produce continuous absorbance profiles at 254 nm. Eighty µl of each fraction was used for protein analyses, and 200 µl were used for RNA analyses.

3.4.8 Pull-down assays

The ORFs encoding Bfr2, Dbp4 and Enp2 were cloned into the following plasmids: pMAL-c5 (NEB), pET-23a(+) (Novagen) and pGEX-4T-1 (GE Healthcare). Proteins were expressed in Rosetta™(DE3) pLysS cells (Novagen). Chloramphenicol and ampicillin were supplemented to the LB medium. Overnight cultures were grown at 37°C, then diluted and grown again to an A_{600} of ~0.6 before induction of 1 mM IPTG. After 2 to 4 hours of induction at 30°C, the cells were harvested, and the pellet was resuspended in lysis buffer (BugBuster®, Novagen). The MBP-Bfr2 extract was precipitated with ammonium sulphate (40%), and the pellet was resuspended in TMN100. The binding and elution of MBP or MBP-Bfr2 fusion protein was carried

out according to pMAL protein fusion and purification system manual (NEB), using amylose magnetic beads (NEB). MBP-Bfr2 coated beads were incubated with Dbp4-His or GST-Enp2, washed with TMN100, and eluted with amylose. Pull-down experiments were also done in the presence of yeast total RNA isolated by the hot acidic phenol procedure (Ausubel 1999). Eluted proteins were analyzed by SDS-PAGE (8% polyacrylamide).

3.5 Results

3.5.1 Bfr2 interacts with Dbp4 and Enp2

The function of many RNA helicases is likely modulated by interacting protein(s) (Silverman *et al.*, 2003). Our bioinformatics searches revealed that the C-terminal extension of Dbp4 harbors a coiled-coil motif that is conserved in all orthologs of Dbp4 (data not shown). This suggested that Dbp4 could interact with other protein(s) through its coiled-coil motif. To identify potential partners of Dbp4 we carried out extensive two-hybrid screens with yeast genomic libraries (James *et al.*, 1996). Among the two-hybrid hits that were identified (unpublished data), Bfr2 was a very attractive candidate because it is a nucleolar protein that has a role in ribosome biogenesis (Bernstein *et al.*, 2004). Database mining further suggested that Bfr2 was a likely partner of Dbp4, together with Enp2 (Collins *et al.*, 2007; Nash *et al.*, 2007; Riffle *et al.*, 2005). All three proteins are essential for yeast growth; they are phylogenetically conserved, and contain at least one coiled-coil motif (data not shown). Like Bfr2, Enp2 is a nucleolar protein that has been classified as a non-SSU

processome component (Bernstein *et al.*, 2004). We carried out directed two-hybrid assays using full-length Dbp4 as bait, and full-length Bfr2 and Enp2 as prey. We also included Dbp4 as prey because DEAD-box RNA helicases can function as dimers (Tanner and Linder 2001), and Dbp4 might do so as well (Krogan et al. 2004). Controls with empty prey plasmid or empty bait plasmid (Figure 3.2) did not grow on selective media ruling out a possible auto-activation of the reporter gene by the bait or preys. We used the ribosome biogenesis factor Nop6 as an additional negative prey control. We could not use Bfr2 as bait because it is an auto-activator (our unpublished observation). Cell growth was observed when Dbp4 (bait) was tested together with Bfr2, Enp2 or Dbp4 as preys on selective medium lacking 3-AT (data not shown). However, when adding 2 mM 3-AT to eliminate background activation of the *HIS3* reporter gene, or up to 20 mM 3-AT to increase the stringency of the selective medium (Toby and Golemis, 2001), only the Dbp4-Bfr2 combination could grow (Figure 3.2), indicating that Dbp4 interacts more strongly with Bfr2 than with the other proteins.

Similar experiments were carried out using Enp2 as bait (Figure 3.2). Growth on selective medium was seen when Enp2 was co-transformed with either Bfr2 or Dbp4, but only the Enp2 and Bfr2 combination could grow in the presence of 20 mM 3-AT. This result indicates that Enp2 and Bfr2 strongly interact together (Toby and Golemis, 2001). Our data are supported by previous studies that identified Bfr2 and Enp2 as potential partners of Dbp4, and Bfr2 as a potential partner of Enp2 (Gavin *et al.*, 2002; Hazbun *et al.*, 2003; Krogan *et al.*, 2006). Taken together, our two-hybrid

analyses suggest that the association between Dbp4 and Enp2 might be dependent on the presence of Bfr2.

3.5.2 Dbp4 is associated with Bfr2 and Enp2 *in vivo*

To validate the two-hybrid results, we verified the interaction between Dbp4, Bfr2 and Enp2 *in vivo*. We were not able to tag Bfr2 at its C-terminus (see also reference Bernstein et al, 2004), we therefore generated a strain that expresses HA-tagged Bfr2 (HA-Bfr2) under the control of the *GAL1* promoter and myc-tagged Enp2 (Enp2-myc) from its endogenous promoter; this strain was named double-tagged strain. We carried out immunoprecipitation experiments (IPs) with extracts prepared from the double-tagged strain grown in galactose-containing medium (Figure 3.3A). IPs were done using the anti-HA monoclonal antibody (mAb) for Bfr2 IPs, an anti-myc mAb for Enp2 IPs and rabbit polyclonal antibodies raised against Dbp4 (hereafter named anti-Dbp4). Control IPs were done with uncoated agarose beads (BA). These experiments show that Dbp4 is associated with Bfr2 and Enp2 *in vivo* (lane 4 in Figure 3.3A) and Bfr2 and Enp2 also interact together *in vivo* (lanes 3 and 5 in Figure 3A). Thus, IPs confirm the two-hybrid assays showing a strong interaction between Bfr2 and Enp2.

DEAD-box RNA helicases use the energy of ATP to bind and remodel RNA or RNA–protein complexes (Garcia and Uhlenbeck, 2008; Jankowsky, 2011). We tested whether the association between Dbp4 and its two partners was dependent on the presence of RNA. IPs were carried out with cellular extracts pre-treated with RNase A. As shown in Figure 3.3B, the association of Dbp4 with either Bfr2 or Enp2

was lost when using RNase-treated extracts (compare lane 7 with lanes 3 and 5) showing that their association is RNA-dependent in agreement with the recent demonstration that Dbp4 needs additional contacts with the extension flanking the RNA duplex for optimal helicase activity (Garcia *et al.*, 2012). In contrast, the interaction between Bfr2 and Enp2 was not affected by RNase treatment, showing that their association is not dependent on the presence of RNA (Figure 3.3C).

To determine if Bfr2 is required for the association of Dbp4 with Enp2, we carried out IPs with Bfr2-depleted cellular extracts. The double-tagged strain was grown to exponential phase in medium containing galactose (YPGal) and then shifted to dextrose-containing medium (YPD) for 8 hours. We chose the 8-hour time point for our experiments because western blot analysis showed no detectable Bfr2 in the cellular extract (Figure 3.5D, lower panel). Cells were collected from both culture media and IPs were done with anti-Dbp4 Abs (Figure 3.3D). These experiments showed that the interaction between Dbp4 and Enp2 was decreased in Bfr2-depleted cells, and this was not due to loss of Dbp4 in the immunoprecipitate (Figure 3.3D, lower panel). These data corroborate our two-hybrid results suggesting that Bfr2 bridges Dbp4 and Enp2.

3.5.3 Bfr2 and Enp2 are necessary for early cleavages leading to 18S rRNA maturation

It has been shown that Dbp4 is necessary for early pre-rRNA cleavages at sites A0, A1 and A2 (Kos and Tollervey, 2005; see Figure 3.1). Because Bfr2 and Enp2

associate with Dbp4, we decided to investigate their involvement in rRNA maturation.

Cells were grown to exponential phase in YPGal using the following two strains GAL::HA-BFR2 expressing HA-tagged Bfr2, and GAL::ENP2-myc encoding myc-tagged Enp2, both under the control of the *GAL1* promoter. The cells were then shifted to YPD and harvested at different time points after depletion; total RNA was extracted and used for northern analyses. Results of Bfr2-depletion are shown in Figure 3.4A: upon depletion of Bfr2 there is a decrease in the production of the 27SA2 precursor, consistent with the loss of cleavage at site A2. We also observed an increase in the amount of 35S and 23S pre-rRNAs compared to the non-depleted sample. The 35S and 23S pre-rRNA usually accumulate in absence of early cleavages at sites A0-A2 (Venema and Tollervey, 1999). The levels of 20S pre-rRNA and the mature 18S rRNA were decreased, consistent with impaired cleavages at sites A0-A2. There were no changes observed in the abundance of the mature 25S and 5.8S rRNA. The same type of results were obtained with Enp2-depleted cells (Figure 3.4B): 1) high levels of 35S and 23S pre-rRNAs; 2) low levels of 27SA2, 20S pre-rRNAs and mature 18S rRNA; and 3) no change in the levels of 25S and 5.8S rRNAs. Taken together these results indicate that Bfr2 and Enp2 are implicated in early processing events that lead to 18S rRNA production.

Polysome profiles of Bfr2- and Enp2-depleted cells were analyzed by sucrose density gradient sedimentation: we observed decreased amounts of 40S and 80S ribosomes, and an increase of free 60S subunits (data not shown). These defects are

consistent with impaired 40S subunit biogenesis and the altered pre-rRNA processing events seen in Bfr2- and Enp2-depleted cells (Figure 3.4A and 3.4B).

3.5.4 Bfr2 and Enp2 associate with the U3 snoRNA and Mpp10

We know that Dbp4 associates specifically with the U3 snoRNA and the U3-specific protein Mpp10 (our unpublished data). We decided to verify if Bfr2 and Enp2 also associate with these SSU processome components. IPs were carried out with Mpp10 antibodies followed by western analysis (Figure 3.5A). The results show that Mpp10 associates with Bfr2 and Enp2. We also immunoprecipitated Bfr2 and Enp2, and observed that Bfr2 associate with Mpp10 (Figure 3.5B). The fact that Enp2 co-immunoprecipitates with Mpp10 but Mpp10 was not detected in Enp2 IPs suggests that the bulk of Enp2 is not in complex with Mpp10 or that the amount of co-immunoprecipitated Mpp10 is below detection limit. Nevertheless, these results show that Bfr2 and Enp2 can associate with Mpp10. To verify the association of the U3 and U14 snoRNAs with Bfr2, Dbp4 and Enp2, IPs were done using WCEs as described in Figure 5B, followed by northern analysis (Figure 3.5C). The results indicate that Bfr2, Dbp4 and, to a lesser extent, Enp2 associate with the U3 snoRNA. There was no association between U14 snoRNA and Bfr2, Dbp4 or Enp2 (Figure 3.5C, upper panel). We then asked if the absence of Bfr2 affected the interactions between U3 snoRNA and Dbp4 or Enp2. Cellular extracts were prepared from the double-tagged strain after growth in YPD to deplete Bfr2, and IPs were done as described above. In the absence of Bfr2 the interaction between Enp2 and the U3 snoRNA was lost,

whereas the association of Dbp4 with U3 was decreased about 2-fold (Figure 3.5C, lower panel). These data indicate that Bfr2 is necessary for the association of Enp2 with the U3 snoRNA. The absence of Bfr2 also affected the Dbp4-U3 snoRNA interaction (but to a lesser extent). Note that the efficiency of Dbp4 and Enp2 IPs with extracts from undepleted and Bfr2-depleted cells were the same (Figure 3.5D, upper and middle panel).

3.5.5 Dbp4, Bfr2 and Enp2 associate with pre-rRNAs

Our results suggest that Bfr2, Dbp4 and Enp2 could be SSU processome components. To further investigate this possibility, we tested whether these proteins associate with rRNA precursors. Extracts were prepared from undepleted and Bfr2-depleted cells, and we carried out IPs followed by northern analyses (Figure 3.6). The results show that in the presence of Bfr2, the 23S pre-rRNA associates with Bfr2, Dbp4 and Enp2 (lanes 3-5). Interestingly, we observed that Bfr2, Dbp4 and Enp2 also interact with the 20S pre-rRNA (lanes 3-5). This result suggests that Bfr2, Dbp4 and Enp2 stay associated with the pre-rRNA after its cleavage at site A2. We were also able to detect the association of Bfr2 with the 35S and 32S pre-rRNA (lane 3). In the absence of Bfr2, there was a loss of association of Enp2 with the pre-rRNAs (lane 10). In contrast, Dbp4 remained associated with the 23S pre-rRNA, and to a lesser extent with the 35S pre-rRNA (see upper panel in Figure 3.6).

3.5.6 Depletion of Bfr2 alters the sedimentation profile of Dbp4 and Enp2

We carried out sucrose gradient sedimentation analyses to determine the sedimentation behavior of Bfr2, Dbp4 and Enp2. The double-tagged strain was grown in YPGal and then shifted to YPD, and cellular extracts were prepared for ultracentrifugation through sucrose gradients. The gradients were fractionated into 16 fractions, and each fraction was subjected to western and northern analyses. As shown in Figure 3.7A, Dbp4, Bfr2 and Enp2 co-sediment in a peak of about 50S in sucrose gradients. Bfr2 and Enp2 are also enriched in the 80S region of the gradient, which contains very little Dbp4. The distribution of Dbp4 could reflect the transient nature of its interactions with component(s) of the 80S complex (see below). We also analysed the sedimentation profile of Mpp10, which was enriched at the top of the gradient and in the 80S region of the gradient. When cells were depleted of Bfr2 for 8 hours, Dpb4 was distributed in a wide peak of 40-80S; the fact that Dbp4 appears in complexes of various sizes upon depletion of Bfr2 implies that dynamic rearrangements of Dbp4 complexes require the presence of Bfr2. Depletion of Bfr2 also changed the sedimentation profile of Enp2, which sedimented in low-density fractions, suggesting that Bfr2 is required for association of Enp2 with complexes of about 50S and 80S. In contrast, the sedimentation profile of Mpp10 remained almost unchanged. These data indicate that depletion of Bfr2 alters the sedimentation profiles of Dbp4 and Enp2 but not that of Mpp10.

We also analyzed the sedimentation pattern of the U3 and U14 snoRNAs in the presence or the absence of Bfr2 (Figure 3.7B). The U3 snoRNA is normally

detected in low-density fractions and in the 80S region of the gradient (top panel in Figure 3.7B). In the absence of Bfr2, there was no change in the overall sedimentation pattern of the U3 snoRNA (bottom panel in Figure 3.7B). This is similar to what was observed with Mpp10 in Bfr2-depleted cells (see Figure 3.7A). However, there was an important change in the distribution pattern of U14 snoRNA with Bfr2-depleted extracts: U14 accumulated to a much higher extent in the 80S region, and this was accompanied by a decrease in its abundance in fractions 3-5 (Figure 3.7C). These results suggest that Bfr2 affects the release of U14 snoRNA from pre-rRNAs by Dbp4.

3.5.7 Molecular interactions of Bfr2, Dbp4 and Enp2 in the 50S and 80S complexes

We conducted a more refined analysis to investigate the association between Bfr2, Dbp4 and Enp2 in the 50S and 80S peaks. Sucrose gradient fractions were obtained from undepleted and Bfr2-depleted cells; fractions 3-5 ("50S" complex) or 7-8 ("80S" complex) were pooled together, and IPs were carried out on the 50S pool and the 80S pool followed by western blot analyses (Figure 3.8A).

The intensity of the signals in Bfr2, Dbp4 and Enp2 inputs from 50S and 80S peaks in undepleted and Bfr2-depleted cells correlated with their sedimentation profiles in sucrose gradients; for example, upon Bfr2 depletion the amount of Enp2 was reduced in the 80S peak compared to undepleted cells (compare lane 2 and 4 in Figure 3.8A).

IPs with the "50S" and "80S" peak of undepleted cells revealed that Bfr2, Dbp4 and Enp2 co-precipitated (see lanes 5, 9, 13 and 6 in Figure 3.8A). These results suggest that Bfr2, Dbp4 and Enp2 associate together in the 50S and 80S peak. When Bfr2 was depleted, Dbp4 could no longer associate with Enp2 in the 50S and 80S (lanes 7 and 8).

We investigated the association of the U3 snoRNA with Bfr2, Dbp4 and Enp2 in the "50S" and "80S" peaks. IPs were done as described in Figure 3.8A using undepleted cells and the U3 snoRNA was detected by northern hybridization (Figure 3.8B). U3 could be detected in the 50S peak but it did not co-immunoprecipitate with Bfr2, Enp2 or Dbp4. However, the U3 snoRNA present in the 80S peak (SSU processome) did co-immunoprecipitate with Bfr2 and Enp2, and to lesser extent with Dbp4 (detectable upon overexposure; see the bottom panel with the asterisk). Thus, the "50S" complex containing Bfr2, Dbp4 and Enp2 does not include the U3 snoRNA, but Bfr2, Dbp4 and Enp2 associate with U3 in the SSU processome.

We also verified if Bfr2, Dbp4 and Enp2 are associated with U14 snoRNA in the "50S" and "80S" peaks. There is no association between U14 snoRNA and Bfr2 or Enp2 in these peaks (data not shown). In contrast, U14 snoRNA was associated with Dbp4 in the "50S" peak of undepleted cells, and in the "80S" peak of Bfr2-depleted cells (Figure 3.8C). These results correlate well with the sucrose gradient sedimentation profiles (Figure 3.7C). In Bfr2-depleted cells, Dbp4 and U14 snoRNA remained associated in the 80S peak, suggesting the release of U14 snoRNA from the 80S complex was impaired in the absence of Bfr2.

To determine whether the "50S" complex could be a pre-40S ribosome, we verified if Bfr2 and Enp2 were associated with Tsr1, a GTPase-like protein involved in assembly of pre-40S ribosomes (Campbell and Karbstein, 2011; Gelperin *et al.*, 2001). IPs conducted with the 50S and 80S peaks isolated from undepleted cells revealed that Tsr1 did not co-immunoprecipitate with Enp2, nor with Bfr2 (Figure 3.9). Therefore, the "50S" complex containing Enp2 and Bfr2 is not a pre-40S ribosome.

3.5.8 The binding partners of Bfr2

To better define the nature of the interaction between Bfr2, Dbp4 and Enp2, we carried out pull-down experiments using bacterially expressed recombinant proteins. The results show that Bfr2 binds directly to Enp2 but not to Dbp4 (Figure 3.10, left panel). Adding Enp2 to the mixture did not improve Dbp4 binding to Bfr2 (data not shown). Interestingly, when yeast total RNA extracted with hot acidic phenol (and devoid of proteins) was added to the mixture, Dbp4 could bind Bfr2 (Figure 3.10, right panel). These results are in perfect agreement with our IP experiments showing that association of Dbp4 with Bfr2 is RNA-dependent, and that the interaction of Enp2 with Bfr2 is not dependent on the presence of RNA (Figure 3.3).

3.5.9 Association of U3 snoRNA with Mpp10 in depleted cells

In order to test the order of recruitment of Bfr2 and Dbp4 into the SSU processome complex, we determined whether the Mpp10-U3 snoRNA association was perturbed

in the absence of Bfr2 or Dbp4 (Figure 3.11). These experiments showed that U3 snoRNA and Mpp10 remained associated in Bfr2- or Dbp4-depleted cells. Thus, our results suggest that Bfr2 and Dbp4 are recruited into the SSU processome after the incorporation of the U3 snoRNP and Mpp10 subcomplex.

3.6 Discussion

There are more than 200 non-ribosomal factors required for processing, modification and assembly reactions during ribosome biogenesis (Fromont-Racine *et al.*, 2003; Henras *et al.*, 2008; Kressler *et al.*, 2010; Phipps *et al.*, 2011b). A large number of these proteins are part of the SSU processome complex (Lim *et al.*, 2011), which is necessary for the maturation of 18S rRNA (Dragon *et al.*, 2002; Osheim *et al.*, 2004). Some proteins of the SSU processome form specific sub-complexes (Champion *et al.*, 2008; Dosil and Bustelo, 2004; Freed and Baserga, 2010; Gallagher *et al.*, 2004; Granneman *et al.*, 2009; Krogan *et al.*, 2004; Lee and Baserga, 1999; Rudra *et al.*, 2007; Venema *et al.*, 2000; Wegierski *et al.*, 2001; Wehner *et al.*, 2002) but more than a half of its components are not categorized into known sub-complexes (Phipps *et al.*, 2011b). Moreover, most of the protein-protein interactions between SSU processome components have not been identified yet (Phipps *et al.*, 2011b). Thus, studying the protein interactions of the SSU processome is important to refine our understanding of the assembly, architecture and activity of this complex during ribosome biogenesis (Lim *et al.*, 2011; Phipps *et al.*, 2011b). Dbp4 is one of the DEAD-box RNA helicases necessary for the early cleavages of the

pre-rRNA at sites A0-A2, cleavages that lead to the production of 18S rRNA (Kos and Tollervey, 2005; see Figure 1). To get a better understanding of the assembly and function of the SSU processome, we decided to analyze the role of Dbp4 in molecular interactions leading to the production of 18S rRNA.

We identified Bfr2 and Enp2 as partners of Dbp4 using yeast two-hybrid assays (Figure 3.2), and we showed by immunoprecipitation with antibodies to Dbp4 that Bfr2 and Enp2 associate with Dbp4 *in vivo* (Figure 3.3). With the yeast two-hybrid system, there is always a risk that the bait protein binds a secondary factor that mediates (or bridges) the interaction with the prey protein. Pull-down assays with bacterially expressed recombinant proteins revealed that Bfr2 binds directly to Enp2 but not to Dbp4; however, when adding yeast total RNA to the mixture, Dbp4 could bind Bfr2 (Figure 3.10). The RNA used in these experiments is devoid of proteins, ruling out the possible involvement of third protein mediating the interaction. Since Bfr2 does not contain an RNA-binding motif, it is unlikely that RNA acts as a mediator of the interaction with Dbp4. Thus, the simplest explanation is that RNA binding to Dbp4 could induce a conformational change that facilitates its interaction with Bfr2.

When IPs were done *via* the Brf2 or Enp2 component, the results showed that Bfr2 and Enp2 interacted with each other, but not with Dbp4 (Figure 3.3A). It is possible that the amount of co-precipitated Dbp4 in IPs for either Bfr2 or Enp2 was under the detection limit. This may also reflect differences in the stoichiometry or differential accessibility of the tags within the complex. Depletion of Bfr2 impaired

the association of Dbp4 with Enp2 (Figure 3.3D). Note that the association between Dbp4 and Enp2 was not completely lost, possibly because small amounts of Bfr2 could still be present after 8 hours of depletion. Based on the results from two-hybrid assays, IPs and pull-down assays, we propose a model for the interaction between these three proteins. Bfr2 and Enp2 interact directly together in an RNA-independent manner (Figures 3.3 and 3.10). RNA binding to Dbp4 induces a conformational change, which allows interaction with Bfr2. In this scenario, Bfr2 would act as a bridge between Dbp4 and Enp2.

Previous studies showed that Dbp4 is involved in the maturation of 18S rRNA. Our findings indicate that Bfr2 and Enp2 are also implicated in this process (Figure 3.4). In fact, the processing defects observed in either Bfr2- or Enp2-depleted cells are consistent with the involvement of Bfr2 and Enp2 in the early processing events at cleavage sites A0, A1 and A2. The hallmark of such processing defects is the strong accumulation of 23S pre-rRNA, which was observed in Bfr2- and Enp2-depleted cells (Figure 4). Li et al. 2009 reported that Bfr2 and Enp2 are involved in pre-rRNA processing because their depletion led to accumulation of the 35S pre-rRNA; however, they did not see strong accumulation of 23S pre-rRNA upon depletion. The phenotypes observed by Li et al. 2009 could be due to degradation of 23S pre-rRNA upon long depletion times (see also Bernstein et al, 2004).

Formation of the SSU processome is necessary for the maturation of the 18S rRNA (Osheim *et al.*, 2004). The SSU processome complex consists of the U3 snoRNA, Mpp10 (U3-specific protein) and many other nucleolar factors (Bernstein *et*

al., 2004; Dragon *et al.*, 2002; Lim *et al.*, 2011). Previous investigations indicated that Dbp4 associates with U3 snoRNA and Mpp10 (unpublished data), and here we showed that Bfr2 and Enp2 also associate with U3 and Mpp10 (see Figure 3.5). We were able to co-immunoprecipitate Mpp10 with Bfr2 but not with Enp2 (Figure 3.5B), (though the amount of Mpp10 co-precipitated with Enp2 may be too small in order to be detectable by our western analyses). These analyses suggest that Dbp4, Bfr2 and Enp2 could be SSU processome components.

We showed that Bfr2, Dbp4 and Enp2 associate with various pre-rRNAs in non-depleted cells (Figure 3.6). Interestingly, these three proteins associate with the 20S pre-rRNA, suggesting that they remain associated with the rRNA precursor after the A2 cleavage until nuclear export, in line with the findings of Li et al. 2009 who reported that Bfr2 and Enp2 were required for small subunit export. In Bfr2-depleted cells, the interaction of Enp2 with 23S and 20S pre-rRNA was lost. Thus, the presence of Bfr2 is required for the association of Enp2 with these pre-RNAs. In contrast, Dbp4 interacts with the 35S pre-rRNA and stays associated with the 23S pre-rRNA in Bfr2-depleted cells. Therefore, it appears that Bfr2 affects the molecular interactions of Dbp4 with pre-18S rRNAs during processing events leading to the maturation of 18S rRNA.

Analyzing the sedimentation pattern of ribosome biogenesis factors by sucrose gradient sedimentation is useful because co-sedimentation of non-ribosomal factors with the pre-ribosomal particles may suggest physical interaction with these particles. The SSU processome has a sedimentation coefficient of about 80S (Dragon

et al., 2002). The data obtained from sucrose gradient sedimentation and IPs on pooled fractions of the gradient (Figure 3.7 and 3.8) indicate that the 50S complex contains Bfr2, Dbp4, Enp2 and U14 snoRNA (and possibly additional nucleolar factors), whereas the 80S complex (the SSU processome) contains Bfr2, Dbp4, Enp2 and U3 snoRNA (Figure 3.8A and B). These results highlight the dynamic reorganization of large complexes during maturation of 18S rRNA. Note that the "50S" complex is not a pre-40S ribosomal particle since there was no association of Tsr1 with Bfr2 or Enp2 (Figure 3.9). It has been shown that actinomycin D treatment induces accumulation of a 50S U3 snoRNP particle that contains DDX10 (human homologue of Dbp4) in HeLa cells (Turner *et al.*, 2009). Given that the "50S" complex described in this study does not contain the U3 snoRNA, it appears that the 50S complex seen in HeLa cells is not the same as the one we characterized here.

Another interesting observation was that, when using WCEs for IPs, there was no association between U14 snoRNA and Bfr2, Dbp4 or Enp2 (Figure 3.5C). However, Dbp4 was associated with U14 snoRNA in the "50S" peak in undepleted cells (Figure 3.8C). When cells were depleted of Bfr2, U14 snoRNA was associated with Dbp4 in the 80S peak, suggesting that Bfr2 could be implicated in the release of U14 snoRNA from the "80S" complex. Discrepancies between IPs with WCEs and sucrose gradient fractions could be explained by the amount of material used, or simply by the fact that fractions isolated from sucrose gradients are partially purified complexes, which may enhance the efficiency of IPs by eliminating interfering components.

Based on the following data, we propose that Bfr2, Dbp4 and Enp2 are SSU processome components: 1) Bfr2, Dbp4 and Enp2 are nucleolar proteins 2) they are involved in pre-rRNA processing at cleavage sites A0, A1 and A2, 3) these proteins associate with the U3 snoRNA and Mpp10, and also interact with different pre-18S rRNA species, 4) Bfr2, Dbp4 and Enp2 co-sediment in a peak of about 80S, and they associate with U3 snoRNA in that peak.

Nan1 is a component of the t-UTP sub-complex, which assembles at a very early step during SSU processome formation (even before U3 snoRNP incorporation). Depletion of Nan1 changes the sedimentation profile of U3 snoRNA (Dutca *et al.*, 2011; Perez-Fernandez *et al.*, 2007). The absence of Bfr2 did not alter the sedimentation profile of the U3 snoRNA and Mpp10 (Figure 3.7). Moreover, the absence of Bfr2 or Dbp4 did not affect the association between U3 snoRNA and Mpp10 (Figure 3.11). These results suggest that Bfr2 and Dbp4 might assemble into the SSU processome after assembly of the U3 snoRNP and Mpp10 sub-complexes. According to our results and the studies of (Perez-Fernandez *et al.*, 2007), we propose a simplified model for the assembly steps of the SSU processome (Figure 3.12). First the UtpA/t-Utp binds to the pre-rRNA followed by two mutually independent steps: one step includes the assembly of the UtpB and the other involves the association of UtpC with the 35S during later assembly steps. The U3 snoRNP base pairs with the pre-rRNA after UtpB binding, which in turn allows the assembly of the Mpp10 sub-complex on the nascent pre-rRNA. Bfr2, Enp2 and Dbp4 then incorporate into the SSU processome particle. The results from IPs and sucrose gradient sedimentation,

combined with the observation that the absence of Bfr2 did not affect the association of Dbp4 and U3 snoRNA in the 80S peak (data not shown), suggest that Bfr2 and Enp2 are recruited together but Dbp4 could be incorporated independently from Bfr2 and Enp2.

Our results provide new insight into the order of assembly of three nucleolar proteins into the nascent SSU processome. This additional data refines our understanding of SSU processome structure and function.

3.7 Acknowledgments

We would like to thank Korka Ba for carrying the original yeast two-hybrid screen, Sabrina Makhlouf for two-hybrid analyses, Karen Wehner for the anti-HA mAb, Susan Baserga for anti-Mpp10 antibodies, Katrin Karbstein for the anti-Tsr1 antibodies, Tom King and Skip Fournier for the pET23-Dbp4Δcat construct, Vincent Lemay for help with artwork, and Ann Beyer for comments on the manuscript.

3.8 Funding

The National Sciences and Engineering Research Council of Canada (NSERC), RGPIN 249792.

3.9 Figure Legends

Figure 3.1. The pre-rRNA processing pathway in yeast.

The structure of the 35S pre-rRNA (primary transcript) is shown on top. The rectangles represent cellular compartments in which different steps of the processing pathway take place. The pre-rRNA cleavage sites are indicated on the transcripts.

Figure 3.2. Directed yeast two-hybrid assays.

Yeast strain AH109 was transformed with bait plasmid pGBKT7 (Vec) or its derivative pGBK-DBP4 or PGBK-ENP2, and prey plasmid pGADT7 (Vec) or its derivatives pGAD-DBP4, pGAD-ENP2, pGAD-BFR2 and pGAD-NOP6. The bait and prey plasmids respectively carry *TRP1* and *LEU2* auxotrophic markers that allow growth on medium lacking tryptophan and leucine (upper panel). Interactions between bait and prey hybrid proteins activate transcription of the *HIS3* reporter gene, which is monitored by growth on medium lacking histidine; addition of 2 or 20 mM 3-AT to this medium enhances the stringency of the *HIS3* reporter, allowing detection of the strongest two-hybrid interactions (middle and lower panels, respectively).

Figure 3.3. Analyzing interaction between Bfr2, Dbp4 and Enp2 by IPs.

(A) Dbp4 associates with Bfr2 and Enp2 *in vivo*. IPs were carried out with anti-HA, anti-myc, and anti-Dbp4 antibodies using extracts prepared from the double-tagged strain that expresses HA-tagged Bfr2 under the control of the *GAL1* promoter and

myc-tagged Enp2 from its natural promoter. Control IPs were done in absence of antibodies (beads alone, BA). Lane 1 is whole cell extract (T is 6.5% input), and lanes 2-5 are IPs with beads alone (BA), anti-HA mAb (Bfr2), anti-Dbp4 antibodies and anti-myc mAb (Enp2). The same blot was subjected to immunodetection with various antibodies recognizing proteins identified on the right.

(B) Dbp4 associates with Bfr2 and Enp2 in a RNA-dependent manner. Control IPs (lanes 1-3) were done as in Figure 3A. In the Mock (lanes 4-5) the cellular extract was incubated at 37°C for 30 min prior to IP, and in lanes 6 and 7 the cellular extract was treated with RNase A for 37°C for 30 min. IPs were done in absence of antibodies (BA, lane 2) or with anti-Dbp4 antibodies (lanes 3-7), and immunoblotting was performed using anti-myc (Enp2) and anti-HA mAbs (Bfr2). T is 6.5% of input.

(C) Association of Bfr2 with Enp2 is not RNA-dependent. IPs were carried out as in Figure 3B except that anti-myc mAb (Enp2) was used for IP, and immunodetection was performed with anti-HA mAb (Bfr2). T is 6.5% of input.

(D) Bfr2 is required for the association of Dbp4 with Enp2. Cellular extracts were prepared from undepleted cells (0h, lanes 1-2) or Bfr2-depleted cells (8h, lanes 3-4). IPs were carried out with anti-Dbp4 antibodies and western blotting for Enp2 and Dbp4 were done with anti-myc mAb and anti-Dbp4 antibodies respectively. The asterisk indicates the overexposed blot. T is 6.5% of input.

Figure 3.4. Bfr2 and Enp2 are required for pre-rRNA processing.

Total RNA was extracted from depletion strains GAL::HA-BFR2 **(A)** and GAL::ENP2-myc **(B)** grown in YPGal (0h, lane 1), and at different depletion times after the shift in YPD (lanes 2-4). RNAs were analyzed by northern hybridization using probes directed against different rRNA precursors indicated on the right. Mature 18S and 25S rRNAs were visualized by staining with GelRed™. The short and long forms of 5.8S rRNA were detected by northern hybridization.

Figure 3.5. Bfr2 and Enp2 associate with Mpp10 and the U3 snoRNA.

(A) Mpp10 associates with Bfr2 and Enp2. IPs were carried out with anti-Mpp10 antibodies, and immunoblotting was done with anti-myc (Enp2) and anti-HA (Bfr2) antibodies.

(B) Bfr2 interact with Mpp10. IPs were carried out with anti-HA (Bfr2) and anti-myc (Enp2) antibodies and western blotting was done with anti-Mpp10 antibodies.

(C) Association of U3 snoRNA with Bfr2, Dbp4 and Enp2 in presence or absence of Bfr2. IPs were carried out with beads alone (BA), anti-HA (Bfr2), anti-Dbp4 and anti-myc (Enp2) antibodies. Northern analysis was done with a radiolabeled oligonucleotide complementary to the U3 and U14 snoRNAs. In the top panel, cellular extracts were prepared from undepleted cells (0 h). In the bottom panel, cellular extracts were obtained form Bfr2-depleted cells (8 h). T is the input (10%), S is the supernatant (10%), and IP is the immunoprecipitated RNA.

(D) IPs of Dbp4 and Enp2 in undepleted and Bfr2-depleted cells

IPs were done with undepleted (0 h) and Bfr2-depleted cells (8 h) using anti-Dbp4 and anti-myc (Enp2) antibodies, and immunoblotting was done with anti-myc (Enp2), anti-Dbp4 and anti-HA (Bfr2) antibodies. The asterisks indicate the overexposed blots.

Figure 3.6. Bfr2, Dbp4 and Enp2 associate with pre-rRNAs.

Cellular extracts were prepared from undepleted and Bfr2-depleted cells. IPs were done without antibodies (BA) and with anti-HA (Bfr2), anti-Dbp4 and anti-myc (Enp2) antibodies. Northern analysis was done with a radiolabeled oligonucleotide to detect pre-rRNAs. The asterisk indicates the overexposed blot.

Figure 3.7. Sedimentation patterns upon Bfr2-depletion

(A) Sedimentation profiles of Dbp4, Bfr2, Enp2 and Mpp10. Cellular extracts were prepared from undepleted (0h) and Bfr2-depleted cells (8h) and fractionated on 7-47% sucrose density gradients. Fractions 1-16 were subjected to western blot analysis using anti-myc (Enp2), anti-Dbp4, anti-HA (Bfr2) and anti-Mpp10 antibodies. The position of 40S and 60S ribosomal subunits, 80S ribosome and polysomes are indicated.

(B) Sedimentation profile of the U3 and U14 snoRNAs. Sucrose gradient fractions were prepared as in Figure 6A except that RNAs were extracted from fractions 1-16

and subjected to northern blot analysis with radiolabeled oligonucleotides complementary to the U3 or U14 snoRNA.

Figure 3.8. Association of Bfr2, Dbp4 and Enp2 in complexes of "50S" and "80S" isolated from sucrose gradients.

(A) Cellular extracts obtained from undepleted and Bfr2-depleted cells were fractionated on sucrose gradients as in Figure 7A, and two series of inputs (In) were prepared for IPs: pooled fractions 3-5 correspond to the "50S" complex and fractions 7-8 are the "80S" complex. IPs were done with anti-Dbp4 (lanes 5-8), anti-myc (lanes 9-12), and anti-HA Abs (lanes 13 and 14). Western blot analyses were carried out using the same antibodies to detect the presence of Enp2 (myc), Bfr2 (HA) and Dbp4. Input lanes correspond to 12% of pooled fractions.

(B) Gradient fractions were prepared from undepleted cells and IPs were done as in Figure 8A except that RNAs were extracted and subjected to nothern hybridization with a radiolabeled oligonucleotide complementary to the U3 snoRNA. Inputs (In) correspond to 10%. The asterisk indicates the overexposed blot of Dbp4 IP.

(C) IPs were done with anti-Dbp4 Abs as in Figure 8B, except that northern hybridization was carried out with a radiolabeled oligonucleotide complementary to the U14 snoRNA.

Figure 3.9. Bfr2 and Enp2 do not associate withand Tsr1.

IPs were carried out with anti-myc (Enp2; upper panel) and anti-HA (Bfr2; lower panel) mAbs as in Figure 8A, except that western blot analyses were done using anti-Tsr1 polyclonal antibodies.

Figure 3.10. Pull-down assays with recombinant proteins.

Pull-down experiments were carried out using MBP (lanes 2 and 5) or MBP-Bfr2 (lanes 3 and 6) bound to amylose beads. After incubation and elution, the presence of proteins Dbp4-His, GST-Enp2 and MBP-Bfr2 was detected by immunoblotting. Experiments were done in the absence of RNA (w/o RNA; left panels) or in the presence of yeast total RNA (with RNA; right panels).

Figure 3.11. Association of U3 snoRNA and Mpp10 is not affected by depletion of Bfr2 or Dbp4.

IPs with anti-Mpp10 Abs were done with extracts from undepleted cells, or cells depleted of Bfr2 or Dbp4 for 8 hours (as in Figure 5C).

Figure 3.12. Simplified model for the assembly steps of the SSU processome

1) The UtpA/t-Utp sub-complex assembles on the 5'ETS of the nascent pre-rRNA; 2) UtpB then associates with the pre-rRNA followed by binding of the U3 snoRNP complex (3); 4) UtpC interacts with the pre-rRNA independent of UtpB and U3 snoRNP; 5) Mpp10 sub-complex assembly takes place after U3 snoRNP binding; 6) The Bfr2-Enp2 dimer and Dbp4 incorporate the SSU processome particle.

3.10 Figures

Figure 3.1

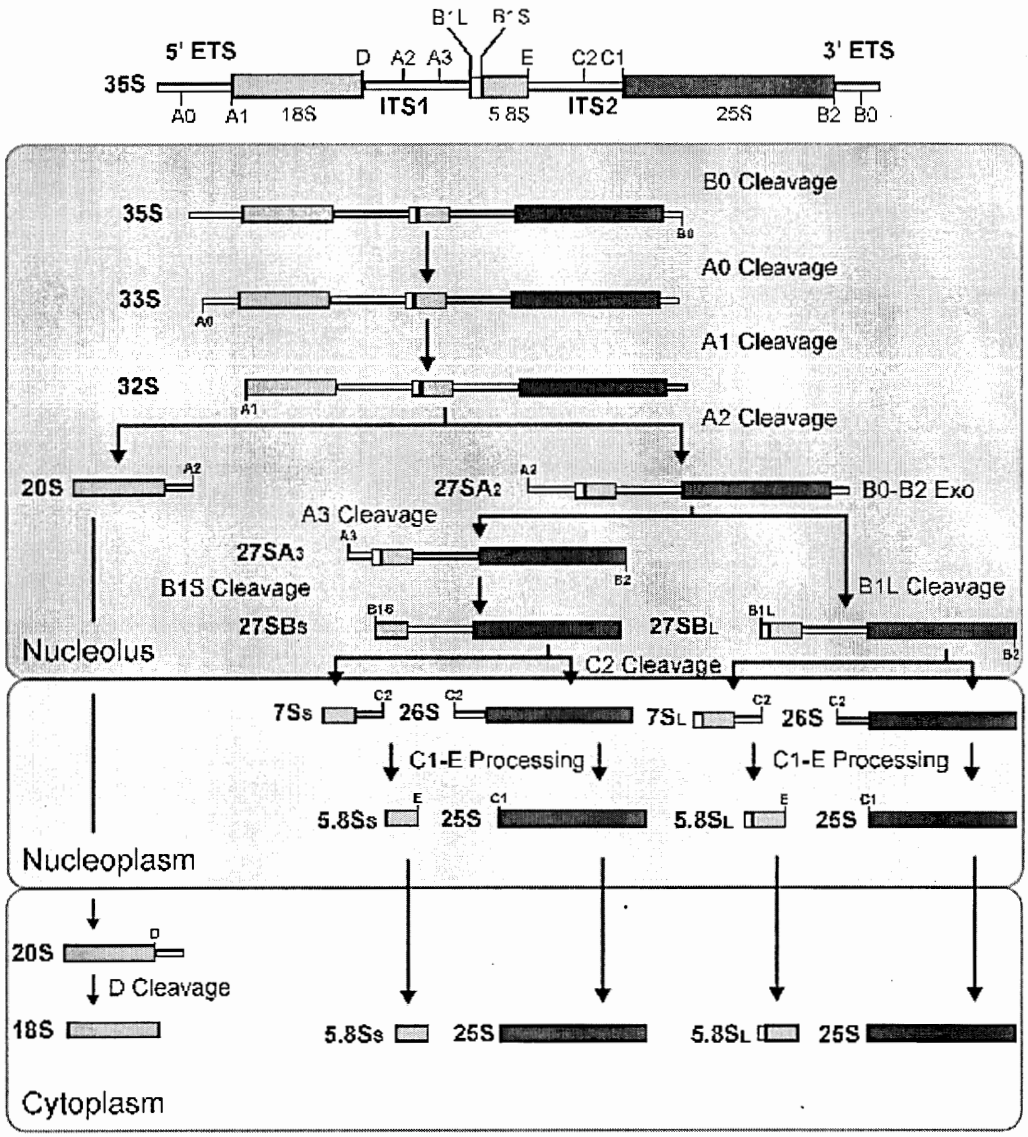

Figure 3.2

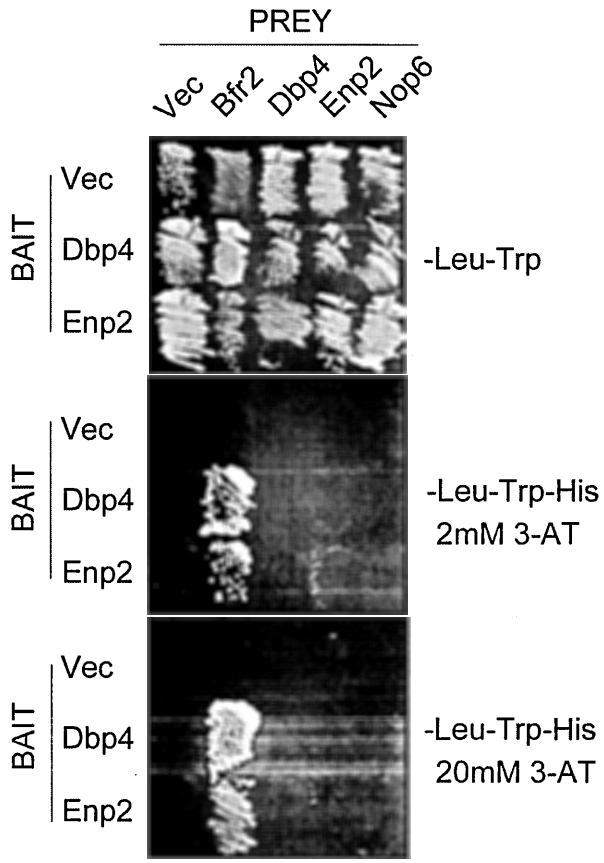
PREY
Vec
Bfr2
Dbp4
Enp2
Nop6
BAIT
Vec
Dbp4
Enp2
-Leu-Trp
BAIT
Vec
Dbp4
Enp2
-Leu-Trp-His
2mM 3-AT
BAIT
Vec
Dbp4
Enp2
-Leu-Trp-His
20mM 3-AT

Figure 3.3

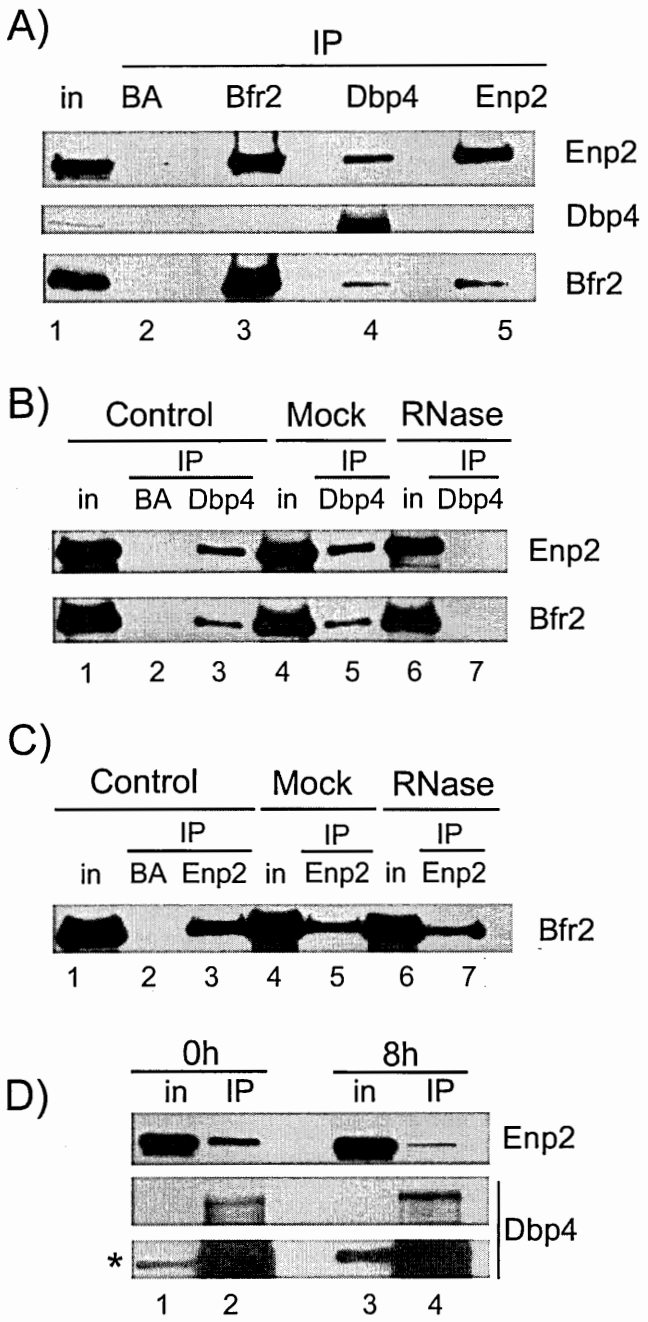
A)
IP
in
BA
Bfr2
Dbp4
Enp2
Enp2
Dbp4
Bfr2
1 2 3 4 5
B)
Control
Mock
RNase
IP
in BA Dbp4 in Dbp4 in Dbp4
Enp2
Bfr2
1 2 3 4 5 6 7
C)
Control
Mock
RNase
IP
in BA Enp2 in Enp2 in Enp2
Bfr2
1 2 3 4 5 6 7
D)
0h
8h
in IP in IP
Enp2
Dbp4
*
1 2 3 4

Figure 3.4

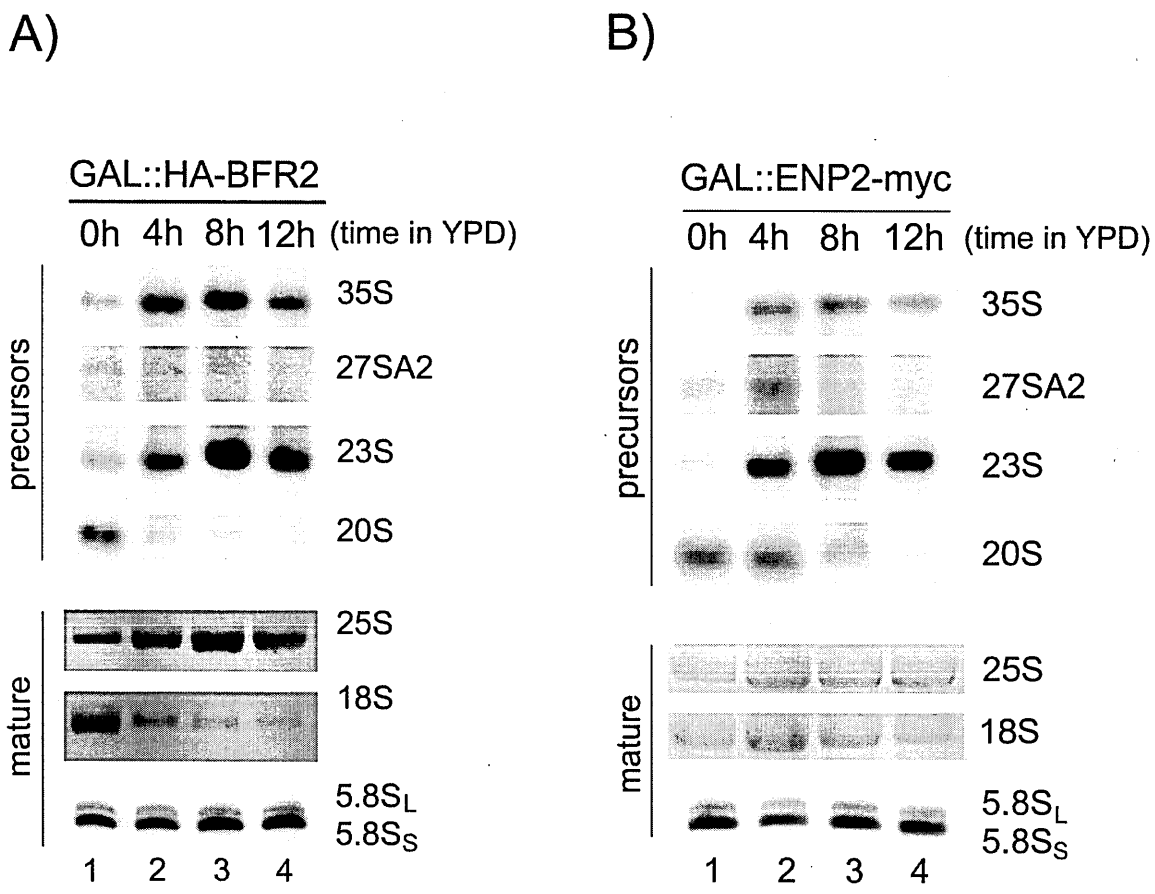
A)
GAL::HA-BFR2
0h 4h 8h 12h (time in YPD)
precursors
35S
27SA2
23S
20S
mature
25S
18S
5.8S$_L$
5.8S$_S$
1 2 3 4
B)
GAL::ENP2-myc
0h 4h 8h 12h (time in YPD)
precursors
35S
27SA2
23S
20S
mature
25S
18S
5.8S$_L$
5.8S$_S$
1 2 3 4

Figure 3.5

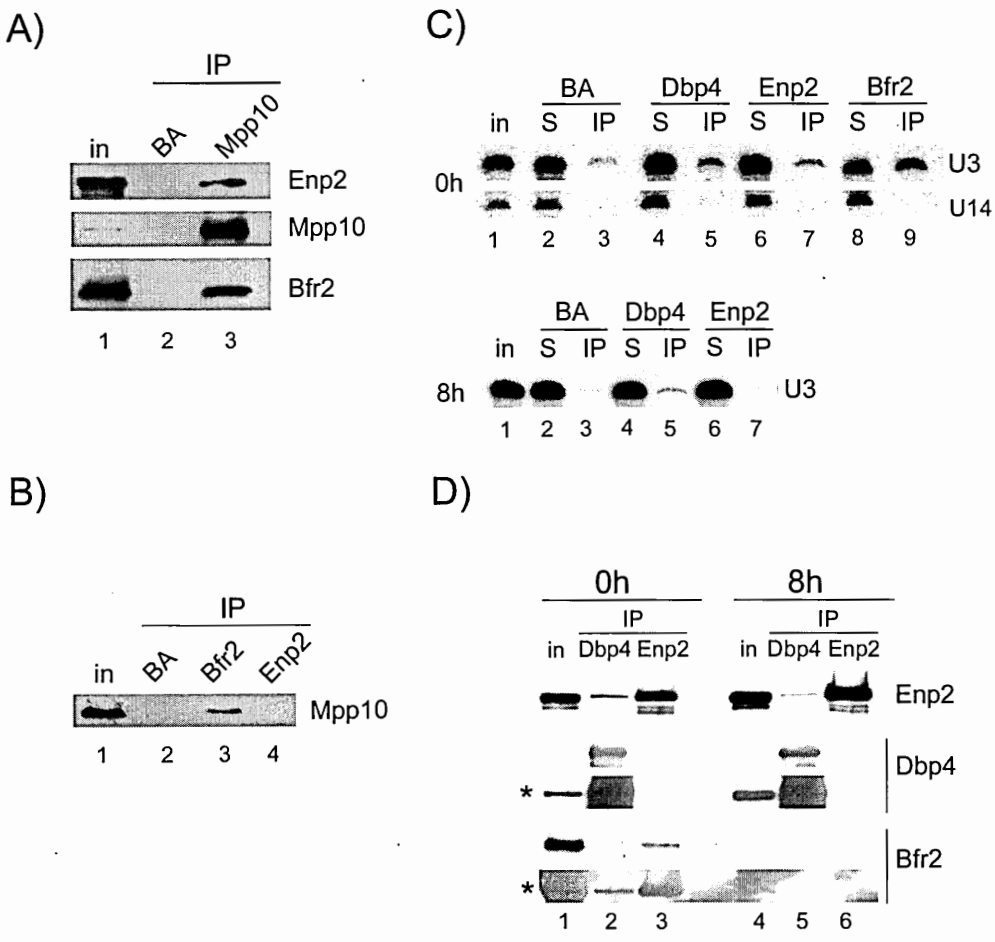
A)
IP
in
BA
Mpp10
Enp2
Mpp10
Bfr2
1 2 3
C)
BA
Dbp4
Enp2
Bfr2
in S IP S IP S IP S IP
0h
U3
U14
1 2 3 4 5 6 7 8 9
BA
Dbp4
Enp2
in S IP S IP S IP
8h
U3
1 2 3 4 5 6 7
B)
IP
in
BA
Bfr2
Enp2
Mpp10
1 2 3 4
D)
0h
8h
IP
in Dbp4 Enp2
IP
in Dbp4 Enp2
Enp2
Dbp4
Bfr2
*
*
1 2 3 4 5 6

Figure 3.6

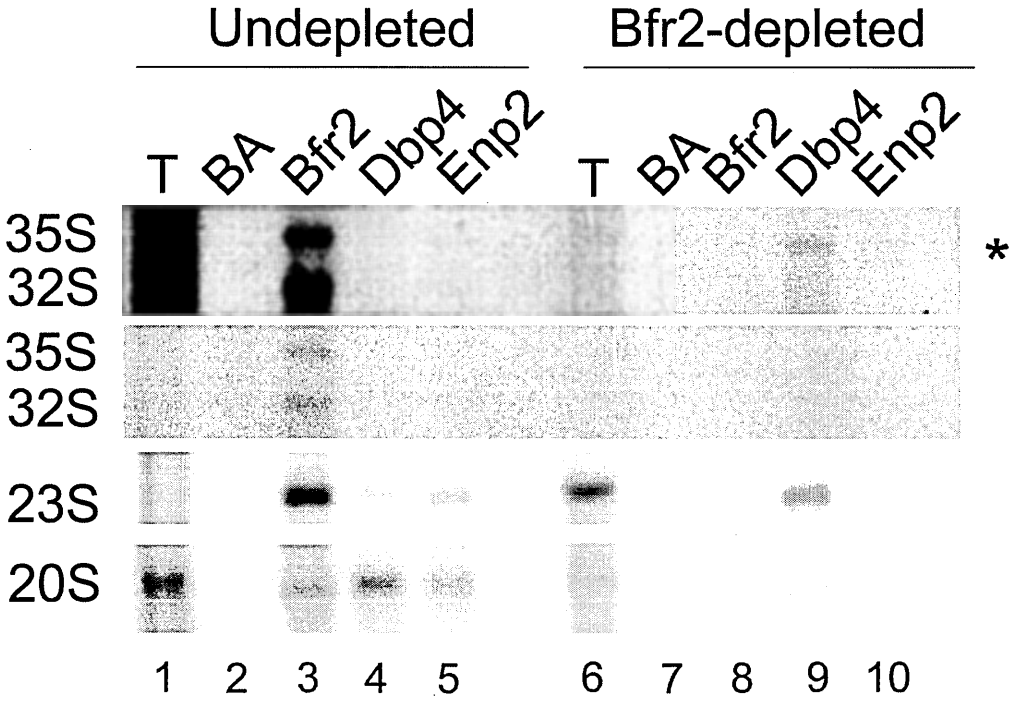
Undepleted
Bfr2-depleted
T
BA
Bfr2
Dbp4
Enp2
T
BA
Bfr2
Dbp4
Enp2
35S
32S
35S
32S
23S
20S
*
1 2 3 4 5 6 7 8 9 10

Figure 3.7

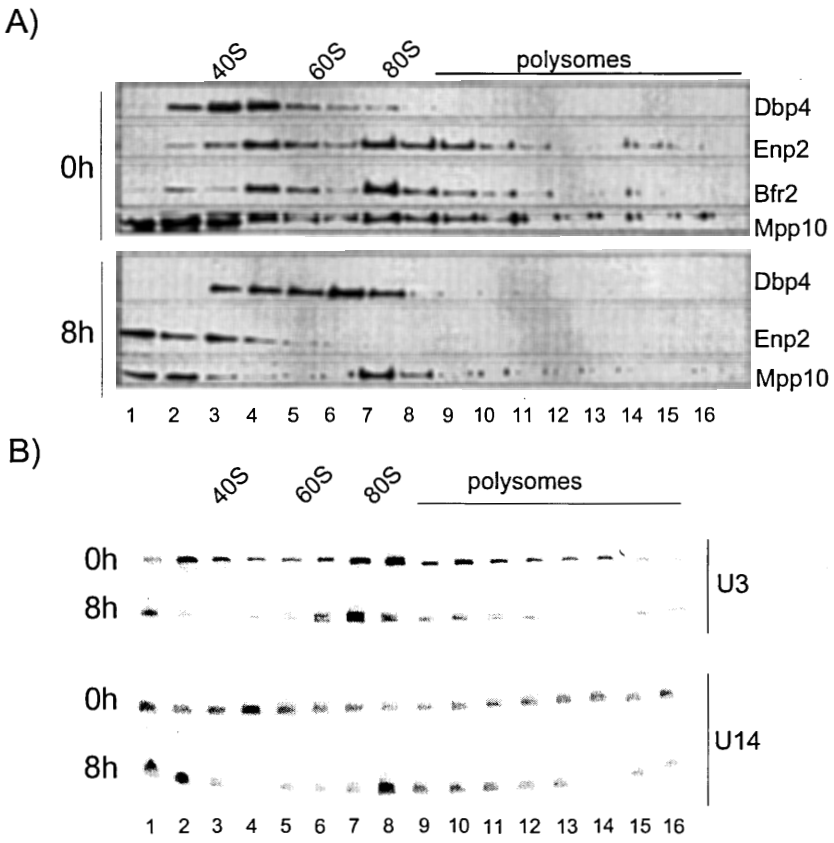
A)
40S
60S
80S
polysomes
0h
8h
Dbp4
Enp2
Bfr2
Mpp10
Dbp4
Enp2
Mpp10
1 2 3 4 5 6 7 8 9 10 11 12 13 14 15 16
B)
40S
60S
80S
polysomes
0h
8h
U3
0h
8h
U14
1 2 3 4 5 6 7 8 9 10 11 12 13 14 15 16

Figure 3.8

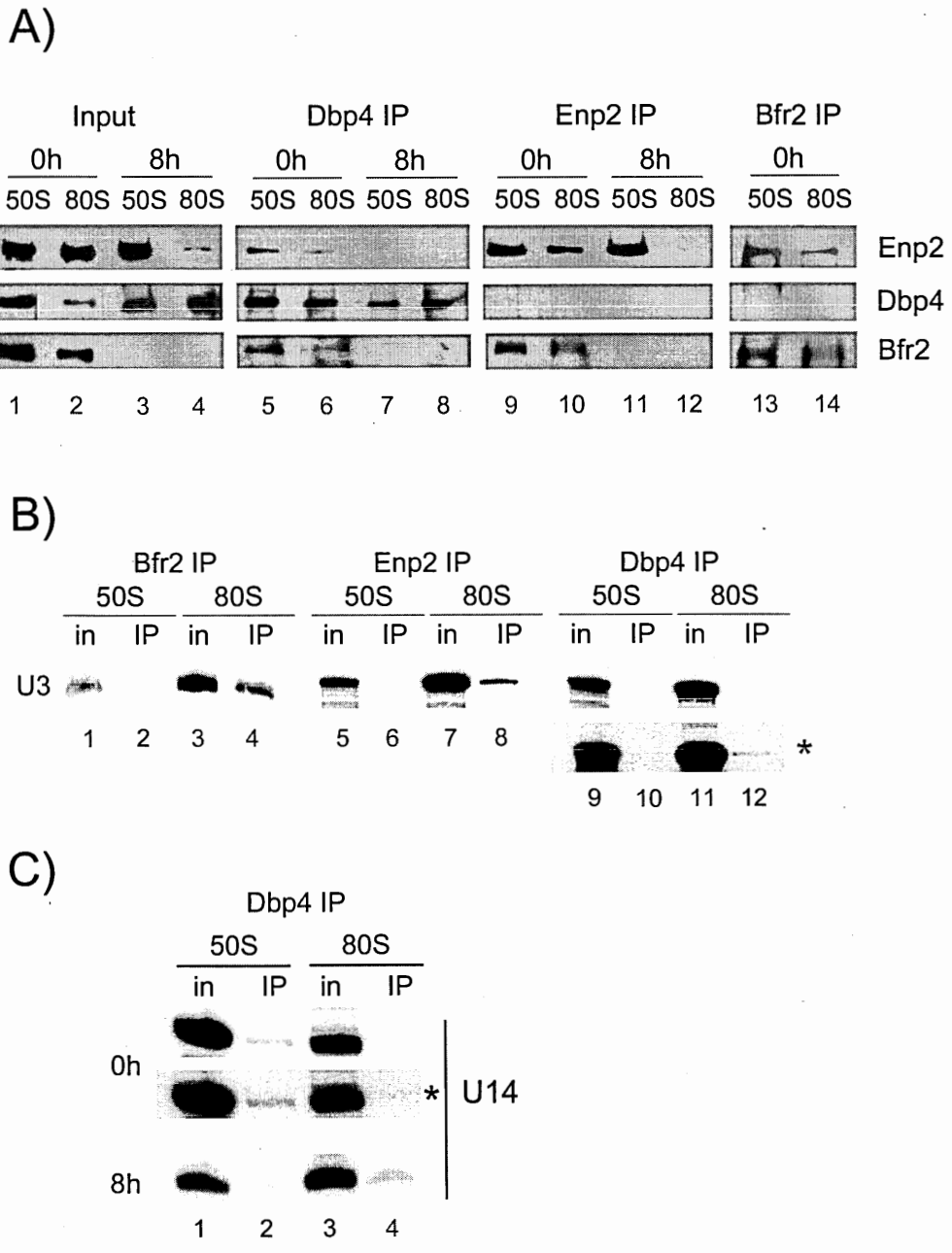
A)
Input
Dbp4 IP
Enp2 IP
Bfr2 IP
0h
8h
0h
8h
0h
8h
0h
50S 80S 50S 80S 50S 80S 50S 80S 50S 80S 50S 80S 50S 80S
Enp2
Dbp4
Bfr2
1 2 3 4 5 6 7 8 9 10 11 12 13 14
B)
Bfr2 IP
Enp2 IP
Dbp4 IP
50S
80S
in IP in IP in IP in IP in IP in IP
U3
1 2 3 4 5 6 7 8
*
9 10 11 12
C)
Dbp4 IP
50S
80S
in IP in IP
0h
*
U14
8h
1 2 3 4

Figure 3.9

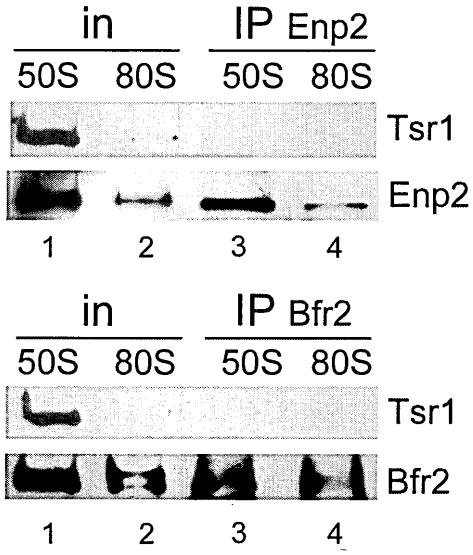
in
IP Enp2
50S 80S 50S 80S
Tsr1
Enp2
1 2 3 4
in
IP Bfr2
50S 80S 50S 80S
Tsr1
Bfr2
1 2 3 4

Figure 3.10

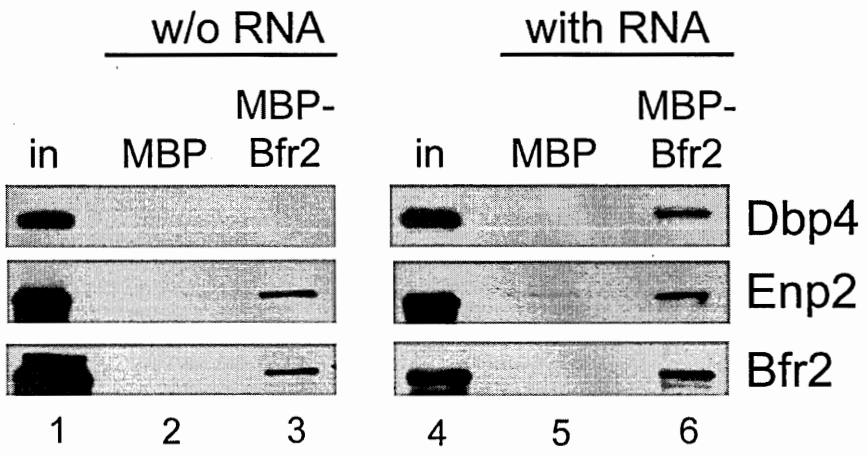
w/o RNA
with RNA
in
MBP
MBP-Bfr2
in
MBP
MBP-Bfr2
Dbp4
Enp2
Bfr2
1
2
3
4
5
6

Figure 3.11

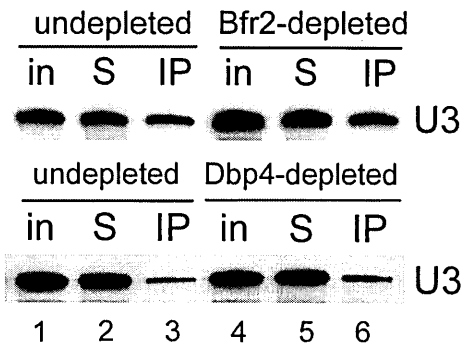
undepleted
Bfr2-depleted
in
S
IP
in
S
IP
U3
undepleted
Dbp4-depleted
in
S
IP
in
S
IP
U3
1
2
3
4
5
6

Figure 3.12

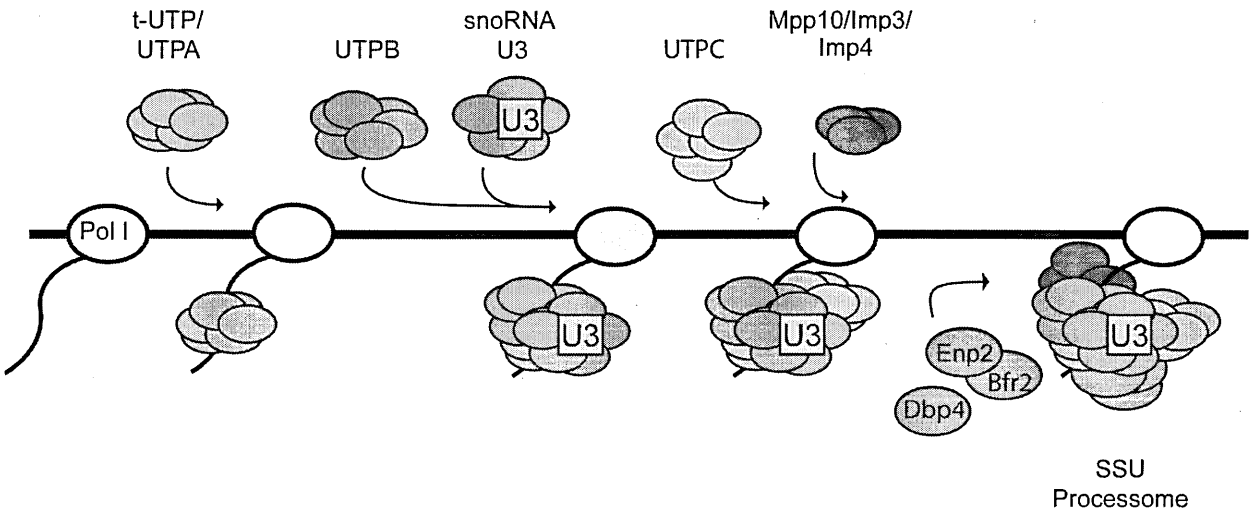
t-UTP/
UTPA
UTPB
snoRNA
U3
UTPC
Mpp10/Imp3/
Imp4
U3
Pol I
U3
U3
Enp2
Bfr2
Dbp4
U3
SSU
Processome

Chapter IV

4.1 Preface

A number of studies showed that human diseases are associated with impaired ribosome biogenesis, but our knowledge about ribosome biogenesis was mostly obtained from studies done in yeast. DDX10 is the human homologue of yeast Dbp4 and it belongs to the DEAD-box family of putative RNA helicases. We showed that DDX10 and Che-1 (the homologue of Bfr2) co-localize with the nucleolar marker fibrillarin, suggesting that DDX10 could participate in ribosome biogenesis. Our results indicated that DDX10 bearing mutations associated with breast cancer also localized to the nucleolus. We tested the effects of DDX10 and Che-1 knock down on rRNA maturation and proliferation of HeLa cells. Loss of DDX10 and Che-1 resulted in decreased production of 18S rRNA. In line with the 18S rRNA defect, immunoprecipitation experiments indicated that DDX10 is associated with the U3 snoRNA, Che-1 and the U3-specific protein DRIM/UTP20. Breast cancer mutations in DDX10 did not affect its interaction with Che-1. Flow cytometry analyses revealed that cells treated with siDDX10 slightly accumulated in the G1 phase of the cell cycle. Immunofluoresence microscopy indicated that treatment with siDDX10 strongly reduced the expression of the proliferation marker Ki-67. Taken together our data indicate that DDX10 is required for cell growth and proliferation, and that it plays a role in pre-18S rRNA maturation.

I did the major part of experiments under the supervision of Dr. François Dragon. Florian Palabaud and Pauline Vermulen performed some of the experiments under

my supervision. Tiziana Bruno carried out the Che-1 knockdown experiment in the laboratory of Maurizio Fanciulli.

RNA helicase DDX10 is implicated in cell growth and ribosome biogenesis.

Sahar Soltanieh[1], Florian Palabaud[1], Pauline Vermeulen[1], Tiziana Bruno[2], Maurizio Fanciulli[2], and François Dragon[1,3]

[1] Département des sciences biologiques and Centre de recherche BioMed, Université du Québec à Montréal, C.P. 8888 Succursale Centre-ville, Montréal (Québec), Canada H3C 3P8

[2] Laboratory B, Department of Therapeutic Programs Development, Regina Elena Cancer Institute, Via Elio Chianesi, Roma 00128, Italy

[3] Corresponding author: dragon.francois@uqam.ca

4.2 Abstract

DDX10 belongs to the DEAD-box family RNA helicases. Here we show that DDX10 localizes to the nucleolus together with the apoptosis-antagonizing transcription factor AATF/Che-1, suggesting they could participate in ribosome biogenesis. Knockdown of *DDX10* or *CHE-1* resulted in pre-rRNA processing defects and decreased production of 18S rRNA. In line with a possible role for DDX10 in 18S rRNA processing, immunoprecipitation experiments with FLAG-tagged DDX10 revealed its association with the U3 snoRNA, Che-1 and the U3-specific protein DRIM (Down-Regulated In Metastasis), also known as UTP20. DDX10 mutations associated with breast cancer did not alter the nucleolar localization of FLAG-tagged DDX10 or the co-immunoprecipitation of Che-1. HeLa cells treated with siDDX10 slightly accumulated in the G1 phase of the cell cycle, and immunofluorescence microscopy revealed that treatment with siDDX10 strongly reduced the expression of the proliferation marker Ki-67. Taken together our data indicate that RNA helicase DDX10 is required for cell growth and proliferation, and that it plays a role in pre-18S rRNA maturation.

4.3 Introduction

The nucleolus is the primary site of eukaryotic ribosome biogenesis. Cancer cells generally harbor multiple, larger nucleoli. This phenotypic change, which likely reflects the high demand for protein synthesis in tumor cells, has been used in the diagnosis of cancer ((Busch, 1990); (Derenzini *et al.*, 2009)). But the nucleolus is not merely a "ribosome factory". Indeed, nucleolar function is far more diverse and includes regulation of mitosis, cell-cycle progression, cellular proliferation, apoptosis and aging (Boisvert *et al.*, 2007; Horky *et al.*, 2002; Maggi and Weber, 2005).

Ribosomes are complex "RNA machines": the tightly compacted rRNA molecules are the catalytic components of ribosomes (Moore and Steitz, 2011). Not surprisingly, ribosome biogenesis is the process that employs the majority of cellular RNA helicases (Bleichert and Baserga, 2007; Martin *et al.*, 2013; Rodriguez-Galan *et al.*, 2013). These enzymes are constituted of a conserved catalytic core flanked by N- and C-terminal extensions that vary in length and composition; these extensions are important for substrate recognition and function of individual helicases (Luking *et al.*, 1998; Rocak and Linder, 2004; Umate *et al.*, 2011). In yeast, most RNA helicases are essential for viability, indicating that they perform critical, non-redundant biological functions. Bioinformatics searches led to the identification of 64 RNA helicases in humans (Umate *et al.*, 2011) ; 36 of those belong to the DEAD-box family and likely have homologues in yeast, which is the case of DDX10 (Abdelhaleem *et al.*, 2003). The yeast homologue of DDX10 is Dbp4, a nucleolar protein that is essential for viability (Huh *et al.*, 2003; Liang *et al.*, 1997). Dbp4

genetically interacts with U14, a conserved small nucleolar RNA (snoRNA) required for pre-rRNA processing (Liang *et al.*, 1997). Cellular depletion of Dbp4 impairs the release of U14 snoRNA from pre-rRNA, suggesting that Dbp4 could unwind snoRNA:pre-rRNA duplexes (Kos and Tollervey, 2005). Curiously however, pre-rRNA processing defects in Dbp4-depleted cells are identical to those of U3-depleted cells (Kos and Tollervey, 2005). U3 is another highly conserved snoRNA that is essential for pre-rRNA processing (Venema and Tollervey, 1999). The functionally active U3 particle is a very large RNP of ~80S that we have coined the SSU processome (Dragon *et al.*, 2002); this complex is constituted of the U3 snoRNA and 72 proteins, 36 of which are U3-specific and generally named Utp proteins (Bernstein *et al.*, 2004; Dragon *et al.*, 2002; Lim *et al.*, 2011). We recently proposed that Dbp4 might be a SSU processome component (Soltanieh *et al.*, 2014).

The SSU processome forms at the 5' end of nascent pre-rRNA transcripts upon association of numerous proteins with the U3 snoRNA (Dragon *et al.*, 2002; Gallagher *et al.*, 2004; Osheim *et al.*, 2004). Most proteins of the SSU processome are conserved in higher eukaryotes (Bernstein *et al.*, 2004; Dragon *et al.*, 2002), suggesting that this complex likely exists in humans (Takahashi *et al.*, 2003). Some components of the human SSU processome have been linked to cancer. To name a few, PDCD11 (programmed cell death 11), also named NFBP (NF-κB binding protein), is associated with the U3 snoRNA and is involved in pre-18S rRNA processing (Sweet *et al.*, 2008). DRIM (Down-Regulated In Metastasis) is a nucleolar

protein first identified in a human breast carcinoma cell line (Liu *et al.*, 2006; Schwirzke *et al.*, 1998). DRIM is the functional homologue of yeast Utp20 (Wang *et al.*, 2007). UTP14A is required for pre-18S rRNA processing and interacts not only with the U3 snoRNA but also with p53, and promotes p53 degradation (Hu *et al.*, 2011). Thus, a number of proteins involved in SSU processome assembly and function are linked to cancer, highlighting the importance of ribosome biogenesis in cell homeostasis.

Ribosome synthesis is a highly complex and coordinated process, which takes place in the nucleolus and involves rRNA synthesis, maturation, and assembly of rRNA and ribosomal proteins into the small and large ribosome subunits. The major steps in ribosome synthesis are conserved throughout eukaryotes (Tollervey, 1996a). This process is regulated throughout the cell cycle, primarily at the level of rRNA synthesis (Hannan *et al.*, 1998b). In humans, RNA polymerase I transcribes the 47S precursor, which is processed into 18S, 5.8S and 28S rRNAs, and RNA polymerase III transcribes 5S rRNA (Henras *et al.*, 2008).

Initial proteomic studies of HeLa cell nucleoli identified around 400 proteins that are stable or transient components of the nucleolus (Andersen *et al.*, 2002; Scherl *et al.*, 2002). Based on the online database of (Andersen *et al.*, 2005), about 700 proteins were identified from purified nucleoli, but according to a more recent study this number was increased to 4500 proteins in humans (Ahmad *et al.*, 2009). Among those, DEAD-box RNA helicase DDX10 and the apoptosis-antagonizing transcription factor AATF/Che-1 are highly conserved in eukaryotes, and their

orthologs are present in the budding yeast *Saccharomyces cerevisiae* (Chabane *et al.*, 1998; Liang *et al.*, 1997) as well as in plants, nematodes, fruit flies, birds, frogs and mammals (our unpublished results). Che-1/AATF is an RNA polymerase binding protein implicated in gene transcription regulation (Fanciulli *et al.*, 2000; Floridi and Fanciulli, 2007). Che-1 is also implicated in cell cycle, DNA repair and apoptosis (Floridi and Fanciulli, 2007; Passananti and Fanciulli, 2007). Moreover, Che-1 is also a retinoblastoma (Rb) binding protein affecting cellular growth (Bruno *et al.*, 2002). Besides the anti-apoptotic role of Che-1 in cancer cells, it may have an opposite role in regulating apoptosis in adult neurons (Barbato *et al.*, 2003). Che-1 activates p53 transcription and many of its target genes upon DNA damage (Bruno *et al.*, 2006).

Here we show that DDX10 and Che-1 localize to the nucleolus, which speaks in favor of a role in ribosome biogenesis, but DDX10 could also have other function(s) in the cell. Our data indicate that DDX10 is associated with the U3 snoRNA, Che-1 and DRIM/UTP20, and that DDX10 and Che-1 are implicated in maturation of the pre-18S rRNA. Moreover, knockdown of *DDX10* perturbs cell cycle progression and cellular proliferation.

4.4 Materials and Methods

4.4.1 Plasmids

The open reading frame (Westendorf *et al.*) encoding human DDX10 (Savitsky *et al.*, 1996) was amplified by PCR from a cDNA library derived from a human Namalwa

(Burkitt lymphoma) cell line (Strubin *et al.*, 1995) with primers DDX10-EcoRI-for (5'-CCG GAA TTC ATG GGC AAA ACG GCC AAC TC-3') and DDX10-EcoRI-rev (5'-CCG GAA TTC TTA GCT TTG ACT TCT TAG CAG AT-3'), and cloned into the *Eco*RI restriction site of pBluescript SK(-) to generate pBS-DDX10. The ORF encoding DDX10 was independently subcloned into the *Eco*RI site of the mammalian expression vector pBact-FLAG, which is identical to pBact-myc (Cravchik and Matus, 1993) except that the sequence encoding the myc epitope has been replaced by that encoding FLAG: vector pBact-myc was cleaved with *Hind*III to remove the small DNA fragment encoding the myc tag, and this piece of DNA was replaced by another one encoding the FLAG tag, following the shot-gun ligation method (Grundstrom *et al.*, 1985) with oligonucleotides FLAG-top1 (5'-AGC TTC GGA CCA TGG ACT ACA AA GAC-3'), FLAG-top2 (5'-GAT GAC GAT AAA GCA GAA TTC ATC GAT A-3'), FLAG-bottom1 (5'-GTC ATC GTC TTT GTA GTC CAT GGT CCG A-3') and FLAG-bottom2 (5'-AGC TTA TCG ATG AAT TCT GCT TTA TC-3'). Recombinant proteins produced from pBact-FLAG bear the FLAG epitope at their N-terminus. Site-directed mutagenesis (Higuchi *et al.*, 1988) was carried out to introduce mutations associated with breast cancer (Sjoblom *et al.*, 2006) in the ORF of DDX10 (mutation L566V and deletion of residues K595 to V619). Plasmid pBact-FLAG-DDX10 and its mutant derivatives were used for transfection of HeLa cells (see below). The integrity of all constructs was verified by automated sequencing at the McGill University and Génome Québec Innovation Center.

4.4.2 Antibodies

The rabbit anti-Che-1 antibodies have been described previously (Fanciulli *et al.*, 2000). Rabbit anti-DDX10 antibodies used for western blotting were purchased from Bethyl Laboratories. Immunolocalization of endogenous DDX10 was done with a goat anti-DDX10 antibody (Santa Cruz Biotechnology, sc-132640). FLAG-tagged DDX10 was detected with two different anti-FLAG antibodies: a rabbit polyclonal antibody (Rockland, 600-401-383) and a mouse monoclonal antibody (Sigma, F7425). Mouse monoclonal anti-DRIM antibody was purchased from Novus Biochemicals (H00027340-A01). Rabbit anti-Ki-67 was purchased from Abcam. Mouse monoclonal anti-fibrillarin antibody 72B9 (Reimer *et al.*, 1987) was kindly provided by Dr. Michael Pollard. GAPDH was detected on western blots with a mouse monoclonal antibody (Santa Cruz Biotechnology, sc-47724). HRP-conjugated secondary antibodies used in western analyses were from GE Healthcare.

4.4.3 Cell culture and transfections

HeLa cells (ATCC CCL-2) were grown in DMEM containing 10% FBS and penicillin-streptomycin (Wisent) at 37°C in a 5% CO_2 humidified atmosphere. For transient expression of recombinant proteins, 600 000 cells were seeded in 10 cm Petri dishes; after 16 h, plasmids encoding human DDX10 or its mutant derivatives were transfected with FuGene (Roche) following the manufacturer's instructions, and cells were harvested 48 h post-transfection. Transfection efficiencies were about 30%. For Transfection with siRNAs, 2×10^5 cells were seeded in each well of 6-well

plates the day before transfection. The anti-DDX10 siRNAs were obtained from Qiagen (siRNA5: 5'-TAGAAGCGATCGTATCTCCAA-3' S103226629, siRNA6: 5'-AACCTTGGTTATGACTGCGTA-3' S1041422551). The siRNAneg (AllStars Negative Control siRNA, S103650318) is a scrambled sequence that is not specific to DDX10; it was designed to serve as a negative control, and its sequence is proprietary (Qiagen). To knockdown *DDX10*, 450 ng siRNA in 100 µl culture medium (DMEM) without serum were used (final siRNA concentration of 15 nM), and 12 µl of HiPerFect Transfection Reagent (Qiagen) were added to the diluted siRNA. This mix was added to cells, which were previously washed and contained in 2.3 ml of grown medium. Cells were incubated at 37°C for 48 hours. Transfection with siRNA against Che-1 was done according to (Bruno *et al.*, 2010).

4.4.4 Immunoprecipitation experiments (IPs)

IPs were carried out essentially as described previously (Pogacic *et al.*, 2000), except that 20 µl of M2 beads (Sigma) were incubated with 1 ml whole cell extracts prepared from about 5 million transfected HeLa cells. Whole-cell extracts were prepared in NET-2 buffer (20 mM Tris-HCl [pH 7.5], 150 mM NaCl, 0.05% Nonidet P-40) by sonication (six times for 15 s at 10 W; Sonic Dismembrator sonicator, FISHER). To analyze the immunoprecipitated proteins, samples were separated on 8% polyacrylamide-SDS gels and analyzed by western blotting. Immunoprecipitated RNAs were extracted with phenol-chloroform, precipitated with ethanol, and further analyzed by RT-PCR (see below).

4.4.5 Immunofluorescence microscopy

Coverslips were placed in 6-well plates (Corning), and 100 000 HeLa cells were seeded in each well. When required, plasmids were transfected 16 h later as described above, and cells were processed for immunolocalization 48 h post-transfection. Cells were fixed with fresh 3.7% paraformaldehyde solution in PBS for 20 minutes, permeabilized with 0.5% Triton X-100 for 10 minutes, and incubated for 20 minutes with blocking solution (3% BSA in PBS). Cells were incubated for 1h with the primary antibodies (goat anti-DDX10 antibody, dilution 1/500; mouse anti-fibrillarin antibody, dilution 1/10; rabbit anti-Che-1, dilution1/1000; mouse anti-FLAG, dilution1/1000; rabbit anti-Ki-67, dilution 1/1000) prepared in 3% BSA, followed by two washes with 3% BSA. Cells were then incubated with the appropriate secondary antibodies diluted in 3% BSA following the manufacturer's recommendations (anti-goat IgG Alexa Fluor® 555, anti-mouse IgG Alexa Fluor® 488, anti-mouse IgG Alexa Fluor® 555, anti-rabbit IgG Alexa Fluor® 488 or anti-rabbit IgG Alexa Fluor® 555; Invitrogen) for 30 minutes at room temperature in a dark chamber. The first wash was done with 3% BSA containing DAPI (Sigma, 1:1000 dilution) in PBS for 10 minutes, followed by two washes with PBS for 10 minutes. Cells were mounted with ProLong® Gold antifade reagent (Invitrogen) and visualized under a fluorescence microscope (Observer A1 Microscope, Zeiss). Images were analysed with the software ImageJ (Collins, 2007).

4.4.6 RNA analyses

In order to have enough RNA, we worked with samples in triplicate. After transfection of HeLa cells with siRNAs, cells were washed with PBS and centrifuged for 5 minutes at 300 g. The triplicates were then pooled, and RNA was extracted with Trizol reagent (1 ml) and chloroform (0.2 ml). Samples were centrifuged at 4°C for 15 minutes at 15 000 g. The supernatant was kept and 0.5 ml isopropanol was used to precipitate the RNA. Samples were centrifuged at 4°C for 10 minutes at 15 000 g. The pellet was washed with 1 ml 70% ethanol. Samples were centrifuged at 4°C for 5 minutes at 15 000 g. The pellet was resuspended in 10 µl RNase-free water and quantified with a NanoDrop.

To detect U3 and U14 snoRNAs after IPs, reverse transcription was done using AffinityScript Multiple Temperature Reverse Transcriptase (Agilent) with 1 µg of RNA and the following oligonucleotides: 5' GTT TCT CTG AAC GTG TAG AGC ACC G 3' and 5' ACC ACT CAG ACC GCG TTC TCT C 3' for U3 snoRNA, 5' TCA CTG TGA TGA TGG TTT TCC AAC ATT C 3'and 5' CTC ACT CAG ACA TCC AAG GAA GGT TTA C 3' for U14 snoRNA. The reaction was performed according to the manufacturer's instructions. The cDNAs were amplified by PCR in a final volume of 50 µl with Taq DNA polymerase (New England Biolabs) using 2 µl of reverse transcription product.

To detect *DDX10* and *GAPDH* after treatment with anti-DDX10 siRNAs, reverse transcription was carried out with the qScript cDNA SuperMix kit (Quanta). For cDNA synthesis, 1 µg of total RNA was added to 4 µl of SuperMix and

completed to 20 µl with RNase-free water. Samples were incubated 5 minutes at 25°C, 30 minutes at 42°C and 5 minutes at 85°C. PCRs were carried out with Taq DNA polymerase using 2 µl of the previous mix and the following oligonucleotides: 5'-CGT AGC CGG CAA AAC ACT CG-3' and 5'-GCA CCC CTG CCA CTT TGG A-3' for DDX10, 5'-TCC TGC ACC ACC AAC TGC TTA GC-3' and 5'-AGG TCC ACC ACC CTG TTG CTG TA-3' for GAPDH. The PCR products were separated by electrophoresis on 2% agarose 0.5% TBE gels containing GelRed (Biotium) and visualized with a UV transilluminator.

For northern hybridization analyses of pre-rRNAs, 10 µg of total RNA were separated in 1.2% agarose gels containing 7% formaldehyde and MOPS buffer (0.2 M MOPS, pH 7, 0.5 M sodium acetate, 10 mM EDTA). Electrophoresis was carried out for 21 h at 59 volts. The RNAs were transferred onto a Hybond-XL membrane (GE Healthcare) by capillarity overnight in 20X SSC (3 M NaCl, 0.3 M trisodium citrate $2H_2O$, pH 7). Membranes were hybridized overnight with 5'-labeled oligonucleotide probes (20,000,000 cpm each) and washed with 20X SSPE (3 M NaCl, 0.2 M NaH_2PO_4-$1H_2O$, 0.2 M Na_2EDTA, pH 7.4) and 1%SDS. To detect rRNAs precursors, the following probes were used (Gerus *et al.*, 2010): probe d 5'-AGA CGA GAA CGC CTG ACA CGC ACG GCA C-3', probe e 5'-CCT CGC CCT CCG GGC TCC GTT AAT GAT C-3', probe f 5'-GCG CGA CGG CGG ACG ACA CCG CGG CGT C-3'.

To analyse mature 18S and 28S rRNAs, total RNA was loaded on a 1.2% agarose gel containing 7% formaldehyde and MOPS. Electrophoresis was done for 3

h at 50 volts. RNAs were stained with GelRed (Biotium) and detected with a UV transilluminator.

To analyse mature 5.8S rRNA, total RNA was loaded on an 8% denaturing acrylamide gel, and electrophoresis was carried out for 1 h 45 min at 45 watts. The samples were transferred onto GE Hybond-XL membranes in a TransBlot Cell (Bio-Rad) with TBE at 30 volts for 16h at 4°C. The hybridization and the wash steps were done as previously described (Soltanieh et al. 2014). We used probe 5.8S 5'-CAATGTGTCCTGCAATTCAC-3' (Gerus *et al.*, 2010).

4.4.7 Western blotting

Proteins were separated on 8% polyacrylamide-SDS gels and transferred onto a PVDF membrane (Millipore). DDX10 was detected with anti-DDX10 antibodies diluted 1/2000 in TBS-T (100 mM Tris-HCl, pH 7.5, 0.9% NaCl, 0.2% Tween-20) and HRP-conjugated anti-rabbit antibody diluted 1/100000. For GAPDH, anti-GAPDH antibody was diluted to 1/1000 in TBS-T and detected with HRP-conjugated anti-mouse antibody diluted 1/10000. Anti-Che-1 antibodies were diluted 1/1000 in PBS and detected with HRP-conjugated anti-rabbit antibody. Anti-DRIM antibodies were diluted 1/1000 TBS-T detected with HRP-conjugated anti-mouse antibody.

4.4.8 Flow cytometry analyses

About 1 x 10^6 growing cells were fixed in 4 ml of cold ethanol (70%) and kept at 4°C for one week. Before analysis, cells were centrifuged for 5 minutes at 500 g and

resuspended in the following mixture: 950 µl of PBS, 10 µl RNase A (10 mg/ml) and 40 µl of propidium iodide (1 mg/ml). Samples were kept at 37°C for 30 minutes and analyzed with the FACScan system (Becton Dickinson).

4.5 Results

4.5.1 DDX10 and Che-1 localize to the nucleolus of HeLa cells

DDX10 and AATF/Che-1 have been detected in nucleolar preparations of large-scale proteomics studies, suggesting they are nucleolar proteins (Andersen *et al.*, 2002; Scherl *et al.*, 2002). To determine if DDX10 and Che-1 are only transiting through the nucleolus or if they reside in this nuclear compartment, we did indirect immunofluorescence studies with HeLa cells. As seen in Figure 1, DDX10 and Che-1 co-localized with fibrillarin, a nucleolar marker specific for the dense fibrillar component (Pogacic *et al.*, 2000). This localization is consistent with a role for DDX10 and Che-1 in pre-rRNA processing because fibrillarin is a common component of box C/D snoRNPs, which are required for maturation of rRNAs (Henras *et al.*, 2008).

DDX10 was identified as a candidate breast cancer gene (Sjoblom *et al.*, 2006). This group identified two different mutations in *DDX10*: a missense mutation (L566V) and a deletion mutation (residues 594-619). We decided to analyze the cellular localization of FLAG-tagged DDX10 bearing mutations associated with breast cancer. These mutations did not alter the nucleolar localization of FLAG-tagged DDX10 or that of Che-1 (data not shown).

4.5.2 DDX10 associates SSU processome components and Che-1

We carried out immunoprecipitation experiments (IPs) with extracts from HeLa cells transiently expressing the FLAG-tagged DDX10 constructs to determine whether DDX10 is associated with the U3 snoRNA. This was prompted by the observation that in yeast, IPs carried out with whole cell extracts indicated that Dbp4 (the ortholog of DDX10) is specifically associated with U3 snoRNA and not with U14 snoRNA (Soltanieh et al. 2014), as originally suspected (Liang *et al.*, 1997). RNAs recovered from IPs were used for RT-PCR with primers specific for the U3 or U14 snoRNAs. IPs conducted with FLAG-DDX10 co-immunoprecipitated U3 but not U14 (Figure 4.2 A). Control experiments with extracts of non-transfected HeLa cells did not show any signal for U3 or U14 snoRNAs. The immunoprecipitates were also analyzed by western blotting to determine if proteins that associate with the U3 snoRNA were also co-immunoprecipitated. The blot was probed with antibodies against DRIM (Down-Regulated In Metastasis) and Che-1 (Figure 4.2 B). DRIM is the ortholog of yeast Utp20 (Peng *et al.*, 2010; Wang *et al.*, 2007), a component of the functionally active U3 RNP (Bernstein *et al.*, 2004; Dragon *et al.*, 2002).

Since yeast Dbp4 strongly interacts with the SSU processome component Bfr2, yeast homologue of Che-1, (Soltanieh et al. 2014), the blot was probed with antibodies against Che-1. The co-IP of Che-1 with FLAG-DDX10 was efficient (Figure 4.2 B), even more so than that of DRIM (compare IP lanes with input lanes for DRIM and Che-1 in Figure 4.2B). These results suggest that the interaction of

DDX10 with Che-1 is more stable or that a larger proportion of DDX10 associates with Che-1 rather than with DRIM. Co-immunoprecipitation of U3 snoRNA and DRIM suggests that DDX10 interacts with the human SSU processome. We also verified if breast cancer mutations in DDX10 affected its interaction with Che-1. As seen in Figure 4.2C, DDX10 mutants remained associated with Che-1, showing that breast cancer mutations in DDX10 did not affect the interaction between these two proteins. DDX10 mutants also remained associated with DRIM (data not shown).

4.5.3 DDX10 and Che-1 are required for pre-rRNA processing

The nucleolar localization of DDX10 and Che-1 (Figure 4.1) and the association of DDX10 with SSU processome components (Figure 4.2) led us to analyze the effects of DDX10 and Che-1 knockdown on pre-rRNA processing. We tested various siRNAs against DDX10 to analyze the efficiency of siRNAs on expression DDX10. An example of RT-PCR analysis is shown in Figure 4.3 A, where siRNA5 more efficiently reduced *DDX10* mRNA levels than siRNA6; however, both siRNAs efficiently reduced DDX10 protein levels (Figure 4.3 B). To investigate the role of DDX10 in ribosome biogenesis, HeLa cells were treated with siRNAs to knock down its expression and we analyzed rRNA synthesis. Because it was routinely found to be more efficient (as judged by RT-PCR analyses), we decided to pursue our studies with siRNA5, which we now refer to as siDDX10. The amount of 18S rRNA was decreased in samples transfected with DDX10 siRNAs but 28S rRNA levels were nearly unchanged (Figure 4.4 A). Thus, only the 18S rRNA seems to be affected

upon *DDX10* knock down. We further analyzed the pre-rRNA processing defects after treatment with siDDX10. Our results showed that upon depletion of DDX10, there was a decrease in the amount of 21S and 18S-E pre-rRNAs (Figure 4.4 A). Because the homologue of Che-1 (Bfr2) is necessary for 18S rRNA maturation in yeast and Che-1 associates with DDX10, we analyzed the role of Che-1 in ribosome biogenesis. We used siChe-1 (Bruno *et al.*, 2010) to knock down Che-1 expression, and we observed a decrease in the amount of mature18S rRNA in siChe-1 treated cells compared to non-tranfected cells; in contrast, there was no change in the levels of the mature 28S rRNA (Figure 4.4). Nothern blot analyses indicated that in the absence of Che-1 levels of 21S and 18S-E pre-rRNAs decreased, and this was accompanied by an accumulation of 45S pre-rRNA (Figure 4.4.B), a phenotype that is similar to that seen upon DDX10 depletion (Figure 4.4 A). These data indicate that DDX10 and Che-1 are implicated in pre-rRNA processing events leading to the production of 18S rRNA.

4.5.4 Knockdown of DDX10 alters G1/S transition and reduces proliferation of HeLa cells

Cell cycle progression upon *DDX10* silencing was analyzed by FACS (Figure 4.5 A). In comparison with HeLa cells transfected with the negative control siRNA (siRNA neg), cells transfected with siDDX10 slightly accumulated in G1 phase; this was accompanied by a concomitant decrease of cells in S phase, indicating that knock down of DDX10 affects the G1/S transition of the cell cycle. Ki-67 is a

nuclear/nucleolar protein (Endl and Gerdes, 2000; Scholzen and Gerdes, 2000), and it is associated with cell proliferation because it is only detected in cells that proliferate (Schluter *et al.*, 1993). The signal for Ki-67 was decreased when cells were treated with siDDX10 (Figure 4.5 B), indicating that knock down of *DDX10* perturbs cell proliferation.

In unstressed cells, low levels of p53 protein are maintained by reducing its stability using negative feedback regulators like MDM2 (Vogelstein *et al.*, 2000; Vousden and Lu, 2002). We examined p53 proteins levels after silencing DDX10 expression (Figure 4.5 C). Knock down of *DDX10* resulted in elevated levels of p53. This result is consistent with nucleolar stress response where excess of free ribosomal proteins caused by 40S ribosome synthesis defects lead to stabilization of p53 protein (Fumagalli *et al.*, 2012).

4.6 Discussion

Ribosome biogenesis is one the highest energy consuming processes in the cell (Warner, 1999) and it is tightly regulated during development, cell growth, cell cycle and stress (Ruggero and Pandolfi, 2003). Several human diseases are associated with increasing risk of cancer development without genetic alterations of oncogenes or tumor suppressors, such as quantitative or qualitative changes in ribosome synthesis (Montanaro *et al.*, 2012). Up-regulation of ribosome biogenesis increases the possibility of tumorigenesis (Montanaro *et al.*, 2012). Thus to obtain more useful insight into ribosomopathies, more profound understanding of ribosome biogenesis in

humans is required. For years, ribosome synthesis has been studied using the yeast *Saccharomyces cerevisiae* as a model organism because this process is highly conserved in eukaryotes. But there are human factors that have different or additional function compared to their yeast orthologs (Tafforeau *et al.*, 2013). Pre-rRNA maturation is one of the many aspects of ribosome biogenesis. RNA helicases are among the trans-acting factors involved in this process. Deregulation of numerous RNA helicases is observed in cancer, usually due to chromosomal translocation, down-regulation and overexpression (Abdelhaleem, 2004). One of the genetic rearrangements, which occur in myeloid leukemia is the NUP98-DDX10 fusion (Arai *et al.*, 1997); it has been shown that a helicase motif of DDX10 plays a role in leukemogenesis (Yassin *et al.*, 2010).

We investigated the function of the human RNA helicase DDX10, the homologue of yeast Dbp4, in ribosome biogenesis. We showed that DDX10 and Che-1 localize to the nucleolus, suggesting that they could be involved in ribosome biogenesis (Figure 4.1). DDX10 constructs bearing mutations associated with breast cancer (Sjoblom *et al.*, 2006) also localized to nucleolus, showing that the point mutation L566V and deletion of residues 594-619 did not alter the localization of DDX10 or Che-1. We tested different siRNAs against *DDX10* to analyze the efficiency of DDX10 knock down in HeLa cells (Figure 4.3). Although the synthesis of 18S rRNA was decreased upon depletion of DDX10, this did not affect the production of 28S rRNAs (Figure 4.4 A). Further analyses showed that knock down of DDX10 altered pre-rRNA processing events leading to the production of 18S

rRNA: this was revealed by the reduction of the signals corresponding to the 21S and 18S-E pre-rRNAs (Figure 4.4 A), suggesting defects at cleavage sites 01, A0, 1, 2 and C (Tafforeau *et al.*, 2013). Similar patterns were observed when Che-1 was knocked down: the data indicated a decrease in the levels of the mature18S rRNA as well as the 21S and 18S-E pre-rRNAs, with a concomitant accumulation of the 45S pre-rRNA (Figure 4.4 B). This phenotype suggests that the absence of Che-1 affects the cleavage of the 45S precursor at sites 01 and 02 (Tafforeau *et al.*, 2013), leading to the accumulation of the 45S pre-rRNA. In contrast, there was only a slight accumulation of 45S pre-rRNA (about 5%) upon DDX10 depletion. These differences could be explained by the fact that knock down of DDX10 did not have a strong effect on the early cleavages of the 45S precursor. The group of Lafontaine (Tafforeau *et al.*, 2013) showed that knock down of DDX10 and Che-1 resulted in strong accumulation of 45S (47S) pre-rRNA. This might be due to differences in experimental procedures such growth conditions or siRNA design and treatment.

In addition to the pre-18S rRNA processing defect, IPs showed that DDX10 is associated with the U3 snoRNA, the U3-specific protein DRIM/UTP20 and Che-1 (Figure 4.2). These results suggest that DDX10 might be a SSU processome component. DDX10 mutations associated with breast cancer did not affect the interaction between DDX10 and Che-1 (Figure 4.2 C) or DRIM (data not shown). According to our bioinformatics analyses, DDX10 contains two coil-coiled motifs, which could be implicated in protein-protein interactions. Both DDX10 mutations examined in this study are located in one of the coil-coiled motifs. It remains to be

determined whether mutation of the other coil-coiled motif (or mutation of the two motifs) might be necessary to disrupt the association of DDX10 and Che-1.

FACS analyses revealed that siDDX10-treated HeLa cells slightly accumulated in the G1 phase of the cell cycle (Figure 4.5 A), suggesting that knock down of DDX10 affects cellular growth. In line with this view, immunofluoresence microscopy showed that expression of the proliferation marker Ki-67 was heavily reduced upon siDDX10 treatment (Figure 5B). In addition, DDX10 knock-down resulted in increased levels of p53 protein in those cells (Figure 5C), a phenomenon that is often observed upon nucleolar stress (Mayer and Grummt, 2005). Taken together, our data suggest that RNA helicase DDX10 is necessary for cellular growth and proliferation, and that it is required for pre-rRNA processing events leading to the production of 18S rRNA.

4.7 Acknowledgements

We are very grateful to Patrick Matthias (Friedrich Miescher Institute for Biomedical Research) for the cDNA library, to Michael Pollard (The Scripps Research Institute) for the generous gift of anti-fibrillarin antibodies, and to Anthony Henras for insightful discussions. We also thank Denis Flipo for help with microscopy. This work was supported by grants from the Cancer Research Society and the Quebec Breast Cancer Foundation, and a Chercheur-boursier award of the Fonds de la recherche en santé du Québec to FD.

4.8 Figures legends

Figure 4.1. Localization of DDX10 and Che-1 in HeLa cells. A) The subcellular localization of endogenous DDX10 was evaluated by immunofluorescence microscopy. Nuclei were stained with DAPI (blue). The images of DDX10 (red channel) and fibrillarin (green channel) were superimposed (Merge). The yellow signal results from superimposition of the red and green signals. B) The experiment was performed as in Figure 1A except that Che-1 was detected using a red fluophore.

Figure 4.2. DDX10 is associated with the U3 snoRNA, DRIM and Che-1. Extracts of HeLa cells expressing FLAG-tagged DDX10 and mutant derivatives were used for IPs with an anti-FLAG mAb. A) The presence of U3 and U14 snoRNAs was analyzed by RT-PCR carried out in the presence (+) or the absence (–) of reverse transcriptase. Lanes T are RT-PCR done with total RNA and lanes IP are RT-PCR done with immunoprecipitated RNAs. B) Western analyses with anti-DRIM and anti-Che-1 antibodies. Whole cell extracts (lanes T) and anti-FLAG immunoprecipitates (lanes IP) from non-transfected cells (NT) or cells expressing FLAG-tagged DDX10. C) Western analyses carried out as in Figure 2B after transfection of HeLa cells with FLAG-tagged DDX10 constructs: wild-type (WT, lanes 1-2), mutant L566V (lanes 3-4), or mutant Δ lacking residues 594-619. In addition to Che-1, DDX10 constructs were detected with anti-FLAG mAb.

Figure 4.3. Silencing of DDX10 with siRNAs. A) HeLa cells were treated for 48h with two different anti-DDX10 siRNAs (siRNA 5 and siRNA 6), a scrambled siRNA (siRNA neg) or non-transfected (NT). Total RNA was used for RT-PCR analyses. RT-PCR on *GAPDH* mRNA was used as loading control. B) Cellular expression of DDX10 protein was assessed by western blot analysis. The blot was also subjected to immunodetection with anti-GAPDH antibodies (loading control).

Figure 4.4. Effects of DDX10 and Che-1 knock down on the maturation of ribosomal RNAs.

A) Total RNA was extracted 48 hours post-transfection with siDDX10 (siRNA 5, lane 2) or from non-transfected HeLa cells (NT, lane 1), and RNAs were resolved on a 1.2% agarose gel containing 7% formaldehyde and transferred onto a Hybond-XL membrane. Blots were probed with radiolabeled oligonucleotides to detect various precursors. The 18S and 28S rRNAs were detected by staining the agarose-formaldehyde gel B) RNA analysis was carried out as in Figure 4A except that the cells were treated with siRNA against Che-1 (lane 2).

Figure 4.5. Loss of DDX10 alters cell cycle progression and proliferation. A) HeLa cells were transfected for 48 hours with siDDX10 or siRNA neg (negative control). Analyses by flow cytometry were performed, and data were presented in histograms. B) Localization of Ki-67 in HeLa cells. In non-transfected cells (NT; left panel), Ki-67 (green channel) is expressed in each cell and co-localize with the

nucleolar marker fibrillarin (red channel). In siDDX10-treated cells (right panel), Ki-67 expression was reduced and barely detected (in green), so that only the nucleolar marker fibrillarin was detected (in red) in these cells. Images are overlays of the green and red channels together with the DAPI staining of nuclear DNA. C) Expression of p53 protein was analyzed in DDX10 silenced HeLa cells. Western blot analysis was carried on non-transfected cells (NT) and siDDX10-treated cells; p53 and GAPDH proteins were detected with appropriate antibodies.

4.9 Figures

Figures 4.1

A)

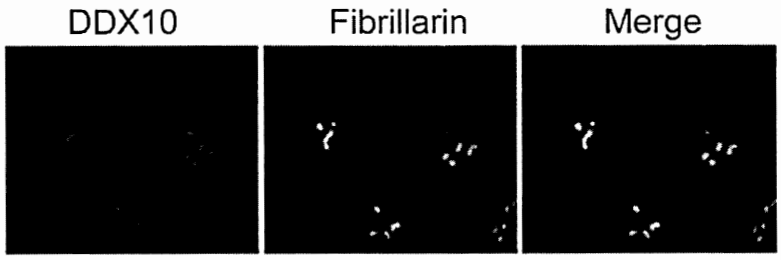

B)

Figure 4.2

A)

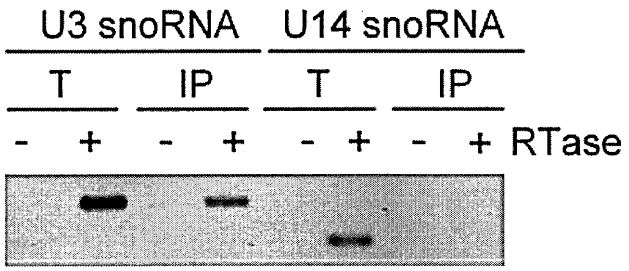

B)

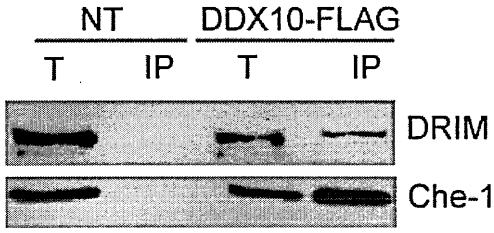

C)

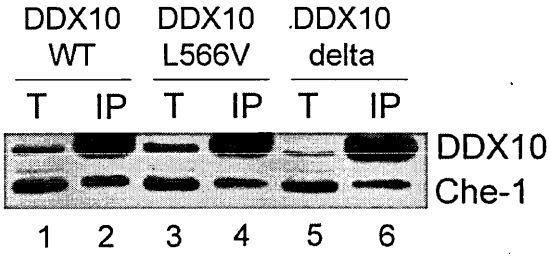

Figure 4.3

A)

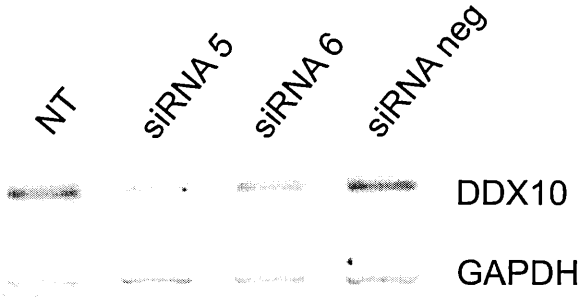
NT
siRNA 5
siRNA 6
siRNA neg
DDX10
GAPDH

B)

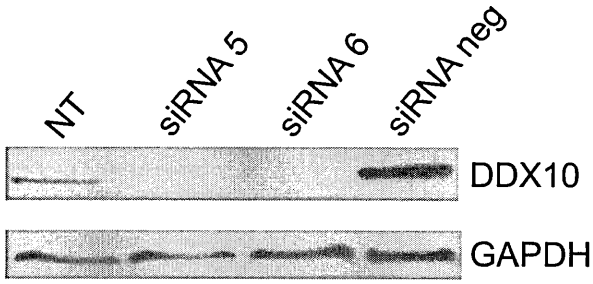
NT
siRNA 5
siRNA 6
siRNA neg
DDX10
GAPDH

Figure 4.4

A)

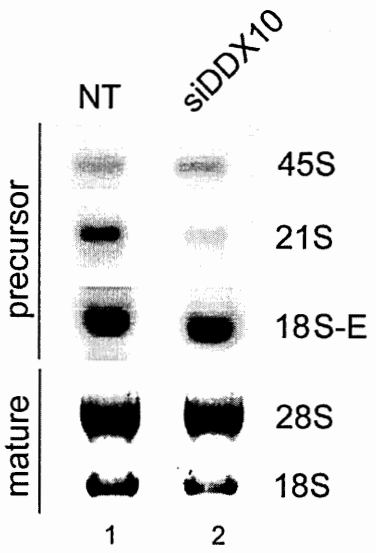
NT
siDDX10
precursor
mature
45S
21S
18S-E
28S
18S
1
2

B)

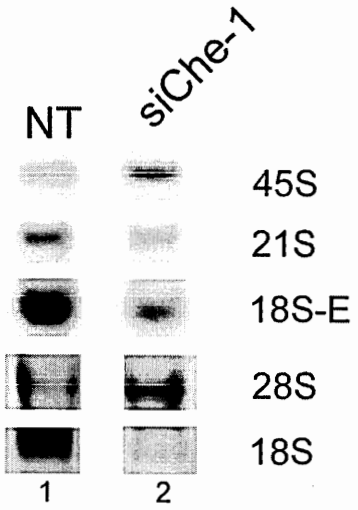
NT
siChe-1
45S
21S
18S-E
28S
18S
1
2

Figure 4.5

A)

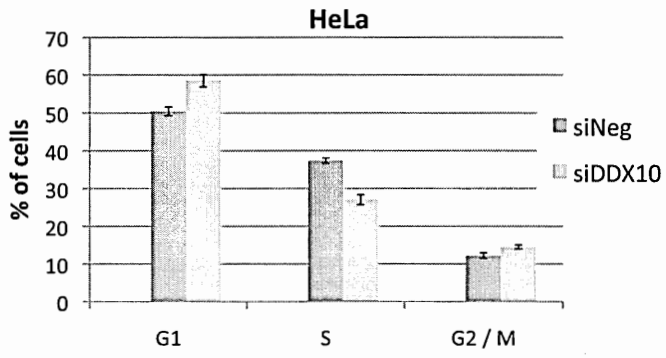

B)

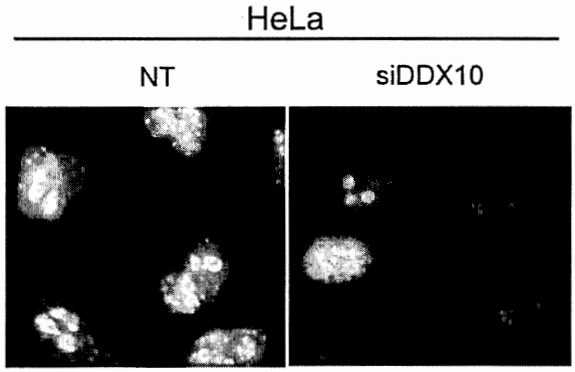

C)

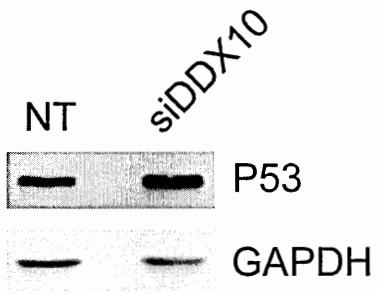

Chapter V

Discussion and perspectives

Protein synthesis is an essential cellular process and ribosomes are the main players of it. Ribosome synthesis is very complex and is a major metabolic task in a cell and conserved among all eukaryotes. About 80% of the total cellular RNA is found in ribosomes. In yeast, more than 75% of cellular transcription is related to ribosome biogenesis, from which about 60% is implicated in transcription of rRNAs (Moss *et al.*, 2007; Warner, 1999). Eukaryotic ribosome biogenesis starts in the nucleolus with rRNA transcription, and then folding, binding with ribosomal proteins and assembly factors while being modified and processed to produce mature ribosomal subunits. Maturation of pre-ribosomal particles involves a dynamic series of protein-protein, RNA-protein and RNA-RNA interactions, which are formed, disrupted and rearranged (Fromont-Racine *et al.*, 2003; Granneman and Baserga, 2004; Henras *et al.*, 2008; Karbstein, 2011; Kressler *et al.*, 2010; Panse and Johnson, 2010; Staley and Woolford, 2009; Tschochner and Hurt, 2003; Venema and Tollervey, 1999). Thus, a variety of pre-ribosomal complexes are formed in this pathway. The pre-ribosome subunits composition is highly dynamic and there are more than 200 trans-acting factors implicated in the assembly of ribosomes in yeast (Fromont-Racine *et al.*, 2003; Granneman and Baserga, 2004; Henras *et al.*, 2008; Kressler *et al.*, 2010; Tschochner and Hurt, 2003; Venema and Tollervey, 1999). *Saccharomyces cerevisiae* is the best-studied organism for ribosome biogenesis. This process has been the subject of intense study over the last decades in order to determine how pre-

ribosomal particles are assembled, and which proteins or RNA elements are directly involved in the cleavage events required to remove spacer sequences from rRNA precursors. RNA helicases are among the enzymes that are implicated in the maturation steps. DEAD-box protein Dbp4 is one of the RNA helicases involved in this process.

5.1. Involvement of DEAD-box RNA helicase Dbp4 in ribosome biogenesis

Due to the complexity of ribosome biogenesis; little is known about Dbp4's specific function *in vivo* and the discrete pre-rRNA processing steps in which this helicase functions. Thus, the objective of my thesis was to better understand the cellular roles of Dbp4. Immunoprecipitation experiments using whole cell extracts showed that Dbp4 associates with U3 snoRNA but not with U14 snoRNA, both of which are required for pre-18S rRNA processing. IPs also indicated that Dbp4 interacts with Mpp10, a U3- specific protein, suggesting that it interacts with the functionally active SSU processome. Electron microscopy analyses revealed that loss of Dbp4 impaired SSU processome formation and co-transcriptional cleavage of the pre-rRNA. Sucrose gradient analyses showed that the release of U14 snoRNA from pre-rRNA was disturbed upon loss of U3 snoRNA or Mpp10 protein, like what is observed in Dbp4-depleted cells, indicating that alteration of the SSU processome affects U14 snoRNA dynamics.

The following future perspectives will give more insight on the role of Dbp4 in rRNA maturation. It is supposed that the catalytic core of RNA helicases interacts

transiently with its substrates, while often additional domains or cofactors provide specificity (Linder and Jankowsky, 2011). Under our experimental conditions, and based on the probable nature of the transient interaction between Dbp4 and its substrate, we observed no association between Dbp4 and U14 snoRNA using whole cell extracts (Chapter II). To verify whether there is an interaction between these two molecules, RNA immunoprecipitation (RIP) experiments should be carried out (Gilbert and Svejstrup, 2006). Cells could be treated with formaldehyde to induce RNA-protein crosslinks before conducting IPs for Dbp4. Reverse transcription-PCR using U14 snoRNA specific oligonucleotides would be carried out to detect the presence of U14.

Dbp4 is one the RNA helicases for which the target site on the RNA is not identified. Thus the CRAC method could be used to identify the binding sites of Dbp4. CRAC is a UV cross-linking and analysis of cDNA method, and it is being used to identify binding sites of ribosome synthesis factors on snoRNAs and/or pre-rRNAs (Bohnsack *et al.*, 2009; Granneman *et al.*, 2009; Granneman *et al.*, 2010; Granneman *et al.*, 2011; Segerstolpe *et al.*, 2013). CRAC uses a bipartite tag on the protein of interest and involves a purification step under highly denaturing conditions followed by partial RNase digestion and deep sequencing (Bohnsack *et al.*, 2012; Granneman *et al.*, 2009).

Dbp4 was first identified as a multicopy suppressor of mutations in the Y domain of U14 snoRNA (Liang *et al.*, 1997). This yeast specific Y domain of U14 snoRNA is a highly folded stem-loop structure, and it is necessary for its activity (Li

and Fournier, 1992; Samarsky *et al.*, 1996). The pentanucleotide sequence GAACC (nt 62-66) in the loop is conserved in yeasts and point mutations or deletions in this sequence caused slow growth or lethal phenotypes. To further analyze the genetic link between Dbp4 and U14 snoRNA, the effect of U14 snoRNA mutations on molecular interactions involving Dbp4 and U3 snoRNA should be studied. The Y domain mutations could be expressed as described by Liang et al. (1997). A multi-copy plasmid carrying the *DBP4* gene along with plasmid-encoded U14 mutants could be transformed into the GAL::U14 strain (chapter II). The strains containing U14 mutants and the over-expressed Dbp4 would be grown in galactose-containing media, and afterwards the cells would be shifted to glucose-containing media to shut down production of genome-encoded U14. Thus the wild type genomic U14 would be depleted and only the U14 mutants would be expressed. The sedimentation pattern of U14 mutants could be compared with the wild-type U14 snoRNA by sucrose gradient analyses in order to find out whether the U14 mutants sediment differently from wild-type U14. The sedimentation profile of U3 snoRNA and Dbp4 would be analyzed in parallel. These experiments could reveal whether the expression of U14 mutants affects the molecular interactions and dynamics of U3 snoRNA and Dbp4 during ribosome biogenesis.

5.2. Nucleolar proteins Bfr2 and Enp2 are partners of Dbp4

Many of the factors involved in ribosome biogenesis have already been discovered and now it is important to find out how these factors are implicated in the

rearrangement of pre-rRNAs and pre-rRNPs. Genetic analyses and affinity purification of pre-ribosomes were used to identify assembly factors and their associated pre-rRNAs. These data helped us to obtain a timeline of assembly for the different factors during ribosome biogenesis but this assembly pathway includes more detailed steps than those already defined by the approaches mentioned above. Therefore, we need to obtain a higher resolution for the recruitment of the various trans-acting factors. Pre-rRNA processing and assembly steps are accompanied with numerous changes in the set of trans-acting factors associated with pre-rRNAs. Thus, pre-ribosomes are distinguishable by composition of pre-rRNAs and associated factors (Bernstein *et al.*, 2004; Milkereit *et al.*, 2003; Perez-Fernandez *et al.*, 2007; Schafer *et al.*, 2003). Most of the ribosome biogenesis factors associate transiently with nascent ribosomal subunits to form specific pre-ribosomal intermediates. The SSU processome is a ribonucleoprotein of about 80S implicated in the processing, assembly and maturation of the small subunit of the ribosome (Dragon *et al.*, 2002). An inclusive interactome map of the SSU processome will give us more detailed information about the assembly, function and regulation of this complex. Studying the assembly of the SSU processome is important to better understand its function in ribosome biogenesis. Based on the database analyses done by the group of Baserga (Lim *et al.*, 2011), about 70% of the physical protein-protein interactions in the SSU processome need to be determined in order to find out exactly how this complex is assembled. The missing data includes proteins with no known partners and unidentified protein-protein interactions. The second objective of my thesis was to get

a better understanding of the assembly and function of the SSU processome by analyzing molecular interactions of trans-acting factors involving RNA helicase Dbp4.

We identified Bfr2 and Enp2 as potential partners of Dbp4. Bfr2 and Enp2 are nucleolar proteins essential for viability of yeast cells. We also found that, like Dbp4, Bfr2 and Enp2 are required for the early processing steps that lead to the production of 18S rRNA. We demonstrated that Bfr2, Enp2 and Dbp4 associate with the U3 snoRNA, the U3-specific protein Mpp10, and also with different pre-rRNA species. These results led us to propose that Bfr2, Dbp4 and Enp2 are components of the SSU processome (80S complex). Sucrose gradient sedimentation analyses revealed that Dbp4, Bfr2 and Enp2 sediment in a peak of about 50S, as well as in a peak of ~80S, suggesting a dynamic reorganization of large complexes that likely contain other nucleolar factors. Our studies revealed that Bfr2, Dbp4 and Enp2 associate together in the 50S peak, which does not include the U3 snoRNA. However these proteins associate with U3 snoRNA in the 80S peak. U14 snoRNA associates with Dbp4 in the 50S peak but does not interact with Bfr2 or Enp2. A set of our experiments suggested that Bfr2, Enp2 and Dbp4 are incorporated at late steps during assembly of the SSU processome. The proposed subsequent experiments should give us additional data about ribosome biogenesis factors and molecular interactions required for rRNA maturation. To identify the protein composition of the "50S complex" including Dbp4, Bfr2 and Enp2, a yeast strain will be constructed in which Dbp4 will be TAP-tagged (Ghaemmaghami *et al.*, 2003) and sucrose gradient fractions corresponding to

the 50S peak will be prepared. Tandem affinity purification (TAP) (Rigaut *et al.*, 1999) of the 50S complex followed by mass spectrometry will be carried out. The identified proteins would be further analyzed to find out whether they are implicated in ribosome biogenesis and whether they are components of the SSU processome.

Many pre-ribosomal particles have complex protein compositions. Isolation of free ribosome biogenesis factor complexes provides better perception of the architecture of pre-ribosomes. It remains unclear if these complexes form and persist independently from pre-ribosome particles (Merl *et al.*, 2010). To verify whether our "50S complex" can form independently of (pre)-rRNAs, the following experiments could be carried out. The RNA polymerase I machinery can be shut down by expressing a conditional temperature-sensitive mutant of Rrn3, which is an essential RNA polymerase I transcription factor (Merl *et al.*, 2010). The phenotype of the mutant rrn3-8 would be expressed by shifting the cells from permissive to restrictive temperature according to (Merl *et al.*, 2010). Then sucrose gradient analyses will be performed to compare the sedimentation patterns of Dbp4, Bfr2 and Enp2 in cells with or without ongoing rRNA synthesis, and to find out if shutting down rRNA synthesis affects the sedimentation profile of these proteins. If there is no change in the sedimentation pattern of these proteins and they remain associated together in the 50S peak, this would suggest that formation of the 50S complex might be independent of the synthesis of rRNA. The protein composition of the 50S complex would be identified in rrn3-8 mutant using tandem affinity purification and mass spectrometry, as described above. The next step would be to verify if the absence of

the U3 snoRNA affects the formation of the 50S complex. A strain will be used in which U3 snoRNA could be depleted by shifting the cells from galactose to glucose (described in chapter II). In this strain one of the U3 snoRNA genes is disrupted and the other is under the control of the galactose promoter (Hughes and Ares, 1991; Samarsky and Fournier, 1998). The sedimenation profiles of Bfr2 and Enp2 could be analyzed in undepleted and U3-depleted cells using sucrose gradients. To find out whether these proteins remain associated in the absence of U3 snoRNA, IPs will be carried out using whole cell extracts and fractions of the sucrose gradient corresponding to the 50S peak. These experiments could tell us whether the 50S complex is formed independently from the SSU processome being assembled, or if it depends on the assembly of U3 snoRNP on the nascent pre-rRNA.

5.3. RNA helicase DDX10 is the human homolgue of yeast Dbp4

Our understanding of the molecular mechanisms underlying ribosome biogenesis has enormously increased over the past decades. Yet there are still questions left unanswered. Over the past 10 years, numerous studies have identified factors implicated in ribosome biogenesis mostly in yeast *Saccharomyces cerevisiae.* The various ribosome biogenesis studies in yeast led to a better understanding of ribosome biogenesis pathway (Li *et al.*, 2009; Tschochner and Hurt, 2003). In higher eukaryotes, model systems like cultured cells and frog oocytes were used to study rRNA transcription, rRNA processing, snoRNP biogenesis and nuclear export (Grummt, 2007; Henras *et al.*, 2008; Kiss *et al.*, 2006; Smith and Steitz, 1997). We

know that the major steps of ribosome biogenesis are highly conserved from yeast to humans, and most of the transacting factors in yeast have homologs in mammals (Adachi *et al.*, 2007; Coute *et al.*, 2008; Ginisty *et al.*, 1998; Holzel *et al.*, 2007; Holzel *et al.*, 2005; Prieto and McStay, 2007; Rohrmoser *et al.*, 2007; Rouquette *et al.*, 2005; Strezoska *et al.*, 2000; Thomas and Kutay, 2003; Trotta *et al.*, 2003; Turner *et al.*, 2009; Wang *et al.*, 2007; Westendorf *et al.*, 1998; Zemp and Kutay, 2007). However in mammals the complexity of ribosome biogenesis is much higher and it is less studied than in yeast. There are differences between yeast and mammalian ribosome synthesis, like rDNA genomic organization (Richard *et al.*, 2008) and stress response pathways (Zhang and Lu, 2009), which are unique to higher eukaryotes. There are also considerable differences in pre-rRNA maturation steps, and the human nucleolar proteome contains many more proteins (Ahmad *et al.*, 2009; Mullineux and Lafontaine, 2012). The making of ribosomes is one of most energy consuming processes in a cell. Because of its importance and crucial role in the cell, defects in ribosome biogenesis negatively affect cellular metabolism and vitality. Ribosome synthesis is related to cell size regulation, cell growth and division, and it affects cell-cycle progression (Bernstein *et al.*, 2007; Dez and Tollervey, 2004; Jorgensen *et al.*, 2004) and it is up-regulated in cancer (Ruggero and Pandolfi, 2003). The role of ribosome biogenesis in cancer is not well studied. Cell growth (change in cell mass) and cell proliferation (change in cell number) are very intimately linked. There is an increase in protein synthesis during cell growth and ribosome biogenesis is an important metabolic effort in proliferating cells. It is

known that the number of synthesized ribosomes controls the G1-S phase transition, thus affecting cell cycle progression (Donati *et al.*, 2012). Genetic abnormalities leading to impaired ribosome biogenesis and function, which show specific clinical phenotypes, are called ribosomopathies. Defects in ribosome biogenesis activate a cell-cycle checkpoint through the activation of the tumor suppressor p53 causing cell-cycle arrest and apoptosis (Deisenroth and Zhang, 2010; Mayer and Grummt, 2005; Zhang and Lu, 2009). In more than half of human tumours the function of p53 is impaired, therefore it is one of the most recurrent gene alteration in cancers (Soussi *et al.*, 2000). Thus activation of p53 by ribosome biogenesis inhibition could be used as target in ribosomepathies where the pathogenic role p53 has been proven. There are a number of diseases associated with defects in ribosome synthesis pathway (Freed *et al.*, 2010; Narla and Ebert, 2010). A study has shown that ribosome synthesis is implicated in stem cell differentiation in *Drosophila* (Fichelson *et al.*, 2009). In the case of HIV infection, the virus may use ribosome biogenesis to modulate host response (Ponti *et al.*, 2008). Haplo-insufficiencies of some ribosomal proteins are related to defects in pre-rRNA processing steps causing different ribosompathies (Liu and Ellis, 2006). Many ribosomal proteins have extraribosomal functions like replication and DNA repair showing that defects caused by mutations in these genes could be independent of their role in ribosome function (Warner and McIntosh, 2009). The number of RNA helicases in humans are two times higher than in yeast (Fairman-Williams *et al.*, 2010; Umate *et al.*, 2011). Among the different RNA helicases in humans (Umate *et al.*, 2011), 40 localize to the nucleolus, and 25 of them

are probably involved in ribosome biogenesis (Ahmad *et al.*, 2009; Rodriguez-Galan *et al.*, 2013). Several human RNA helicases have yeast homologues. Therefore the molecular functions of helicases in human and yeast could be similar (Rodriguez-Galan *et al.*, 2013). DDX10 is the human homologue of Dbp4 (Liang *et al.*, 1997). One of the goals of my thesis was to determine whether DDX10 is involved in ribosomes synthesis, and to analyze the effects of DDX10 down-regulation on cellular growth and proliferation. Knock down of DDX10 resulted in pre-rRNA processing defects and decreased production of 18S rRNA. We showed that DDX10 is associated with the U3 snoRNA, the U3-specific protein DRIM/UTP20 and Che-1 (human homologue of Bfr2). Flow cytometry analyses revealed that cells slightly accumulated in the G1 phase of the cell cycle upon loss of DDX10. Immunofluoresence microscopy indicated that treatment with siDDX10 strongly reduced the expression of the proliferation marker Ki-67. Based on our results, we suggested that DDX10 is necessary for cell growth and proliferation, and that it is implicated in pre-18S rRNA maturation.

The following experiments could provide additional data to better understand the role of DDX10 in ribosome biogenesis and its possible implication in human diseases. We found that DDX10 is associated with Che-1/AATF, Apoptosis Antagonizing Transcription Factor (Fanciulli *et al.*, 2000). Che-1 is a multifunctional protein involved in transcription regulation, cell-cycle control, DNA damage response and apoptosis (Passananti *et al.*, 2007). Our bioinformatics analysis showed that DDX10 contains two predicted coiled-coil (CC) motifs, which mediate protein-

protein interactions. Based on the results from chapter IV, DDX10 associated with Che-1 and the mutant DDX10 did not affect the interaction between these two proteins. To further study the nature of the interaction between DDX10 and Che-1, mutant DDX10 constructs bearing deletions of the second coiled coil or both coiled-coils will be expressed. IPs will be carried out to determine if these mutants remain associated with Che-1. In yeast, Dbp4 binds directly to Bfr2, the yeast homologue of Che-1 (Soltanieh *et al.*, 2014) Therefore it would be interesting to find out if there is a direct association between DDX10 and Che-1 using GST-pull down experiments. Nucleolar stress induced by impaired ribosome biogenesis triggers p53 signaling pathway (Chakraborty *et al.*, 2011). In order to analyze the effect of DDX10 knockdown on cell apoptosis, cells treated with siDDX10 and control siRNA will be double stained with annexin V and propidium iodide, and subjected to FACS analysis. The poly (ADP-ribose) polymerase (PARP) is involved in DNA repair (Trucco *et al.*, 1998). Cleaved PARP is no longer implicated in DNA repair function and therefore might facilitate induction of apoptosis (Smulson *et al.*, 1998; Trucco *et al.*, 1998). To further confirm induced apoptosis by DDX10 knock down, PARP cleavage will be determined using anti-PARP antibody by western blotting.

DDX10 was identified as a candidate breast cancer gene (Sjoblom et al. 2006): two mutations in DDX10 were associated with breast cancer, the point mutation L556V and the deletion of amino acids 593-618 (delta). DDX10 is expressed in a variety of human tissues (Savitsky *et al.*, 1996). Cell type and tissue specific expression of a target protein at the gene and protein level provide the

starting point for further studies to explore its specific role and function. Thus it could be helpful to analyze expression levels of DDX10 in different cell lines like MCF7 and MDA-MB-231 (breast cancer cell lines), HeLa (cervical cancer cell line), HEK293 (human embryonic kidney cell line) and other cancer and non-cancer cell lines. It would be interesting to analyze the effect of the two breast cancer mutations in DDX10 on cellular growth and proliferation in the different cell lines mentioned above. To verify cellular growth, cell counting and FACS analysis will be performed on cells expressing wild type and mutant DDX10 L566V and delta. To analyze cellular proliferation, BrdU Cell Proliferation Assay Kit (5-bromo-2'-deoxyuridine), immunofluoresence microscopy and western blot analysis using anti-Ki-67 antibodies proliferation maker could be carried out. Estrogens (E2) are hormones that are involved in initiation and progress of breast and uterine cancer (Yager and Davidson, 2006). Estrogen receptor α mediates E2 response in breast cancer (Bjornstrom and Sjoberg, 2005) and MCF7 is an estrogen receptor (ER) positive control cell line. DDX10 is an E2 responsive gene based on the study of (Hua *et al.*, 2008). Because DDX10 is a candidate breast cancer gene (Sjoblom *et al.*, 2006), it would be interesting to find out if DDX10 is a mediator of E2-stimulated cell proliferation. This would provide additional data to support the involvement of DDX10 in breast cancer. Cellular proliferation of siDDX10-treated and control cells will be measured under E2-depleted and E2-stimulated conditions using MCF7 cell lines.

5.4. General Conclusion

RNA helicases are ubiquitous and they participate in all aspects of RNA metabolism including ribosome biogenesis (Rocak and Linder, 2004), a complex process involving various components and different orderly steps. My work allowed a better understanding of the role of DEAD-box RNA helicase Dbp4 in ribosome biogenesis. The involvement of different RNA helicases in complexes with RNA and/or proteins and factors during ribosome biogenesis needs to be studied in detail. My experimental approaches and results provided insight into the order of assembly of Dbp4, Bfr2 and Enp2 into the SSU processome. There are growing evidences for various links between human diseases and ribosome biogenesis and function (Dai and Lu, 2008; Freed *et al.*, 2010; Narla and Ebert, 2010). Understanding how ribosome biogenesis factors like RNA helicases contribute to cancer initiation and progress and human diseases is a challenge, and progress in this field is needed. Chapter IV of my thesis presents additional findings in this regard. We showed that the human RNA helicase DDX10, homologue of yeast Dbp4, is involved in ribosome biogenesis, and is implicated in cellular growth and proliferation.

References

Abdelhaleem, M. (2004). Do human RNA helicases have a role in cancer? *Biochim Biophys Acta, 1704*(1), 37-46.

Abdelhaleem, M., Maltais, L. and Wain, H. (2003). The human DDX and DHX gene families of putative RNA helicases. *Genomics, 81*(6), 618-622.

Adachi, K., Soeta-Saneyoshi, C., Sagara, H. and Iwakura, Y. (2007). Crucial role of Bysl in mammalian preimplantation development as an integral factor for 40S ribosome biogenesis. *Mol Cell Biol, 27*(6), 2202-2214.

Adhikary, S. and Eilers, M. (2005). Transcriptional regulation and transformation by Myc proteins. *Nat Rev Mol Cell Biol, 6*(8), 635-645.

Ahmad, Y., Boisvert, F.M., Gregor, P., Cobley, A. and Lamond, A.I. (2009). NOPdb: Nucleolar Proteome Database--2008 update. *Nucleic Acids Res, 37*(Database issue), D181-184.

Anantharaman, V., Koonin, E.V. and Aravind, L. (2002). Comparative genomics and evolution of proteins involved in RNA metabolism. *Nucleic Acids Res, 30*(7), 1427-1464.

Andersen, J.S., Lam, Y.W., Leung, A.K., Ong, S.E., Lyon, C.E., Lamond, A.I. and Mann, M. (2005). Nucleolar proteome dynamics. *Nature, 433*(7021), 77-83.

Andersen, J.S., Lyon, C.E., Fox, A.H., Leung, A.K., Lam, Y.W., Steen, H., Mann, M. and Lamond, A.I. (2002). Directed proteomic analysis of the human nucleolus. *Curr Biol, 12*(1), 1-11.

Arai, Y., Hosoda, F., Kobayashi, H., Arai, K., Hayashi, Y., Kamada, N., Kaneko, Y. and Ohki, M. (1997). The inv(11)(p15q22) chromosome translocation of de novo and therapy-related myeloid malignancies results in fusion of the nucleoporin gene, NUP98, with the putative RNA helicase gene, DDX10. *Blood, 89*(11), 3936-3944.

Ausubel , B.R., Kingston RE, Moore DD, Seidman JG, SMITH JA, Struhl K (dir.). (1999). *Short protocols in molecular biology*. New York: John Wiley & Sons, Inc.

Bachellerie, J.P., Cavaille, J. and Huttenhofer, A. (2002). The expanding snoRNA world. *Biochimie, 84*(8), 775-790.

Balakin, A.G., Lempicki, R.A., Huang, G.M. and Fournier, M.J. (1994). Saccharomyces cerevisiae U14 small nuclear RNA has little secondary structure and appears to be produced by post-transcriptional processing. *J Biol Chem, 269*(1), 739-746.

Balakin, A.G., Smith, L. and Fournier, M.J. (1996). The RNA world of the nucleolus: two major families of small RNAs defined by different box elements with related functions. *Cell, 86*(5), 823-834.

Ban, N., Beckmann, R., Cate, J.H., Dinman, J.D., Dragon, F., Ellis, S.R., Lafontaine, D.L., Lindahl, L., Liljas, A., Lipton, J.M., McAlear, M.A., Moore, P.B., Noller, H.F., Ortega, J., Panse, V.G., Ramakrishnan, V., Spahn, C.M., Steitz, T.A., Tchorzewski, M., Tollervey, D., Warren, A.J., Williamson, J.R., Wilson, D., Yonath, A. and Yusupov, M. (2014). A new system for naming ribosomal proteins. *Curr Opin Struct Biol, 24*, 165-169.

Barbato, C., Corbi, N., Canu, N., Fanciulli, M., Serafino, A., Ciotti, M., Libri, V., Bruno, T., Amadoro, G., De Angelis, R., Calissano, P. and Passananti, C. (2003). Rb binding protein Che-1 interacts with Tau in cerebellar granule neurons. Modulation during neuronal apoptosis. *Mol Cell Neurosci, 24*(4), 1038-1050.

Beltrame, M., Henry, Y. and Tollervey, D. (1994a). Mutational analysis of an essential binding site for the U3 snoRNA in the 5' external transcribed spacer of yeast pre-rRNA. *Nucleic Acids Res, 22*(20), 4057-4065.

Beltrame, M., Henry, Y. and Tollervey, D. (1994b). Mutational analysis of an essential binding site for the U3 snoRNA in the 5' external transcribed spacer of yeast pre-rRNA. *Nucleic Acids Res, 22*(23), 5139-5147.

Beltrame, M. and Tollervey, D. (1992). Identification and functional analysis of two U3 binding sites on yeast pre-ribosomal RNA. *EMBO J, 11*(4), 1531-1542.

Beltrame, M. and Tollervey, D. (1995). Base pairing between U3 and the pre-ribosomal RNA is required for 18S rRNA synthesis. *EMBO J, 14*(17), 4350-4356.

Bernstein, D.A. and Keck, J.L. (2003). Domain mapping of Escherichia coli RecQ defines the roles of conserved N- and C-terminal regions in the RecQ family. *Nucleic Acids Res, 31*(11), 2778-2785.

Bernstein, K.A., Bleichert, F., Bean, J.M., Cross, F.R. and Baserga, S.J. (2007). Ribosome biogenesis is sensed at the Start cell cycle checkpoint. *Mol Biol Cell, 18*(3), 953-964.

Bernstein, K.A., Gallagher, J.E., Mitchell, B.M., Granneman, S. and Baserga, S.J. (2004). The small-subunit processome is a ribosome assembly intermediate. *Eukaryot Cell, 3*(6), 1619-1626.

Billy, E., Wegierski, T., Nasr, F. and Filipowicz, W. (2000). Rcl1p, the yeast protein similar to the RNA 3'-phosphate cyclase, associates with U3 snoRNP and is required for 18S rRNA biogenesis. *EMBO J, 19*(9), 2115-2126.

Bizebard, T., Ferlenghi, I., Iost, I. and Dreyfus, M. (2004). Studies on three E. coli DEAD-box helicases point to an unwinding mechanism different from that of model DNA helicases. *Biochemistry, 43*(24), 7857-7866.

Bjornstrom, L. and Sjoberg, M. (2005). Mechanisms of estrogen receptor signaling: convergence of genomic and nongenomic actions on target genes. *Mol Endocrinol, 19*(4), 833-842.

Bleichert, F. and Baserga, S.J. (2007). The long unwinding road of RNA helicases. *Mol Cell, 27*(3), 339-352.

Bohnsack, M.T., Martin, R., Granneman, S., Ruprecht, M., Schleiff, E. and Tollervey, D. (2009). Prp43 bound at different sites on the pre-rRNA performs distinct functions in ribosome synthesis. *Mol Cell, 36*(4), 583-592.

Bohnsack, M.T., Tollervey, D. and Granneman, S. (2012). Identification of RNA helicase target sites by UV cross-linking and analysis of cDNA. *Methods Enzymol, 511*, 275-288.

Boisvert, F.M., van Koningsbruggen, S., Navascues, J. and Lamond, A.I. (2007). The multifunctional nucleolus. *Nat Rev Mol Cell Biol, 8*(7), 574-585.

Boocock, G.R., Morrison, J.A., Popovic, M., Richards, N., Ellis, L., Durie, P.R. and Rommens, J.M. (2003). Mutations in SBDS are associated with Shwachman-Diamond syndrome. *Nat Genet, 33*(1), 97-101.

Borovjagin, A.V. and Gerbi, S.A. (1999). U3 small nucleolar RNA is essential for cleavage at sites 1, 2 and 3 in pre-rRNA and determines which rRNA processing pathway is taken in Xenopus oocytes. *J Mol Biol, 286*(5), 1347-1363.

Bratkovic, T. and Rogelj, B. (2011). Biology and applications of small nucleolar RNAs. *Cell Mol Life Sci, 68*(23), 3843-3851.

Brown, J.W., Echeverria, M., Qu, L.H., Lowe, T.M., Bachellerie, J.P., Huttenhofer, A., Kastenmayer, J.P., Green, P.J., Shaw, P. and Marshall, D.F. (2003). Plant snoRNA database. *Nucleic Acids Res, 31*(1), 432-435.

Bruno, T., De Angelis, R., De Nicola, F., Barbato, C., Di Padova, M., Corbi, N., Libri, V., Benassi, B., Mattei, E., Chersi, A., Soddu, S., Floridi, A., Passananti, C. and Fanciulli, M. (2002). Che-1 affects cell growth by interfering with the recruitment of HDAC1 by Rb. *Cancer Cell, 2*(5), 387-399.

Bruno, T., De Nicola, F., Iezzi, S., Lecis, D., D'Angelo, C., Di Padova, M., Corbi, N., Dimiziani, L., Zannini, L., Jekimovs, C., Scarsella, M., Porrello, A., Chersi, A., Crescenzi, M., Leonetti, C., Khanna, K.K., Soddu, S., Floridi, A., Passananti, C., Delia, D. and Fanciulli, M. (2006). Che-1 phosphorylation by ATM/ATR and Chk2 kinases activates p53 transcription and the G2/M checkpoint. *Cancer Cell, 10*(6), 473-486.

Bruno, T., Desantis, A., Bossi, G., Di Agostino, S., Sorino, C., De Nicola, F., Iezzi, S., Franchitto, A., Benassi, B., Galanti, S., La Rosa, F., Floridi, A., Bellacosa, A., Passananti, C., Blandino, G. and Fanciulli, M. (2010). Che-1 promotes tumor cell survival by sustaining mutant p53 transcription and inhibiting DNA damage response activation. *Cancer Cell, 18*(2), 122-134.

Busch, H. (1990). The final common pathway of cancer. *Cancer Res, 50*(16), 4830-4838.

Busch, H., Smetana, K. and (dir.). (1970). *The nucleolus*. New york: Academic Press.

Campbell, M.G. and Karbstein, K. (2011). Protein-protein interactions within late pre-40S ribosomes. *PLoS One, 6*(1), e16194.

Carmo-Fonseca, M., Mendes-Soares, L. and Campos, I. (2000). To be or not to be in the nucleolus. *Nat Cell Biol, 2*(6), E107-112.

Casafont, I., Navascues, J., Pena, E., Lafarga, M. and Berciano, M.T. (2006). Nuclear organization and dynamics of transcription sites in rat sensory ganglia neurons detected by incorporation of 5'-fluorouridine into nascent RNA. *Neuroscience, 140*(2), 453-462.

Chabane, S., Gachet, E. and Kepes, F. (1998). Over-expression of the yeast BFR2 gene partially suppresses the growth defects induced by Brefeldin A and by four ER-to-Golgi mutations. *Curr Genet, 33*(1), 21-28.

Chabane, S. and Kepes, F. (1998). Expression of the yeast BFR2 gene is regulated at the transcriptional level and through degradation of its product. *Mol Gen Genet, 258*(3), 215-221.

Chagnon, P., Michaud, J., Mitchell, G., Mercier, J., Marion, J.F., Drouin, E., Rasquin-Weber, A., Hudson, T.J. and Richter, A. (2002). A missense mutation (R565W) in cirhin (FLJ14728) in North American Indian childhood cirrhosis. *Am J Hum Genet, 71*(6), 1443-1449.

Chakraborty, A., Uechi, T. and Kenmochi, N. (2011). Guarding the 'translation apparatus': defective ribosome biogenesis and the p53 signaling pathway. *Wiley Interdiscip Rev RNA, 2*(4), 507-522.

Champion, E.A., Lane, B.H., Jackrel, M.E., Regan, L. and Baserga, S.J. (2008). A direct interaction between the Utp6 half-a-tetratricopeptide repeat domain and a specific peptide in Utp21 is essential for efficient pre-rRNA processing. *Mol Cell Biol, 28*(21), 6547-6556.

Chanfreau, G., Elela, S.A., Ares, M., Jr. and Guthrie, C. (1997). Alternative 3'-end processing of U5 snRNA by RNase III. *Genes Dev, 11*(20), 2741-2751.

Chanfreau, G., Legrain, P. and Jacquier, A. (1998). Yeast RNase III as a key processing enzyme in small nucleolar RNAs metabolism. *J Mol Biol, 284*(4), 975-988.

Chen, D., Zhang, Z., Li, M., Wang, W., Li, Y., Rayburn, E.R., Hill, D.L., Wang, H. and Zhang, R. (2007). Ribosomal protein S7 as a novel modulator of p53-MDM2 interaction: binding to MDM2, stabilization of p53 protein, and activation of p53 function. *Oncogene, 26*(35), 5029-5037.

Chu, S., Archer, R.H., Zengel, J.M. and Lindahl, L. (1994). The RNA of RNase MRP is required for normal processing of ribosomal RNA. *Proc Natl Acad Sci U S A, 91*(2), 659-663.

Clark, E.L., Coulson, A., Dalgliesh, C., Rajan, P., Nicol, S.M., Fleming, S., Heer, R., Gaughan, L., Leung, H.Y., Elliott, D.J., Fuller-Pace, F.V. and Robson, C.N. (2008). The RNA helicase p68 is a novel androgen receptor coactivator involved in splicing and is overexpressed in prostate cancer. *Cancer Res, 68*(19), 7938-7946.

Cmarko, D., Verschure, P.J., Rothblum, L.I., Hernandez-Verdun, D., Amalric, F., van Driel, R. and Fakan, S. (2000). Ultrastructural analysis of nucleolar transcription in cells microinjected with 5-bromo-UTP. *Histochem Cell Biol, 113*(3), 181-187.

Cokol, M., Nair, R. and Rost, B. (2000). Finding nuclear localization signals. *EMBO Rep, 1*(5), 411-415.

Collins, S.R., Kemmeren, P., Zhao, X.C., Greenblatt, J.F., Spencer, F., Holstege, F.C., Weissman, J.S. and Krogan, N.J. (2007). Toward a comprehensive atlas of the physical interactome of Saccharomyces cerevisiae. *Mol Cell Proteomics, 6*(3), 439-450.

Collins, T.J. (2007). ImageJ for microscopy. *Biotechniques, 43*(1 Suppl), 25-30.

Cordin, O., Banroques, J., Tanner, N.K. and Linder, P. (2006). The DEAD-box protein family of RNA helicases. *Gene, 367*, 17-37.

Cordin, O., Tanner, N.K., Doere, M., Linder, P. and Banroques, J. (2004). The newly discovered Q motif of DEAD-box RNA helicases regulates RNA-binding and helicase activity. *EMBO J, 23*(13), 2478-2487.

Coute, Y., Kindbeiter, K., Belin, S., Dieckmann, R., Duret, L., Bezin, L., Sanchez, J.C. and Diaz, J.J. (2008). ISG20L2, a novel vertebrate nucleolar exoribonuclease involved in ribosome biogenesis. *Mol Cell Proteomics, 7*(3), 546-559.

Cravchik, A. and Matus, A. (1993). A novel strategy for the immunological tagging of cDNA constructs. *Gene, 137*(1), 139-143.

Cui, S., Eisenacher, K., Kirchhofer, A., Brzozka, K., Lammens, A., Lammens, K., Fujita, T., Conzelmann, K.K., Krug, A. and Hopfner, K.P. (2008). The C-terminal regulatory domain is the RNA 5'-triphosphate sensor of RIG-I. *Mol Cell, 29*(2), 169-179.

Dai, M.S., Arnold, H., Sun, X.X., Sears, R. and Lu, H. (2007a). Inhibition of c-Myc activity by ribosomal protein L11. *EMBO J, 26*(14), 3332-3345.

Dai, M.S. and Lu, H. (2004). Inhibition of MDM2-mediated p53 ubiquitination and degradation by ribosomal protein L5. *J Biol Chem, 279*(43), 44475-44482.

Dai, M.S. and Lu, H. (2008). Crosstalk between c-Myc and ribosome in ribosomal biogenesis and cancer. *J Cell Biochem, 105*(3), 670-677.

Dai, M.S., Sears, R. and Lu, H. (2007b). Feedback regulation of c-Myc by ribosomal protein L11. *Cell Cycle, 6*(22), 2735-2741.

Dai, M.S., Zeng, S.X., Jin, Y., Sun, X.X., David, L. and Lu, H. (2004). Ribosomal protein L23 activates p53 by inhibiting MDM2 function in response to

ribosomal perturbation but not to translation inhibition. *Mol Cell Biol, 24*(17), 7654-7668.

David-Pfeuty, T., Nouvian-Dooghe, Y., Sirri, V., Roussel, P. and Hernandez-Verdun, D. (2001). Common and reversible regulation of wild-type p53 function and of ribosomal biogenesis by protein kinases in human cells. *Oncogene, 20*(42), 5951-5963.

de la Cruz, J., Kressler, D. and Linder, P. (1999). Unwinding RNA in Saccharomyces cerevisiae: DEAD-box proteins and related families. *Trends Biochem Sci, 24*(5), 192-198.

Decatur, W.A. and Fournier, M.J. (2002). rRNA modifications and ribosome function. *Trends Biochem Sci, 27*(7), 344-351.

Decatur, W.A. and Fournier, M.J. (2003). RNA-guided nucleotide modification of ribosomal and other RNAs. *J Biol Chem, 278*(2), 695-698.

Deisenroth, C. and Zhang, Y. (2010). Ribosome biogenesis surveillance: probing the ribosomal protein-Mdm2-p53 pathway. *Oncogene, 29*(30), 4253-4260.

Dennis, P.P. and Omer, A. (2005). Small non-coding RNAs in Archaea. *Curr Opin Microbiol, 8*(6), 685-694.

Derenzini, M., Montanaro, L. and Trere, D. (2009). What the nucleolus says to a tumour pathologist. *Histopathology, 54*(6), 753-762.

Dez, C. and Tollervey, D. (2004). Ribosome synthesis meets the cell cycle. *Curr Opin Microbiol, 7*(6), 631-637.

Doetsch, M., Schroeder, R. and Furtig, B. (2011). Transient RNA-protein interactions in RNA folding. *FEBS J, 278*(10), 1634-1642.

Donati, G., Montanaro, L. and Derenzini, M. (2012). Ribosome biogenesis and control of cell proliferation: p53 is not alone. *Cancer Res, 72*(7), 1602-1607.

Dosil, M. and Bustelo, X.R. (2004). Functional characterization of Pwp2, a WD family protein essential for the assembly of the 90 S pre-ribosomal particle. *J Biol Chem, 279*(36), 37385-37397.

Dragon, F., Gallagher, J.E., Compagnone-Post, P.A., Mitchell, B.M., Porwancher, K.A., Wehner, K.A., Wormsley, S., Settlage, R.E., Shabanowitz, J., Osheim, Y., Beyer, A.L., Hunt, D.F. and Baserga, S.J. (2002). A large nucleolar U3

ribonucleoprotein required for 18S ribosomal RNA biogenesis. *Nature, 417*(6892), 967-970.

Dragon, F., Pogacic, V. and Filipowicz, W. (2000). In vitro assembly of human H/ACA small nucleolar RNPs reveals unique features of U17 and telomerase RNAs. *Mol Cell Biol, 20*(9), 3037-3048.

Dunbar, D.A. and Baserga, S.J. (1998). The U14 snoRNA is required for 2'-O-methylation of the pre-18S rRNA in Xenopus oocytes. *RNA, 4*(2), 195-204.

Dunbar, D.A., Wormsley, S., Agentis, T.M. and Baserga, S.J. (1997). Mpp10p, a U3 small nucleolar ribonucleoprotein component required for pre-18S rRNA processing in yeast. *Mol Cell Biol, 17*(10), 5803-5812.

Dutca, L.M., Gallagher, J.E. and Baserga, S.J. (2011). The initial U3 snoRNA:pre-rRNA base pairing interaction required for pre-18S rRNA folding revealed by in vivo chemical probing. *Nucleic Acids Res, 39*(12), 5164-5180.

Eliceiri, G.L. (1999). Small nucleolar RNAs. *Cell Mol Life Sci, 56*(1-2), 22-31.

Emmott, E. and Hiscox, J.A. (2009). Nucleolar targeting: the hub of the matter. *EMBO Rep, 10*(3), 231-238.

Endl, E. and Gerdes, J. (2000). The Ki-67 protein: fascinating forms and an unknown function. *Exp Cell Res, 257*(2), 231-237.

Fabrizio, P., Esser, S., Kastner, B. and Luhrmann, R. (1994). Isolation of S. cerevisiae snRNPs: comparison of U1 and U4/U6.U5 to their human counterparts. *Science, 264*(5156), 261-265.

Fairman, M.E., Maroney, P.A., Wang, W., Bowers, H.A., Gollnick, P., Nilsen, T.W. and Jankowsky, E. (2004). Protein displacement by DExH/D "RNA helicases" without duplex unwinding. *Science, 304*(5671), 730-734.

Fairman-Williams, M.E., Guenther, U.P. and Jankowsky, E. (2010). SF1 and SF2 helicases: family matters. *Curr Opin Struct Biol, 20*(3), 313-324.

Fanciulli, M., Bruno, T., Di Padova, M., De Angelis, R., Iezzi, S., Iacobini, C., Floridi, A. and Passananti, C. (2000). Identification of a novel partner of RNA polymerase II subunit 11, Che-1, which interacts with and affects the growth suppression function of Rb. *FASEB J, 14*(7), 904-912.

Fatica, A. and Tollervey, D. (2002). Making ribosomes. *Curr Opin Cell Biol, 14*(3), 313-318.

Ferreira-Cerca, S., Kiburu, I., Thomson, E., LaRonde, N. and Hurt, E. (2014). Dominant Rio1 kinase/ATPase catalytic mutant induces trapping of late pre-40S biogenesis factors in 80S-like ribosomes. *Nucleic Acids Res, 42*(13), 8635-8647.

Fichelson, P., Moch, C., Ivanovitch, K., Martin, C., Sidor, C.M., Lepesant, J.A., Bellaiche, Y. and Huynh, J.R. (2009). Live-imaging of single stem cells within their niche reveals that a U3snoRNP component segregates asymmetrically and is required for self-renewal in Drosophila. *Nat Cell Biol, 11*(6), 685-693.

Filipowicz, W. and Pogacic, V. (2002). Biogenesis of small nucleolar ribonucleoproteins. *Curr Opin Cell Biol, 14*(3), 319-327.

Floridi, A. and Fanciulli, M. (2007). Che-1: a new effector of checkpoints signaling. *Cell Cycle, 6*(7), 804-806.

Freed, E.F. and Baserga, S.J. (2010). The C-terminus of Utp4, mutated in childhood cirrhosis, is essential for ribosome biogenesis. *Nucleic Acids Res, 38*(14), 4798-4806.

Freed, E.F., Bleichert, F., Dutca, L.M. and Baserga, S.J. (2010). When ribosomes go bad: diseases of ribosome biogenesis. *Mol Biosyst, 6*(3), 481-493.

Fromont-Racine, M., Senger, B., Saveanu, C. and Fasiolo, F. (2003). Ribosome assembly in eukaryotes. *Gene, 313*, 17-42.

Fumagalli, S., Ivanenkov, V.V., Teng, T. and Thomas, G. (2012). Suprainduction of p53 by disruption of 40S and 60S ribosome biogenesis leads to the activation of a novel G2/M checkpoint. *Genes Dev, 26*(10), 1028-1040.

Gallagher, J.E., Dunbar, D.A., Granneman, S., Mitchell, B.M., Osheim, Y., Beyer, A.L. and Baserga, S.J. (2004). RNA polymerase I transcription and pre-rRNA processing are linked by specific SSU processome components. *Genes Dev, 18*(20), 2506-2517.

Ganot, P., Bortolin, M.L. and Kiss, T. (1997a). Site-specific pseudouridine formation in preribosomal RNA is guided by small nucleolar RNAs. *Cell, 89*(5), 799-809.

Ganot, P., Caizergues-Ferrer, M. and Kiss, T. (1997b). The family of box ACA small nucleolar RNAs is defined by an evolutionarily conserved secondary structure and ubiquitous sequence elements essential for RNA accumulation. *Genes Dev, 11*(7), 941-956.

Garcia, I., Albring, M.J. and Uhlenbeck, O.C. (2012). Duplex destabilization by four ribosomal DEAD-box proteins. *Biochemistry, 51*(50), 10109-10118.

Garcia, I. and Uhlenbeck, O.C. (2008). Differential RNA-dependent ATPase activities of four rRNA processing yeast DEAD-box proteins. *Biochemistry, 47*(47), 12562-12573.

Garcia, S.N. and Pillus, L. (1999). Net results of nucleolar dynamics. *Cell, 97*(7), 825-828.

Gari, E., Piedrafita, L., Aldea, M. and Herrero, E. (1997). A set of vectors with a tetracycline-regulatable promoter system for modulated gene expression in Saccharomyces cerevisiae. *Yeast, 13*(9), 837-848.

Gavin, A.C., Bosche, M., Krause, R., Grandi, P., Marzioch, M., Bauer, A., Schultz, J., Rick, J.M., Michon, A.M., Cruciat, C.M., Remor, M., Hofert, C., Schelder, M., Brajenovic, M., Ruffner, H., Merino, A., Klein, K., Hudak, M., Dickson, D., Rudi, T., Gnau, V., Bauch, A., Bastuck, S., Huhse, B., Leutwein, C., Heurtier, M.A., Copley, R.R., Edelmann, A., Querfurth, E., Rybin, V., Drewes, G., Raida, M., Bouwmeester, T., Bork, P., Seraphin, B., Kuster, B., Neubauer, G. and Superti-Furga, G. (2002). Functional organization of the yeast proteome by systematic analysis of protein complexes. *Nature, 415*(6868), 141-147.

Gelperin, D., Horton, L., Beckman, J., Hensold, J. and Lemmon, S.K. (2001). Bms1p, a novel GTP-binding protein, and the related Tsr1p are required for distinct steps of 40S ribosome biogenesis in yeast. *RNA, 7*(9), 1268-1283.

Gerus, M., Bonnart, C., Caizergues-Ferrer, M., Henry, Y. and Henras, A.K. (2010). Evolutionarily conserved function of RRP36 in early cleavages of the pre-rRNA and production of the 40S ribosomal subunit. *Mol Cell Biol, 30*(5), 1130-1144.

Ghaemmaghami, S., Huh, W.K., Bower, K., Howson, R.W., Belle, A., Dephoure, N., O'Shea, E.K. and Weissman, J.S. (2003). Global analysis of protein expression in yeast. *Nature, 425*(6959), 737-741.

Gilbert, C. and Svejstrup, J.Q. (2006). RNA immunoprecipitation for determining RNA-protein associations in vivo. *Curr Protoc Mol Biol, Chapter 27*, Unit 27 24.

Ginisty, H., Amalric, F. and Bouvet, P. (1998). Nucleolin functions in the first step of ribosomal RNA processing. *EMBO J, 17*(5), 1476-1486.

Goessens, G. (1984). Nucleolar structure. *Int Rev Cytol, 87*, 107-158.

Gonzalez-Melendi, P., Wells, B., Beven, A.F. and Shaw, P.J. (2001). Single ribosomal transcription units are linear, compacted Christmas trees in plant nucleoli. *Plant J, 27*(3), 223-233.

Goobie, S., Popovic, M., Morrison, J., Ellis, L., Ginzberg, H., Boocock, G.R., Ehtesham, N., Betard, C., Brewer, C.G., Roslin, N.M., Hudson, T.J., Morgan, K., Fujiwara, T.M., Durie, P.R. and Rommens, J.M. (2001). Shwachman-Diamond syndrome with exocrine pancreatic dysfunction and bone marrow failure maps to the centromeric region of chromosome 7. *Am J Hum Genet, 68*(4), 1048-1054.

Gorbalenya and Koonin. (1993). Helicases: amino acid comparisons and structure-function relationships. *Curr Opin Struct Biol, 3*
, 419-429.

Grandi, P., Rybin, V., Bassler, J., Petfalski, E., Strauss, D., Marzioch, M., Schafer, T., Kuster, B., Tschochner, H., Tollervey, D., Gavin, A.C. and Hurt, E. (2002). 90S pre-ribosomes include the 35S pre-rRNA, the U3 snoRNP, and 40S subunit processing factors but predominantly lack 60S synthesis factors. *Mol Cell, 10*(1), 105-115.

Granneman, S. and Baserga, S.J. (2004). Ribosome biogenesis: of knobs and RNA processing. *Exp Cell Res, 296*(1), 43-50.

Granneman, S. and Baserga, S.J. (2005). Crosstalk in gene expression: coupling and co-regulation of rDNA transcription, pre-ribosome assembly and pre-rRNA processing. *Curr Opin Cell Biol, 17*(3), 281-286.

Granneman, S., Kudla, G., Petfalski, E. and Tollervey, D. (2009). Identification of protein binding sites on U3 snoRNA and pre-rRNA by UV cross-linking and high-throughput analysis of cDNAs. *Proc Natl Acad Sci U S A, 106*(24), 9613-9618.

Granneman, S., Petfalski, E., Swiatkowska, A. and Tollervey, D. (2010). Cracking pre-40S ribosomal subunit structure by systematic analyses of RNA-protein cross-linking. *EMBO J, 29*(12), 2026-2036.

Granneman, S., Petfalski, E. and Tollervey, D. (2011). A cluster of ribosome synthesis factors regulate pre-rRNA folding and 5.8S rRNA maturation by the Rat1 exonuclease. *EMBO J, 30*(19), 4006-4019.

Granneman, S., Pruijn, G.J., Horstman, W., van Venrooij, W.J., Luhrmann, R. and Watkins, N.J. (2002). The hU3-55K protein requires 15.5K binding to the box B/C motif as well as flanking RNA elements for its association with the U3 small nucleolar RNA in Vitro. *J Biol Chem, 277*(50), 48490-48500.

Green and Noller. (1997). Ribosomes and translation. *Annu. Rev. Biochem, 66*, 679-716.

Grummt, I. (1999). Regulation of mammalian ribosomal gene transcription by RNA polymerase I. *Prog Nucleic Acid Res Mol Biol, 62*, 109-154.

Grummt, I. (2007). Different epigenetic layers engage in complex crosstalk to define the epigenetic state of mammalian rRNA genes. *Hum Mol Genet, 16 Spec No 1*, R21-27.

Grundstrom, T., Zenke, W.M., Wintzerith, M., Matthes, H.W., Staub, A. and Chambon, P. (1985). Oligonucleotide-directed mutagenesis by microscale 'shot-gun' gene synthesis. *Nucleic Acids Res, 13*(9), 3305-3316.

Gutmann, B., Gobert, A. and Giege, P. (2012). PRORP proteins support RNase P activity in both organelles and the nucleus in Arabidopsis. *Genes Dev, 26*(10), 1022-1027.

Hadjiolov (dir.). (1985). *The nucleolus and ribosome biogenesis*. New York: Springer.

Hanada, K. and Hickson, I.D. (2007). Molecular genetics of RecQ helicase disorders. *Cell Mol Life Sci, 64*(17), 2306-2322.

Hannan, K.M., Hannan, R.D. and Rothblum, L.I. (1998a). Transcription by RNA polymerase I. *Front Biosci, 3*, d376-398.

Hannan, K.M., Hannan, R.D. and Rothblum, L.I. (1998b). Transcription by RNA polymerase I. *Frontiers in bioscience : a journal and virtual library, 3*, d376-398.

Haupt, Y., Maya, R., Kazaz, A. and Oren, M. (1997). Mdm2 promotes the rapid degradation of p53. *Nature, 387*(6630), 296-299.

Hazbun, T.R., Malmstrom, L., Anderson, S., Graczyk, B.J., Fox, B., Riffle, M., Sundin, B.A., Aranda, J.D., McDonald, W.H., Chiu, C.H., Snydsman, B.E., Bradley, P., Muller, E.G., Fields, S., Baker, D., Yates, J.R., 3rd and Davis, T.N. (2003). Assigning function to yeast proteins by integration of technologies. *Mol Cell, 12*(6), 1353-1365.

He, Y., Andersen, G.R. and Nielsen, K.H. (2010). Structural basis for the function of DEAH helicases. *EMBO Rep, 11*(3), 180-186.

Henras, A.K., Dez, C. and Henry, Y. (2004). RNA structure and function in C/D and H/ACA s(no)RNPs. *Curr Opin Struct Biol, 14*(3), 335-343.

Henras, A.K., Soudet, J., Gerus, M., Lebaron, S., Caizergues-Ferrer, M., Mougin, A. and Henry, Y. (2008). The post-transcriptional steps of eukaryotic ribosome biogenesis. *Cell Mol Life Sci, 65*(15), 2334-2359.

Higuchi, R., Krummel, B. and Saiki, R.K. (1988). A general method of in vitro preparation and specific mutagenesis of DNA fragments: study of protein and DNA interactions. *Nucleic Acids Res, 16*(15), 7351-7367.

Hiscox, J.A. (2007). RNA viruses: hijacking the dynamic nucleolus. *Nat Rev Microbiol, 5*(2), 119-127.

Holzel, M., Grimm, T., Rohrmoser, M., Malamoussi, A., Harasim, T., Gruber-Eber, A., Kremmer, E. and Eick, D. (2007). The BRCT domain of mammalian Pes1 is crucial for nucleolar localization and rRNA processing. *Nucleic Acids Res, 35*(3), 789-800.

Holzel, M., Rohrmoser, M., Schlee, M., Grimm, T., Harasim, T., Malamoussi, A., Gruber-Eber, A., Kremmer, E., Hiddemann, W., Bornkamm, G.W. and Eick, D. (2005). Mammalian WDR12 is a novel member of the Pes1-Bop1 complex and is required for ribosome biogenesis and cell proliferation. *J Cell Biol, 170*(3), 367-378.

Horky, M., Kotala, V., Anton, M. and Wesierska-Gadek, J. (2002). Nucleolus and apoptosis. *Ann N Y Acad Sci, 973*, 258-264.

Hu, L., Wang, J., Liu, Y., Zhang, Y., Zhang, L., Kong, R., Zheng, Z., Du, X. and Ke, Y. (2011). A small ribosomal subunit (SSU) processome component, the human U3 protein 14A (hUTP14A) binds p53 and promotes p53 degradation. *J Biol Chem, 286*(4), 3119-3128.

Hua, S., Kallen, C.B., Dhar, R., Baquero, M.T., Mason, C.E., Russell, B.A., Shah, P.K., Liu, J., Khramtsov, A., Tretiakova, M.S., Krausz, T.N., Olopade, O.I., Rimm, D.L. and White, K.P. (2008). Genomic analysis of estrogen cascade reveals histone variant H2A.Z associated with breast cancer progression. *Mol Syst Biol, 4*, 188.

Huang, G.M., Jarmolowski, A., Struck, J.C. and Fournier, M.J. (1992). Accumulation of U14 small nuclear RNA in Saccharomyces cerevisiae

requires box C, box D, and a 5', 3' terminal stem. *Mol Cell Biol, 12*(10), 4456-4463.

Hughes, J.M. (1996). Functional base-pairing interaction between highly conserved elements of U3 small nucleolar RNA and the small ribosomal subunit RNA. *J Mol Biol, 259*(4), 645-654.

Hughes, J.M. and Ares, M., Jr. (1991). Depletion of U3 small nucleolar RNA inhibits cleavage in the 5' external transcribed spacer of yeast pre-ribosomal RNA and impairs formation of 18S ribosomal RNA. *EMBO J, 10*(13), 4231-4239.

Huh, W.K., Falvo, J.V., Gerke, L.C., Carroll, A.S., Howson, R.W., Weissman, J.S. and O'Shea, E.K. (2003). Global analysis of protein localization in budding yeast. *Nature, 425*(6959), 686-691.

Huttenhofer, A., Kiefmann, M., Meier-Ewert, S., O'Brien, J., Lehrach, H., Bachellerie, J.P. and Brosius, J. (2001). RNomics: an experimental approach that identifies 201 candidates for novel, small, non-messenger RNAs in mouse. *EMBO J, 20*(11), 2943-2953.

James, P., Halladay, J. and Craig, E.A. (1996). Genomic libraries and a host strain designed for highly efficient two-hybrid selection in yeast. *Genetics, 144*(4), 1425-1436.

Jankowsky, A., Guenther, U.P. and Jankowsky, E. (2011). The RNA helicase database. *Nucleic Acids Res, 39*(Database issue), D338-341.

Jankowsky, E. (2011). RNA helicases at work: binding and rearranging. *Trends Biochem Sci, 36*(1), 19-29.

Jankowsky, E. and Bowers, H. (2006). Remodeling of ribonucleoprotein complexes with DExH/D RNA helicases. *Nucleic Acids Res, 34*(15), 4181-4188.

Jankowsky, E. and Fairman, M.E. (2007). RNA helicases--one fold for many functions. *Curr Opin Struct Biol, 17*(3), 316-324.

Jarmolowski, A., Zagorski, J., Li, H.V. and Fournier, M.J. (1990). Identification of essential elements in U14 RNA of Saccharomyces cerevisiae. *EMBO J, 9*(13), 4503-4509.

Jarmoskaite, I. and Russell, R. (2011). DEAD-box proteins as RNA helicases and chaperones. *Wiley Interdiscip Rev RNA, 2*(1), 135-152.

Jiao, X., Hooper, S.D., Djureinovic, T., Larsson, C., Warnberg, F., Tellgren-Roth, C., Botling, J. and Sjoblom, T. (2013). Gene rearrangements in hormone receptor negative breast cancers revealed by mate pair sequencing. *BMC Genomics, 14*, 165.

Jorgensen, P., Rupes, I., Sharom, J.R., Schneper, L., Broach, J.R. and Tyers, M. (2004). A dynamic transcriptional network communicates growth potential to ribosome synthesis and critical cell size. *Genes Dev, 18*(20), 2491-2505.

Karbstein, K. (2011). Inside the 40S ribosome assembly machinery. *Curr Opin Chem Biol, 15*(5), 657-663.

Karbstein, K., Jonas, S. and Doudna, J.A. (2005). An essential GTPase promotes assembly of preribosomal RNA processing complexes. *Mol Cell, 20*(4), 633-643.

Karginov, F.V., Caruthers, J.M., Hu, Y., McKay, D.B. and Uhlenbeck, O.C. (2005). YxiN is a modular protein combining a DEx(D/H) core and a specific RNA-binding domain. *J Biol Chem, 280*(42), 35499-35505.

Kass, S., Tyc, K., Steitz, J.A. and Sollner-Webb, B. (1990). The U3 small nucleolar ribonucleoprotein functions in the first step of preribosomal RNA processing. *Cell, 60*(6), 897-908.

Katsamba, P.S., Myszka, D.G. and Laird-Offringa, I.A. (2001). Two functionally distinct steps mediate high affinity binding of U1A protein to U1 hairpin II RNA. *J Biol Chem, 276*(24), 21476-21481.

Killoran, M.P. and Keck, J.L. (2008). Structure and function of the regulatory C-terminal HRDC domain from Deinococcus radiodurans RecQ. *Nucleic Acids Res, 36*(9), 3139-3149.

King, T.H., Liu, B., McCully, R.R. and Fournier, M.J. (2003). Ribosome structure and activity are altered in cells lacking snoRNPs that form pseudouridines in the peptidyl transferase center. *Mol Cell, 11*(2), 425-435.

Kiss, T. (2001). Small nucleolar RNA-guided post-transcriptional modification of cellular RNAs. *EMBO J, 20*(14), 3617-3622.

Kiss, T., Fayet, E., Jady, B.E., Richard, P. and Weber, M. (2006). Biogenesis and intranuclear trafficking of human box C/D and H/ACA RNPs. *Cold Spring Harb Symp Quant Biol, 71*, 407-417.

Kiss-Laszlo, Z., Henry, Y., Bachellerie, J.P., Caizergues-Ferrer, M. and Kiss, T. (1996). Site-specific ribose methylation of preribosomal RNA: a novel function for small nucleolar RNAs. *Cell, 85*(7), 1077-1088.

Kiss-Laszlo, Z., Henry, Y. and Kiss, T. (1998). Sequence and structural elements of methylation guide snoRNAs essential for site-specific ribose methylation of pre-rRNA. *EMBO J, 17*(3), 797-807.

Klein, D.J., Schmeing, T.M., Moore, P.B. and Steitz, T.A. (2001). The kink-turn: a new RNA secondary structure motif. *EMBO J, 20*(15), 4214-4221.

Klostermeier, D. and Rudolph, M.G. (2009). A novel dimerization motif in the C-terminal domain of the Thermus thermophilus DEAD box helicase Hera confers substantial flexibility. *Nucleic Acids Res, 37*(2), 421-430.

Knop, M., Siegers, K., Pereira, G., Zachariae, W., Winsor, B., Nasmyth, K. and Schiebel, E. (1999). Epitope tagging of yeast genes using a PCR-based strategy: more tags and improved practical routines. *Yeast, 15*(10B), 963-972.

Kos, M. and Tollervey, D. (2005). The Putative RNA Helicase Dbp4p Is Required for Release of the U14 snoRNA from Preribosomes in Saccharomyces cerevisiae. *Mol Cell, 20*(1), 53-64.

Kos, M. and Tollervey, D. (2010). Yeast pre-rRNA processing and modification occur cotranscriptionally. *Mol Cell, 37*(6), 809-820.

Kressler, D., Hurt, E. and Bassler, J. (2010). Driving ribosome assembly. *Biochim Biophys Acta, 1803*(6), 673-683.

Kressler, D., Linder, P. and de La Cruz, J. (1999). Protein trans-acting factors involved in ribosome biogenesis in Saccharomyces cerevisiae. *Mol Cell Biol, 19*(12), 7897-7912.

Krogan, N.J., Cagney, G., Yu, H., Zhong, G., Guo, X., Ignatchenko, A., Li, J., Pu, S., Datta, N., Tikuisis, A.P., Punna, T., Peregrin-Alvarez, J.M., Shales, M., Zhang, X., Davey, M., Robinson, M.D., Paccanaro, A., Bray, J.E., Sheung, A., Beattie, B., Richards, D.P., Canadien, V., Lalev, A., Mena, F., Wong, P., Starostine, A., Canete, M.M., Vlasblom, J., Wu, S., Orsi, C., Collins, S.R., Chandran, S., Haw, R., Rilstone, J.J., Gandi, K., Thompson, N.J., Musso, G., St Onge, P., Ghanny, S., Lam, M.H., Butland, G., Altaf-Ul, A.M., Kanaya, S., Shilatifard, A., O'Shea, E., Weissman, J.S., Ingles, C.J., Hughes, T.R., Parkinson, J., Gerstein, M., Wodak, S.J., Emili, A. and Greenblatt, J.F. (2006). Global landscape of protein complexes in the yeast Saccharomyces cerevisiae. *Nature, 440*(7084), 637-643.

Krogan, N.J., Peng, W.T., Cagney, G., Robinson, M.D., Haw, R., Zhong, G., Guo, X., Zhang, X., Canadien, V., Richards, D.P., Beattie, B.K., Lalev, A., Zhang, W., Davierwala, A.P., Mnaimneh, S., Starostine, A., Tikuisis, A.P., Grigull, J., Datta, N., Bray, J.E., Hughes, T.R., Emili, A. and Greenblatt, J.F. (2004). High-definition macromolecular composition of yeast RNA-processing complexes. *Mol Cell, 13*(2), 225-239.

Kruiswijk, T., Planta, R.J. and Krop, J.M. (1978). The course of the assembly of ribosomal subunits in yeast. *Biochim Biophys Acta, 517*(2), 378-389.

Kruse, J.P. and Gu, W. (2009). Modes of p53 regulation. *Cell, 137*(4), 609-622.

Kubbutat, M.H., Jones, S.N. and Vousden, K.H. (1997). Regulation of p53 stability by Mdm2. *Nature, 387*(6630), 299-303.

la Cour, T., Kiemer, L., Molgaard, A., Gupta, R., Skriver, K. and Brunak, S. (2004). Analysis and prediction of leucine-rich nuclear export signals. *Protein Eng Des Sel, 17*(6), 527-536.

Lafontaine, D.L. (2015). Noncoding RNAs in eukaryotic ribosome biogenesis and function. *Nat Struct Mol Biol, 22*(1), 11-19.

Lafontaine, D.L. and Tollervey, D. (2001). The function and synthesis of ribosomes. *Nat Rev Mol Cell Biol, 2*(7), 514-520.

Leader, D.J., Clark, G.P., Watters, J., Beven, A.F., Shaw, P.J. and Brown, J.W. (1997). Clusters of multiple different small nucleolar RNA genes in plants are expressed as and processed from polycistronic pre-snoRNAs. *EMBO J, 16*(18), 5742-5751.

Leader, D.J., Sanders, J.F., Waugh, R., Shaw, P. and Brown, J.W. (1994). Molecular characterisation of plant U14 small nucleolar RNA genes: closely linked genes are transcribed as polycistronic U14 transcripts. *Nucleic Acids Res, 22*(24), 5196-5203.

Lee, S.J. and Baserga, S.J. (1999). Imp3p and Imp4p, two specific components of the U3 small nucleolar ribonucleoprotein that are essential for pre-18S rRNA processing. *Mol Cell Biol, 19*(8), 5441-5452.

Leger-silvestre and Gas (dir.). (2004). *The nucleolar ultrastructure in yeast.* New York: Kluwer Academic/Plenum Publishers.

Leipe, D.D., Wolf, Y.I., Koonin, E.V. and Aravind, L. (2002). Classification and evolution of P-loop GTPases and related ATPases. *J Mol Biol, 317*(1), 41-72.

Lemay, V., Hossain, A., Osheim, Y.N., Beyer, A.L. and Dragon, F. (2011). Identification of novel proteins associated with yeast snR30 small nucleolar RNA. *Nucleic Acids Res, 39*(22), 9659-9670.

Lestrade, L. and Weber, M.J. (2006). snoRNA-LBME-db, a comprehensive database of human H/ACA and C/D box snoRNAs. *Nucleic Acids Res, 34*(Database issue), D158-162.

Li, D. and Fournier, M.J. (1992). U14 function in Saccharomyces cerevisiae can be provided by large deletion variants of yeast U14 and hybrid mouse-yeast U14 RNAs. *EMBO J, 11*(2), 683-689.

Li, Z., Lee, I., Moradi, E., Hung, N.J., Johnson, A.W. and Marcotte, E.M. (2009). Rational extension of the ribosome biogenesis pathway using network-guided genetics. *PLoS Biol, 7*(10), e1000213.

Liang, W.Q., Clark, J.A. and Fournier, M.J. (1997). The rRNA-processing function of the yeast U14 small nucleolar RNA can be rescued by a conserved RNA helicase-like protein. *Mol Cell Biol, 17*(7), 4124-4132.

Liang, W.Q. and Fournier, M.J. (1995). U14 base-pairs with 18S rRNA: a novel snoRNA interaction required for rRNA processing. *Genes Dev, 9*(19), 2433-2443.

Liang, X.H., Liu, Q., King, T.H. and Fournier, M.J. (2010). Strong dependence between functional domains in a dual-function snoRNA infers coupling of rRNA processing and modification events. *Nucleic Acids Res*

Lim, Y.H., Charette, J.M. and Baserga, S.J. (2011). Assembling a protein-protein interaction map of the SSU processome from existing datasets. *PLoS One, 6*(3), e17701.

Linder, P. and Jankowsky, E. (2011). From unwinding to clamping - the DEAD box RNA helicase family. *Nat Rev Mol Cell Biol, 12*(8), 505-516.

Linder, P., Lasko, P.F., Ashburner, M., Leroy, P., Nielsen, P.J., Nishi, K., Schnier, J. and Slonimski, P.P. (1989). Birth of the D-E-A-D box. *Nature, 337*(6203), 121-122.

Liu, J., Du, X. and Ke, Y. (2006). Mapping nucleolar localization sequences of 1A6/DRIM. *FEBS Lett, 580*(5), 1405-1410.

Liu, J.M. and Ellis, S.R. (2006). Ribosomes and marrow failure: coincidental association or molecular paradigm? *Blood, 107*(12), 4583-4588.

Lohman, T.M., Tomko, E.J. and Wu, C.G. (2008). Non-hexameric DNA helicases and translocases: mechanisms and regulation. *Nat Rev Mol Cell Biol, 9*(5), 391-401.

Longtine, M.S., McKenzie, A., 3rd, Demarini, D.J., Shah, N.G., Wach, A., Brachat, A., Philippsen, P. and Pringle, J.R. (1998). Additional modules for versatile and economical PCR-based gene deletion and modification in Saccharomyces cerevisiae. *Yeast, 14*(10), 953-961.

Lorsch, J.R. and Herschlag, D. (1998). The DEAD box protein eIF4A. 1. A minimal kinetic and thermodynamic framework reveals coupled binding of RNA and nucleotide. *Biochemistry, 37*(8), 2180-2193.

Lowe, S.W., Cepero, E. and Evan, G. (2004). Intrinsic tumour suppression. *Nature, 432*(7015), 307-315.

Luking, A., Stahl, U. and Schmidt, U. (1998). The protein family of RNA helicases. *Crit Rev Biochem Mol Biol, 33*(4), 259-296.

Lygerou, Z., Allmang, C., Tollervey, D. and Seraphin, B. (1996). Accurate processing of a eukaryotic precursor ribosomal RNA by ribonuclease MRP in vitro. *Science, 272*(5259), 268-270.

Maggi, L.B., Jr. and Weber, J.D. (2005). Nucleolar adaptation in human cancer. *Cancer Invest, 23*(7), 599-608.

Martin, R., Straub, A.U., Doebele, C. and Bohnsack, M.T. (2013). DExD/H-box RNA helicases in ribosome biogenesis. *RNA Biol, 10*(1), 4-18.

Martindill, D.M. and Riley, P.R. (2008). Cell cycle switch to endocycle: the nucleolus lends a hand. *Cell Cycle, 7*(1), 17-23.

Matthews, D.A. and Olson, M.O. (2006). What is new in the nucleolus?: workshop on the nucleolus: new perspectives. *EMBO Rep, 7*(9), 870-873.

Maxwell, E.S. and Fournier, M.J. (1995). The small nucleolar RNAs. *Annu Rev Biochem, 64*, 897-934.

Mayer, C. and Grummt, I. (2005). Cellular stress and nucleolar function. *Cell Cycle, 4*(8), 1036-1038.

McKeown, P.C. and Shaw, P.J. (2009). Chromatin: linking structure and function in the nucleolus. *Chromosoma, 118*(1), 11-23.

Meier, U.T. (2005). The many facets of H/ACA ribonucleoproteins. *Chromosoma, 114*(1), 1-14.

Melcak, I., Risueno, M.C. and Raska, I. (1996). Ultrastructural nonisotopic mapping of nucleolar transcription sites in onion protoplasts. *J Struct Biol, 116*(2), 253-263.

Mereau, A., Fournier, R., Gregoire, A., Mougin, A., Fabrizio, P., Luhrmann, R. and Branlant, C. (1997). An in vivo and in vitro structure-function analysis of the Saccharomyces cerevisiae U3A snoRNP: protein-RNA contacts and base-pair interaction with the pre-ribosomal RNA. *J Mol Biol, 273*(3), 552-571.

Merl, J., Jakob, S., Ridinger, K., Hierlmeier, T., Deutzmann, R., Milkereit, P. and Tschochner, H. (2010). Analysis of ribosome biogenesis factor-modules in yeast cells depleted from pre-ribosomes. *Nucleic Acids Res, 38*(9), 3068-3080.

Milkereit, P., Kuhn, H., Gas, N. and Tschochner, H. (2003). The pre-ribosomal network. *Nucleic Acids Res, 31*(3), 799-804.

Miller, O.L., Jr. and Beatty, B.R. (1969). Visualization of nucleolar genes. *Science, 164*(3882), 955-957.

Momand, J., Zambetti, G.P., Olson, D.C., George, D. and Levine, A.J. (1992). The mdm-2 oncogene product forms a complex with the p53 protein and inhibits p53-mediated transactivation. *Cell, 69*(7), 1237-1245.

Mongelard, F. and Bouvet, P. (2007). Nucleolin: a multiFACeTed protein. *Trends Cell Biol, 17*(2), 80-86.

Montanaro, L., Trere, D. and Derenzini, M. (2008). Nucleolus, ribosomes, and cancer. *Am J Pathol, 173*(2), 301-310.

Montanaro, L., Trere, D. and Derenzini, M. (2012). Changes in ribosome biogenesis may induce cancer by down-regulating the cell tumor suppressor potential. *Biochim Biophys Acta, 1825*(1), 101-110.

Montgomery. (1898). Comparative cytological studies, with especial regard to the morphology of the nucleolus. *J. Morphol, 15*, 265-582.

Moore, P.B. and Steitz, T.A. (2002). The involvement of RNA in ribosome function. *Nature, 418*(6894), 229-235.

Moore, P.B. and Steitz, T.A. (2011). The roles of RNA in the synthesis of protein. *Cold Spring Harb Perspect Biol, 3*(11), a003780.

Mosgoller (dir.). (2004). *Nucleolar utrastructure in vertebrates*. New York: Kluwer Avademic/Plenum Publishers.

Moss, T., Langlois, F., Gagnon-Kugler, T. and Stefanovsky, V. (2007). A housekeeper with power of attorney: the rRNA genes in ribosome biogenesis. *Cell Mol Life Sci, 64*(1), 29-49.

Mougey, E.B., O'Reilly, M., Osheim, Y., Miller, O.L., Jr., Beyer, A. and Sollner-Webb, B. (1993). The terminal balls characteristic of eukaryotic rRNA transcription units in chromatin spreads are rRNA processing complexes. *Genes Dev, 7*(8), 1609-1619.

Mullineux, S.T. and Lafontaine, D.L. (2012). Mapping the cleavage sites on mammalian pre-rRNAs: where do we stand? *Biochimie, 94*(7), 1521-1532.

Myong, S., Cui, S., Cornish, P.V., Kirchhofer, A., Gack, M.U., Jung, J.U., Hopfner, K.P. and Ha, T. (2009). Cytosolic viral sensor RIG-I is a 5'-triphosphate-dependent translocase on double-stranded RNA. *Science, 323*(5917), 1070-1074.

Nagahama, M., Hara, Y., Seki, A., Yamazoe, T., Kawate, Y., Shinohara, T., Hatsuzawa, K., Tani, K. and Tagaya, M. (2004). NVL2 is a nucleolar AAA-ATPase that interacts with ribosomal protein L5 through its nucleolar localization sequence. *Mol Biol Cell, 15*(12), 5712-5723.

Narla, A. and Ebert, B.L. (2010). Ribosomopathies: human disorders of ribosome dysfunction. *Blood, 115*(16), 3196-3205.

Nash, R., Weng, S., Hitz, B., Balakrishnan, R., Christie, K.R., Costanzo, M.C., Dwight, S.S., Engel, S.R., Fisk, D.G., Hirschman, J.E., Hong, E.L., Livstone, M.S., Oughtred, R., Park, J., Skrzypek, M., Theesfeld, C.L., Binkley, G., Dong, Q., Lane, C., Miyasato, S., Sethuraman, A., Schroeder, M., Dolinski, K., Botstein, D. and Cherry, J.M. (2007). Expanded protein information at SGD: new pages and proteome browser. *Nucleic Acids Res, 35*(Database issue), D468-471.

Neigeborn, L. and Warner, J.R. (1990). Expression of yeast 5S RNA is independent of the rDNA enhancer region. *Nucleic Acids Res, 18*(14), 4179-4184.

Ni, J., Tien, A.L. and Fournier, M.J. (1997). Small nucleolar RNAs direct site-specific synthesis of pseudouridine in ribosomal RNA. *Cell, 89*(4), 565-573.

Nicoloso, M., Qu, L.H., Michot, B. and Bachellerie, J.P. (1996). Intron-encoded, antisense small nucleolar RNAs: the characterization of nine novel species

points to their direct role as guides for the 2'-O-ribose methylation of rRNAs. *J Mol Biol, 260*(2), 178-195.

Nissan, T.A., Galani, K., Maco, B., Tollervey, D., Aebi, U. and Hurt, E. (2004). A pre-ribosome with a tadpole-like structure functions in ATP-dependent maturation of 60S subunits. *Mol Cell, 15*(2), 295-301.

Nissen, P., Hansen, J., Ban, N., Moore, P.B. and Steitz, T.A. (2000). The structural basis of ribosome activity in peptide bond synthesis. *Science, 289*(5481), 920-930.

Noller, H.F., Hoffarth, V. and Zimniak, L. (1992). Unusual resistance of peptidyl transferase to protein extraction procedures. *Science, 256*(5062), 1416-1419.

Oeffinger, M., Zenklusen, D., Ferguson, A., Wei, K.E., El Hage, A., Tollervey, D., Chait, B.T., Singer, R.H. and Rout, M.P. (2009). Rrp17p is a eukaryotic exonuclease required for 5' end processing of Pre-60S ribosomal RNA. *Mol Cell, 36*(5), 768-781.

Ofengand, J. (2002). Ribosomal RNA pseudouridines and pseudouridine synthases. *FEBS Lett, 514*(1), 17-25.

Olson, M.O., Dundr, M. and Szebeni, A. (2000). The nucleolus: an old factory with unexpected capabilities. *Trends Cell Biol, 10*(5), 189-196.

Omer, A.D., Ziesche, S., Decatur, W.A., Fournier, M.J. and Dennis, P.P. (2003). RNA-modifying machines in archaea. *Mol Microbiol, 48*(3), 617-629.

Ortiz, M.L., Calero, M., Fernandez Patron, C., Patron, C.F., Castellanos, L. and Mendez, E. (1992). Imidazole-SDS-Zn reverse staining of proteins in gels containing or not SDS and microsequence of individual unmodified electroblotted proteins. *FEBS Lett, 296*(3), 300-304.

Osheim, Y.N., French, S.L., Keck, K.M., Champion, E.A., Spasov, K., Dragon, F., Baserga, S.J. and Beyer, A.L. (2004). Pre-18S ribosomal RNA is structurally compacted into the SSU processome prior to being cleaved from nascent transcripts in Saccharomyces cerevisiae. *Mol Cell, 16*(6), 943-954.

Oskarsson, T. and Trumpp, A. (2005). The Myc trilogy: lord of RNA polymerases. *Nat Cell Biol, 7*(3), 215-217.

Panse, V.G. and Johnson, A.W. (2010). Maturation of eukaryotic ribosomes: acquisition of functionality. *Trends Biochem Sci, 35*(5), 260-266.

Passananti, C. and Fanciulli, M. (2007). The anti-apoptotic factor Che-1/AATF links transcriptional regulation, cell cycle control, and DNA damage response. *Cell Div, 2*, 21.

Passananti, C., Floridi, A. and Fanciulli, M. (2007). Che-1/AATF, a multivalent adaptor connecting transcriptional regulation, checkpoint control, and apoptosis. *Biochem Cell Biol, 85*(4), 477-483.

Peck, M.L. and Herschlag, D. (2003). Adenosine 5'-O-(3-thio)triphosphate (ATPgammaS) is a substrate for the nucleotide hydrolysis and RNA unwinding activities of eukaryotic translation initiation factor eIF4A. *RNA, 9*(10), 1180-1187.

Pederson, T. (1998a). Growth factors in the nucleolus? *J Cell Biol, 143*(2), 279-281.

Pederson, T. (1998b). The plurifunctional nucleolus. *Nucleic Acids Res, 26*(17), 3871-3876.

Pelengaris, S., Khan, M. and Evan, G. (2002a). c-MYC: more than just a matter of life and death. *Nat Rev Cancer, 2*(10), 764-776.

Pelengaris, S., Khan, M. and Evan, G.I. (2002b). Suppression of Myc-induced apoptosis in beta cells exposes multiple oncogenic properties of Myc and triggers carcinogenic progression. *Cell, 109*(3), 321-334.

Peng, Q., Wu, J., Zhang, Y., Liu, Y., Kong, R., Hu, L., Du, X. and Ke, Y. (2010). 1A6/DRIM, a novel t-UTP, activates RNA polymerase I transcription and promotes cell proliferation. *PLoS One, 5*(12), e14244.

Perez-Fernandez, J., Martin-Marcos, P. and Dosil, M. (2011). Elucidation of the assembly events required for the recruitment of Utp20, Imp4 and Bms1 onto nascent pre-ribosomes. *Nucleic Acids Res, 39*(18), 8105-8121.

Perez-Fernandez, J., Roman, A., De Las Rivas, J., Bustelo, X.R. and Dosil, M. (2007). The 90S preribosome is a multimodular structure that is assembled through a hierarchical mechanism. *Mol Cell Biol, 27*(15), 5414-5429.

Pestov, D.G., Strezoska, Z. and Lau, L.F. (2001). Evidence of p53-dependent cross-talk between ribosome biogenesis and the cell cycle: effects of nucleolar protein Bop1 on G(1)/S transition. *Mol Cell Biol, 21*(13), 4246-4255.

Phipps, K.R., Charette, J. and Baserga, S.J. (2011a). The small subunit processome in ribosome biogenesis-progress and prospects. *Wiley Interdiscip Rev RNA, 2*(1), 1-21.

Phipps, K.R., Charette, J.M. and Baserga, S.J. (2011b). The small subunit processome in ribosome biogenesis-progress and prospects. *Wiley Interdiscip Rev RNA, 2*(1), 1-21.

Piekna-Przybylska, D., Decatur, W.A. and Fournier, M.J. (2007). New bioinformatic tools for analysis of nucleotide modifications in eukaryotic rRNA. *RNA, 13*(3), 305-312.

Planta, R.J. (1997). Regulation of ribosome synthesis in yeast. *Yeast, 13*(16), 1505-1518.

Pogacic, V., Dragon, F. and Filipowicz, W. (2000). Human H/ACA small nucleolar RNPs and telomerase share evolutionarily conserved proteins NHP2 and NOP10. *Mol Cell Biol, 20*(23), 9028-9040.

Ponti, D., Troiano, M., Bellenchi, G.C., Battaglia, P.A. and Gigliani, F. (2008). The HIV Tat protein affects processing of ribosomal RNA precursor. *BMC Cell Biol, 9*, 32.

Prieto, J.L. and McStay, B. (2007). Recruitment of factors linking transcription and processing of pre-rRNA to NOR chromatin is UBF-dependent and occurs independent of transcription in human cells. *Genes Dev, 21*(16), 2041-2054.

Pyle, A.M. (2008). Translocation and unwinding mechanisms of RNA and DNA helicases. *Annu Rev Biophys, 37*, 317-336.

Rajkowitsch, L., Chen, D., Stampfl, S., Semrad, K., Waldsich, C., Mayer, O., Jantsch, M.F., Konrat, R., Blasi, U. and Schroeder, R. (2007). RNA chaperones, RNA annealers and RNA helicases. *RNA Biol, 4*(3), 118-130.

Raska, I. (2003). Oldies but goldies: searching for Christmas trees within the nucleolar architecture. *Trends Cell Biol, 13*(10), 517-525.

Raska, I. (2004). Searching for active ribosomal genes. *Prog Mol Subcell Biol, 35*, 23-56.

Raska, I., Shaw, P.J. and Cmarko, D. (2006). Structure and function of the nucleolus in the spotlight. *Curr Opin Cell Biol, 18*(3), 325-334.

Reichow, S.L., Hamma, T., Ferre-D'Amare, A.R. and Varani, G. (2007). The structure and function of small nucleolar ribonucleoproteins. *Nucleic Acids Res, 35*(5), 1452-1464.

Reimer, G., Pollard, K.M., Penning, C.A., Ochs, R.L., Lischwe, M.A., Busch, H. and Tan, E.M. (1987). Monoclonal autoantibody from a (New Zealand black x New Zealand white)F1 mouse and some human scleroderma sera target an Mr 34,000 nucleolar protein of the U3 RNP particle. *Arthritis Rheum, 30*(7), 793-800.

Richard, G.F., Kerrest, A. and Dujon, B. (2008). Comparative genomics and molecular dynamics of DNA repeats in eukaryotes. *Microbiol Mol Biol Rev, 72*(4), 686-727.

Richard, P., Darzacq, X., Bertrand, E., Jady, B.E., Verheggen, C. and Kiss, T. (2003). A common sequence motif determines the Cajál body-specific localization of box H/ACA scaRNAs. *EMBO J, 22*(16), 4283-4293.

Riffle, M., Malmstrom, L. and Davis, T.N. (2005). The Yeast Resource Center Public Data Repository. *Nucleic Acids Res, 33*(Database issue), D378-382.

Rigaut, G., Shevchenko, A., Rutz, B., Wilm, M., Mann, M. and Seraphin, B. (1999). A generic protein purification method for protein complex characterization and proteome exploration. *Nat Biotechnol, 17*(10), 1030-1032.

Rocak, S. and Linder, P. (2004). DEAD-box proteins: the driving forces behind RNA metabolism. *Nat Rev Mol Cell Biol, 5*(3), 232-241.

Rodriguez-Galan, O., Garcia-Gomez, J.J. and de la Cruz, J. (2013). Yeast and human RNA helicases involved in ribosome biogenesis: current status and perspectives. *Biochim Biophys Acta, 1829*(8), 775-790.

Rogers, G.W., Jr., Richter, N.J. and Merrick, W.C. (1999). Biochemical and kinetic characterization of the RNA helicase activity of eukaryotic initiation factor 4A. *J Biol Chem, 274*(18), 12236-12244.

Rohrmoser, M., Holzel, M., Grimm, T., Malamoussi, A., Harasim, T., Orban, M., Pfisterer, I., Gruber-Eber, A., Kremmer, E. and Eick, D. (2007). Interdependence of Pes1, Bop1, and WDR12 controls nucleolar localization and assembly of the PeBoW complex required for maturation of the 60S ribosomal subunit. *Mol Cell Biol, 27*(10), 3682-3694.

Rouquette, J., Choesmel, V. and Gleizes, P.E. (2005). Nuclear export and cytoplasmic processing of precursors to the 40S ribosomal subunits in mammalian cells. *EMBO J, 24*(16), 2862-2872.

Rubbi, C.P. and Milner, J. (2003). Disruption of the nucleolus mediates stabilization of p53 in response to DNA damage and other stresses. *EMBO J, 22*(22), 6068-6077.

Rudra, D., Mallick, J., Zhao, Y. and Warner, J.R. (2007). Potential interface between ribosomal protein production and pre-rRNA processing. *Mol Cell Biol, 27*(13), 4815-4824.

Ruggero, D. and Pandolfi, P.P. (2003). Does the ribosome translate cancer? *Nat Rev Cancer, 3*(3), 179-192.

Rujkijyanont, P., Adams, S.L., Beyene, J. and Dror, Y. (2009). Bone marrow cells from patients with Shwachman-Diamond syndrome abnormally express genes involved in ribosome biogenesis and RNA processing. *Br J Haematol, 145*(6), 806-815.

Samarsky, D.A. and Fournier, M.J. (1998). Functional mapping of the U3 small nucleolar RNA from the yeast Saccharomyces cerevisiae. *Mol Cell Biol, 18*(6), 3431-3444.

Samarsky, D.A. and Fournier, M.J. (1999). A comprehensive database for the small nucleolar RNAs from Saccharomyces cerevisiae. *Nucleic Acids Res, 27*(1), 161-164.

Samarsky, D.A., Schneider, G.S. and Fournier, M.J. (1996). An essential domain in Saccharomyces cerevisiae U14 snoRNA is absent in vertebrates, but conserved in other yeasts. *Nucleic Acids Res, 24*(11), 2059-2066.

Savino, R. and Gerbi, S.A. (1990). In vivo disruption of Xenopus U3 snRNA affects ribosomal RNA processing. *EMBO J, 9*(7), 2299-2308.

Savitsky, K., Ziv, Y., Bar-Shira, A., Gilad, S., Tagle, D.A., Smith, S., Uziel, T., Sfez, S., Nahmias, J., Sartiel, A., Eddy, R.L., Shows, T.B., Collins, F.S., Shiloh, Y. and Rotman, G. (1996). A human gene (DDX10) encoding a putative DEAD-box RNA helicase at 11q22-q23. *Genomics, 33*(2), 199-206.

Schafer, T., Strauss, D., Petfalski, E., Tollervey, D. and Hurt, E. (2003). The path from nucleolar 90S to cytoplasmic 40S pre-ribosomes. *EMBO J, 22*(6), 1370-1380.

Scheer, U. and Benavente, R. (1990). Functional and dynamic aspects of the mammalian nucleolus. *Bioessays, 12*(1), 14-21.

Scheer, U. and Hock, R. (1999). Structure and function of the nucleolus. *Curr Opin Cell Biol, 11*(3), 385-390.

Scherl, A., Coute, Y., Deon, C., Calle, A., Kindbeiter, K., Sanchez, J.C., Greco, A., Hochstrasser, D. and Diaz, J.J. (2002). Functional proteomic analysis of human nucleolus. *Mol Biol Cell, 13*(11), 4100-4109.

Schluter, C., Duchrow, M., Wohlenberg, C., Becker, M.H., Key, G., Flad, H.D. and Gerdes, J. (1993). The cell proliferation-associated antigen of antibody Ki-67: a very large, ubiquitous nuclear protein with numerous repeated elements, representing a new kind of cell cycle-maintaining proteins. *J Cell Biol, 123*(3), 513-522.

Schmidt-Zachmann, M.S. and Nigg, E.A. (1993). Protein localization to the nucleolus: a search for targeting domains in nucleolin. *J Cell Sci, 105 (Pt 3)*, 799-806.

Schmitt, M.E. and Clayton, D.A. (1993). Nuclear RNase MRP is required for correct processing of pre-5.8S rRNA in Saccharomyces cerevisiae. *Mol Cell Biol, 13*(12), 7935-7941.

Scholzen, T. and Gerdes, J. (2000). The Ki-67 protein: from the known and the unknown. *J Cell Physiol, 182*(3), 311-322.

Schwirzke, M., Gnirke, A., Bork, P., Tarin, D. and Weidle, U.H. (1998). Differential gene expression in mammary carcinoma cell lines: identification of DRIM, a new gene down-regulated in metastasis. *Anticancer Res, 18*(3A), 1409-1421.

Segerstolpe, A., Granneman, S., Bjork, P., de Lima Alves, F., Rappsilber, J., Andersson, C., Hogbom, M., Tollervey, D. and Wieslander, L. (2013). Multiple RNA interactions position Mrd1 at the site of the small subunit pseudoknot within the 90S pre-ribosome. *Nucleic Acids Res, 41*(2), 1178-1190.

Seidel, R., Bloom, J.G., Dekker, C. and Szczelkun, M.D. (2008). Motor step size and ATP coupling efficiency of the dsDNA translocase EcoR124I. *EMBO J, 27*(9), 1388-1398.

Sharma, K. and Tollervey, D. (1999). Base pairing between U3 small nucleolar RNA and the 5' end of 18S rRNA is required for pre-rRNA processing. *Mol Cell Biol, 19*(9), 6012-6019.

Sharma, K., Venema, J. and Tollervey, D. (1999). The 5' end of the 18S rRNA can be positioned from within the mature rRNA. *RNA, 5*(5), 678-686.

Shaw, P.J. and Brown, J.W. (2004). Plant nuclear bodies. *Curr Opin Plant Biol, 7*(6), 614-620.

Shaw, P.J. and Jordan, E.G. (1995). The nucleolus. *Annu Rev Cell Dev Biol, 11*, 93-121.

Shereda, R.D., Reiter, N.J., Butcher, S.E. and Keck, J.L. (2009). Identification of the SSB binding site on E. coli RecQ reveals a conserved surface for binding SSB's C terminus. *J Mol Biol, 386*(3), 612-625.

Sikorski, R.S. and Hieter, P. (1989). A system of shuttle vectors and yeast host strains designed for efficient manipulation of DNA in Saccharomyces cerevisiae. *Genetics, 122*(1), 19-27.

Silverman, E., Edwalds-Gilbert, G. and Lin, R.J. (2003). DExD/H-box proteins and their partners: helping RNA helicases unwind. *Gene, 312*, 1-16.

Singleton, M.R., Dillingham, M.S. and Wigley, D.B. (2007). Structure and mechanism of helicases and nucleic acid translocases. *Annu Rev Biochem, 76*, 23-50.

Sjoblom, T., Jones, S., Wood, L.D., Parsons, D.W., Lin, J., Barber, T.D., Mandelker, D., Leary, R.J., Ptak, J., Silliman, N., Szabo, S., Buckhaults, P., Farrell, C., Meeh, P., Markowitz, S.D., Willis, J., Dawson, D., Willson, J.K., Gazdar, A.F., Hartigan, J., Wu, L., Liu, C., Parmigiani, G., Park, B.H., Bachman, K.E., Papadopoulos, N., Vogelstein, B., Kinzler, K.W. and Velculescu, V.E. (2006). The consensus coding sequences of human breast and colorectal cancers. *Science, 314*(5797), 268-274.

Smith, C.M. and Steitz, J.A. (1997). Sno storm in the nucleolus: new roles for myriad small RNPs. *Cell, 89*(5), 669-672.

Smulson, M.E., Pang, D., Jung, M., Dimtchev, A., Chasovskikh, S., Spoonde, A., Simbulan-Rosenthal, C., Rosenthal, D., Yakovlev, A. and Dritschilo, A. (1998). Irreversible binding of poly(ADP)ribose polymerase cleavage product to DNA ends revealed by atomic force microscopy: possible role in apoptosis. *Cancer Res, 58*(16), 3495-3498.

Soltanieh, S., Lapensee, M. and Dragon, F. (2014). Nucleolar proteins Bfr2 and Enp2 interact with DEAD-box RNA helicase Dbp4 in two different complexes. *Nucleic Acids Res, 42*(5), 3194-3206.

Sorensen, P.D. and Frederiksen, S. (1991). Characterization of human 5S rRNA genes. *Nucleic Acids Res, 19*(15), 4147-4151.

Soultanas, P., Dillingham, M.S., Wiley, P., Webb, M.R. and Wigley, D.B. (2000). Uncoupling DNA translocation and helicase activity in PcrA: direct evidence for an active mechanism. *EMBO J, 19*(14), 3799-3810.

Soussi, T., Dehouche, K. and Beroud, C. (2000). p53 website and analysis of p53 gene mutations in human cancer: forging a link between epidemiology and carcinogenesis. *Hum Mutat, 15*(1), 105-113.

Staley, J.P. and Guthrie, C. (1998). Mechanical devices of the spliceosome: motors, clocks, springs, and things. *Cell, 92*(3), 315-326.

Staley, J.P. and Woolford, J.L., Jr. (2009). Assembly of ribosomes and spliceosomes: complex ribonucleoprotein machines. *Curr Opin Cell Biol, 21*(1), 109-118.

Stanek, D. and Neugebauer, K.M. (2006). The Cajal body: a meeting place for spliceosomal snRNPs in the nuclear maze. *Chromosoma, 115*(5), 343-354.

Stark, L.A. and Taliansky, M. (2009). Old and new faces of the nucleolus. Workshop on the Nucleolus and Disease. *EMBO Rep, 10*(1), 35-40.

Strezoska, Z., Pestov, D.G. and Lau, L.F. (2000). Bop1 is a mouse WD40 repeat nucleolar protein involved in 28S and 5. 8S RRNA processing and 60S ribosome biogenesis. *Mol Cell Biol, 20*(15), 5516-5528.

Strubin, M., Newell, J.W. and Matthias, P. (1995). OBF-1, a novel B cell-specific coactivator that stimulates immunoglobulin promoter activity through association with octamer-binding proteins. *Cell, 80*(3), 497-506.

Strunk, B.S. and Karbstein, K. (2009). Powering through ribosome assembly. *RNA, 15*(12), 2083-2104.

Strunk, B.S., Loucks, C.R., Su, M., Vashisth, H., Cheng, S., Schilling, J., Brooks, C.L., 3rd, Karbstein, K. and Skiniotis, G. (2011). Ribosome assembly factors prevent premature translation initiation by 40S assembly intermediates. *Science, 333*(6048), 1449-1453.

Strunk, B.S., Novak, M.N., Young, C.L. and Karbstein, K. (2012). A translation-like cycle is a quality control checkpoint for maturing 40S ribosome subunits. *Cell, 150*(1), 111-121.

Sweet, T., Yen, W., Khalili, K. and Amini, S. (2008). Evidence for involvement of NFBP in processing of ribosomal RNA. *J Cell Physiol, 214*(2), 381-388.

Tafforeau, L., Zorbas, C., Langhendries, J.L., Mullineux, S.T., Stamatopoulou, V., Mullier, R., Wacheul, L. and Lafontaine, D.L. (2013). The complexity of human ribosome biogenesis revealed by systematic nucleolar screening of Pre-rRNA processing factors. *Mol Cell, 51*(4), 539-551.

Takahashi, N., Yanagida, M., Fujiyama, S., Hayano, T. and Isobe, T. (2003). Proteomic snapshot analyses of preribosomal ribonucleoprotein complexes formed at various stages of ribosome biogenesis in yeast and mammalian cells. *Mass Spectrom Rev, 22*(5), 287-317.

Tanner, N.K. (2003). The newly identified Q motif of DEAD box helicases is involved in adenine recognition. *Cell Cycle, 2*(1), 18-19.

Tanner, N.K., Cordin, O., Banroques, J., Doere, M. and Linder, P. (2003). The Q motif: a newly identified motif in DEAD box helicases may regulate ATP binding and hydrolysis. *Mol Cell, 11*(1), 127-138.

Tanner, N.K. and Linder, P. (2001). DExD/H box RNA helicases: from generic motors to specific dissociation functions. *Mol Cell, 8*(2), 251-262.

Terns, M.P. and Terns, R.M. (2002). Small nucleolar RNAs: versatile trans-acting molecules of ancient evolutionary origin. *Gene Expr, 10*(1-2), 17-39.

Theissen, B., Karow, A.R., Kohler, J., Gubaev, A. and Klostermeier, D. (2008). Cooperative binding of ATP and RNA induces a closed conformation in a DEAD box RNA helicase. *Proc Natl Acad Sci U S A, 105*(2), 548-553.

Thomas, F. and Kutay, U. (2003). Biogenesis and nuclear export of ribosomal subunits in higher eukaryotes depend on the CRM1 export pathway. *J Cell Sci, 116*(Pt 12), 2409-2419.

Tijerina, P., Bhaskaran, H. and Russell, R. (2006). Nonspecific binding to structured RNA and preferential unwinding of an exposed helix by the CYT-19 protein, a DEAD-box RNA chaperone. *Proc Natl Acad Sci U S A, 103*(45), 16698-16703.

Toby, G.G. and Golemis, E.A. (2001). Using the yeast interaction trap and other two-hybrid-based approaches to study protein-protein interactions. *Methods, 24*(3), 201-217.

Tollervey, D. (1987). A yeast small nuclear RNA is required for normal processing of pre-ribosomal RNA. *EMBO J, 6*(13), 4169-4175.

Tollervey, D. (1996a). Trans-acting factors in ribosome synthesis. *Experimental cell research, 229*(2), 226-232.

Tollervey, D. (1996b). Trans-acting factors in ribosome synthesis. *Exp Cell Res, 229*(2), 226-232.

Tollervey, D. and Guthrie, C. (1985). Deletion of a yeast small nuclear RNA gene impairs growth. *EMBO J, 4*(13B), 3873-3878.

Tollervey, D. and Kiss, T. (1997). Function and synthesis of small nucleolar RNAs. *Curr Opin Cell Biol, 9*(3), 337-342.

Trotta, C.R., Lund, E., Kahan, L., Johnson, A.W. and Dahlberg, J.E. (2003). Coordinated nuclear export of 60S ribosomal subunits and NMD3 in vertebrates. *EMBO J, 22*(11), 2841-2851.

Trubetskoy, D., Proux, F., Allemand, F., Dreyfus, M. and Iost, I. (2009). SrmB, a DEAD-box helicase involved in Escherichia coli ribosome assembly, is specifically targeted to 23S rRNA in vivo. *Nucleic Acids Res, 37*(19), 6540-6549.

Trucco, C., Oliver, F.J., de Murcia, G. and Menissier-de Murcia, J. (1998). DNA repair defect in poly(ADP-ribose) polymerase-deficient cell lines. *Nucleic Acids Res, 26*(11), 2644-2649.

Tschochner, H. and Hurt, E. (2003). Pre-ribosomes on the road from the nucleolus to the cytoplasm. *Trends Cell Biol, 13*(5), 255-263.

Turner, A.J., Knox, A.A., Prieto, J.L., McStay, B. and Watkins, N.J. (2009). A novel small-subunit processome assembly intermediate that contains the U3 snoRNP, nucleolin, RRP5, and DBP4. *Mol Cell Biol, 29*(11), 3007-3017.

Tycowski, K.T., Smith, C.M., Shu, M.D. and Steitz, J.A. (1996). A small nucleolar RNA requirement for site-specific ribose methylation of rRNA in Xenopus. *Proc Natl Acad Sci U S A, 93*(25), 14480-14485.

Umate, P., Tuteja, N. and Tuteja, R. (2011). Genome-wide comprehensive analysis of human helicases. *Commun Integr Biol, 4*(1), 118-137.

Valentin (dir.). (1839). *Repertorium fur Anatomie und Physiologie* (Vol. 4). Bern, St. Gallen: Verlag von Huber und comp.

Venema, J. and Tollervey, D. (1999). Ribosome synthesis in Saccharomyces cerevisiae. *Annu Rev Genet, 33*, 261-311.

Venema, J., Vos, H.R., Faber, A.W., van Venrooij, W.J. and Raue, H.A. (2000). Yeast Rrp9p is an evolutionarily conserved U3 snoRNP protein essential for early pre-rRNA processing cleavages and requires box C for its association. *RNA, 6*(11), 1660-1671.

Vilardell, J. and Warner, J.R. (1997). Ribosomal protein L32 of Saccharomyces cerevisiae influences both the splicing of its own transcript and the processing of rRNA. *Mol Cell Biol, 17*(4), 1959-1965.

Vogelstein, B., Lane, D. and Levine, A.J. (2000). Surfing the p53 network. *Nature, 408*(6810), 307-310.

Vousden, K.H. and Lane, D.P. (2007). p53 in health and disease. *Nat Rev Mol Cell Biol, 8*(4), 275-283.

Vousden, K.H. and Lu, X. (2002). Live or let die: the cell's response to p53. *Nat Rev Cancer, 2*(8), 594-604.

Vulliamy, T., Beswick, R., Kirwan, M., Marrone, A., Digweed, M., Walne, A. and Dokal, I. (2008). Mutations in the telomerase component NHP2 cause the premature ageing syndrome dyskeratosis congenita. *Proc Natl Acad Sci U S A, 105*(23), 8073-8078.

Walne, A.J. and Dokal, I. (2009). Advances in the understanding of dyskeratosis congenita. *Br J Haematol, 145*(2), 164-172.

Walne, A.J., Vulliamy, T., Marrone, A., Beswick, R., Kirwan, M., Masunari, Y., Al-Qurashi, F.H., Aljurf, M. and Dokal, I. (2007). Genetic heterogeneity in autosomal recessive dyskeratosis congenita with one subtype due to mutations in the telomerase-associated protein NOP10. *Hum Mol Genet, 16*(13), 1619-1629.

Wang, Y., Liu, J., Zhao, H., Lu, W., Zhao, J., Yang, L., Li, N., Du, X. and Ke, Y. (2007). Human 1A6/DRIM, the homolog of yeast Utp20, functions in the 18S rRNA processing. *Biochim Biophys Acta, 1773*(6), 863-868.

Warner, J.R. (1989). Synthesis of ribosomes in Saccharomyces cerevisiae. *Microbiol Rev, 53*(2), 256-271.

Warner, J.R. (1999). The economics of ribosome biosynthesis in yeast. *Trends Biochem Sci, 24*(11), 437-440.

Warner, J.R. and McIntosh, K.B. (2009). How common are extraribosomal functions of ribosomal proteins? *Mol Cell, 34*(1), 3-11.

Watkins, N.J., Leverette, R.D., Xia, L., Andrews, M.T. and Maxwell, E.S. (1996). Elements essential for processing intronic U14 snoRNA are located at the termini of the mature snoRNA sequence and include conserved nucleotide boxes C and D. *RNA, 2*(2), 118-133.

Wegierski, T., Billy, E., Nasr, F. and Filipowicz, W. (2001). Bms1p, a G-domain-containing protein, associates with Rcl1p and is required for 18S rRNA biogenesis in yeast. *RNA, 7*(9), 1254-1267.

Wehner, K.A., Gallagher, J.E. and Baserga, S.J. (2002). Components of an interdependent unit within the SSU processome regulate and mediate its activity. *Mol Cell Biol, 22*(20), 7258-7267.

Westendorf, J.M., Konstantinov, K.N., Wormsley, S., Shu, M.D., Matsumoto-Taniura, N., Pirollet, F., Klier, F.G., Gerace, L. and Baserga, S.J. (1998). M phase phosphoprotein 10 is a human U3 small nucleolar ribonucleoprotein component. *Mol Biol Cell, 9*(2), 437-449.

White, R.J. (2005). RNA polymerases I and III, growth control and cancer. *Nat Rev Mol Cell Biol, 6*(1), 69-78.

Wiederkehr, T., Pretot, R.F. and Minvielle-Sebastia, L. (1998). Synthetic lethal interactions with conditional poly(A) polymerase alleles identify LCP5, a gene involved in 18S rRNA maturation. *RNA, 4*(11), 1357-1372.

Woolford, J.L., Jr. (1991). The structure and biogenesis of yeast ribosomes. *Adv Genet, 29*, 63-118.

Woolford, J.L., Jr. and Baserga, S.J. (2013). Ribosome biogenesis in the yeast Saccharomyces cerevisiae. *Genetics, 195*(3), 643-681.

Xiao, S., Houser-Scott, F. and Engelke, D.R. (2001). Eukaryotic ribonuclease P: increased complexity to cope with the nuclear pre-tRNA pathway. *J Cell Physiol, 187*(1), 11-20.

Yager, J.D. and Davidson, N.E. (2006). Estrogen carcinogenesis in breast cancer. *N Engl J Med, 354*(3), 270-282.

Yang, Q., Del Campo, M., Lambowitz, A.M. and Jankowsky, E. (2007). DEAD-box proteins unwind duplexes by local strand separation. *Mol Cell, 28*(2), 253-263.

Yang, Q. and Jankowsky, E. (2006). The DEAD-box protein Ded1 unwinds RNA duplexes by a mode distinct from translocating helicases. *Nat Struct Mol Biol, 13*(11), 981-986.

Yassin, E.R., Abdul-Nabi, A.M., Takeda, A. and Yaseen, N.R. (2010). Effects of the NUP98-DDX10 oncogene on primary human CD34+ cells: role of a conserved helicase motif. *Leukemia, 24*(5), 1001-1011.

Yoneyama, M. and Fujita, T. (2008). Structural mechanism of RNA recognition by the RIG-I-like receptors. *Immunity, 29*(2), 178-181.

Yusupov, M.M., Yusupova, G.Z., Baucom, A., Lieberman, K., Earnest, T.N., Cate, J.H. and Noller, H.F. (2001). Crystal structure of the ribosome at 5.5 A resolution. *Science, 292*(5518), 883-896.

Zafarullah, M., Wisniewski, J., Shworak, N.W., Schieman, S., Misra, S. and Gedamu, L. (1992). Molecular cloning and characterization of a constitutively expressed heat-shock-cognate hsc71 gene from rainbow trout. *Eur J Biochem, 204*(2), 893-900.

Zemp, I. and Kutay, U. (2007). Nuclear export and cytoplasmic maturation of ribosomal subunits. *FEBS Lett, 581*(15), 2783-2793.

Zhang, S. and Grosse, F. (2004). Multiple functions of nuclear DNA helicase II (RNA helicase A) in nucleic acid metabolism. *Acta Biochim Biophys Sin (Shanghai), 36*(3), 177-183.

Zhang, Y. and Lu, H. (2009). Signaling to p53: ribosomal proteins find their way. *Cancer Cell, 16*(5), 369-377.

Zhang, Y., Wolf, G.W., Bhat, K., Jin, A., Allio, T., Burkhart, W.A. and Xiong, Y. (2003). Ribosomal protein L11 negatively regulates oncoprotein MDM2 and mediates a p53-dependent ribosomal-stress checkpoint pathway. *Mol Cell Biol, 23*(23), 8902-8912.

Zhu, Y., Poyurovsky, M.V., Li, Y., Biderman, L., Stahl, J., Jacq, X. and Prives, C. (2009). Ribosomal protein S7 is both a regulator and a substrate of MDM2. *Mol Cell, 35*(3), 316-326.